

RECOVERY OF NATURAL GAS LIQUIDS WITH
MEMBRANES FROM ASSOCIATED GAS ON
NEWFOUNDLAND AND LABRADOR OFFSHORE
PRODUCTION FACILITIES

by

Erika Beronich

A thesis submitted to the
School of Graduates Studies
in partial fulfilment of the
requirement for the degree of
Master of Engineering
Faculty of Engineering and Applied Science
Memorial University of Newfoundland
August 2006

St John's

Newfoundland



Library and
Archives Canada

Bibliothèque et
Archives Canada

Published Heritage
Branch

Direction du
Patrimoine de l'édition

395 Wellington Street
Ottawa ON K1A 0N4
Canada

395, rue Wellington
Ottawa ON K1A 0N4
Canada

Your file *Votre référence*
ISBN: 978-0-494-30449-5
Our file *Notre référence*
ISBN: 978-0-494-30449-5

NOTICE:

The author has granted a non-exclusive license allowing Library and Archives Canada to reproduce, publish, archive, preserve, conserve, communicate to the public by telecommunication or on the Internet, loan, distribute and sell theses worldwide, for commercial or non-commercial purposes, in microform, paper, electronic and/or any other formats.

The author retains copyright ownership and moral rights in this thesis. Neither the thesis nor substantial extracts from it may be printed or otherwise reproduced without the author's permission.

AVIS:

L'auteur a accordé une licence non exclusive permettant à la Bibliothèque et Archives Canada de reproduire, publier, archiver, sauvegarder, conserver, transmettre au public par télécommunication ou par l'Internet, prêter, distribuer et vendre des thèses partout dans le monde, à des fins commerciales ou autres, sur support microforme, papier, électronique et/ou autres formats.

L'auteur conserve la propriété du droit d'auteur et des droits moraux qui protègent cette thèse. Ni la thèse ni des extraits substantiels de celle-ci ne doivent être imprimés ou autrement reproduits sans son autorisation.

In compliance with the Canadian Privacy Act some supporting forms may have been removed from this thesis.

Conformément à la loi canadienne sur la protection de la vie privée, quelques formulaires secondaires ont été enlevés de cette thèse.

While these forms may be included in the document page count, their removal does not represent any loss of content from the thesis.

Bien que ces formulaires aient inclus dans la pagination, il n'y aura aucun contenu manquant.


Canada

ABSTRACT

The market for natural gas has been rapidly increasing and is becoming one of the most important sources of energy in the world. Natural gas is a “cleaner” burning fuel when compared to other fossil fuels and therefore environmental impacts are minimized. Gas produced (associated gas) with oil is largely methane with heavier fractions referred to as NGL (Natural Gas Liquids). NGL is used as feedstock for petrochemical processes or as fuel for industrial and domestic purposes. The recovery of NGL is commonly carried out at onshore oil and gas operations where space and weight are not critical design parameters. The limited space on offshore platforms makes NGL recovery a challenge. Currently, in the Newfoundland and Labrador Offshore, the associated gas is re-injected, used for power on the platforms, and some is flared but not recovered due to the difficulties to storage and transport in this remote location. This associated gas contains high levels of NGL, making attractive its recovery from the economical and environmental points of view. This thesis describes in detail the development of a membrane process to recover NGL. Different processes such as turbo-expander, absorption, adsorption, external refrigeration and membranes are reviewed and compared. As a result of this comparison, membranes are proposed as a feasible option for NGL recovery. Several membrane models are investigated. Membranes are placed in different locations in a three-stage separation train on an offshore platform, and the effect of pressure, inlet temperature process, flow pattern, and location in the process are analysed. The analyses are then extended by incorporating the recycle of the permeate and residue streams of the membranes to separators. Twelve alternative configurations of the original process are investigated with the objective of evaluating the impact of the membranes on the production of crude oil base. As a result, it is demonstrated that some of the configurations considered increase the production of crude oil.

ACKNOWLEDGEMENTS

First, I would like to deeply thank my supervisors Dr. Kelly Hawboldt and Dr. Majid Abdi, who believed in me and gave me this great opportunity. They provided me with useful and helpful assistance, advice and support.

This work has received a generous financial support from National Science and Engineering Research Council of Canada (NSERC) and School of Graduate Studies, Memorial University of Newfoundland.

I would also like to thanks Ms Moya Crocker, Secretary to the Associated Dean of Graduate Studies and Research, and Dr Venkatesan, Associated Dean of Graduate Studies and Research, for their efficiency and kindness.

In addition, Dr. O Anunziata, Dr. L Pierella, and all the people involved with the Physical-Chemistry Group of New Materials (GFNM), part of the Center for Research and Development of Chemistry (CITeQ), National Technological University, Argentina (UTN-FRC), who initiated me in the research world and encouraged me to continue with my studies.

Finally, I would like to thank my family and friends for their loving support, and to express my special gratitude to my husband, Martin, who is always shoulder-to-shoulder providing me confidence and support.

TABLE OF CONTENTS

ABSTRACT	i
ACKNOWLEDGEMENT	ii
TABLE OF CONTENTS	iii
LIST OF FIGURES	viii
LIST OF TABLES	xii
NOMENCLATURE	xii
INTRODUCTION.....	1
1.1 Stranded gas	1
1.2 Environmental Risk of the Emissions in Offshore Newfoundland	2
1.3 Objectives of Study	4
1.4 Scope of Study	4
1.5 Thesis Outline	5
2 ALTERNATIVES TO OFFSHORE NGLS RECOVERY	7
2.1 External Refrigeration/Cryogenic Processes.....	7
2.1.1 General Characteristics	7
2.1.2 Advantages and drawbacks	8
2.2 Turbine expansion	9
2.2.1 General Characteristics	9
2.2.2 Advantages and drawbacks	10
2.3 Absorption.....	11

2.3.1 General Characteristics	11
2.3.2 Advantages and drawbacks	12
2.4 Adsorption	13
2.4.1 General Characteristics	13
2.4.1 Advantages and drawbacks	13
2.5 Membranes Separation Technologies	14
2.5.1 General Characteristics	14
2.5.2 Advantages and drawbacks	15
2.6 Comparison of the Alternatives and Possibilities of installation in Newfoundland's Offshore	16
3 APPLICATION OF MEMBRANES IN NATURAL GAS PROCESSING	19
3.1 Membrane description.....	19
3.2 Gas Membrane Systems	20
3.2.1 Flat membranes	20
3.2.2 Hollow fibre membranes	20
3.2.3 Spiral membranes	22
3.3 Classification of membranes	23
3.4 Transport of gases through nonporous membranes.....	24
3.5 Nonporous membrane materials.....	25
4 COMPARISON OF MEMBRANE SEPARATION MODELS	29
4.1 Co-current Flow Models	29
4.1.1 Model based on differential equations	29
4.1.2 Model based on discrete equations.....	34

4.2 Counter-current Flow Models	37
4.2.1 Model based on differential equations	37
4.2.2 Model with discrete equations.....	38
4.3 Example for Comparison of the Models	42
4.3.1 Co-current Models comparison	43
4.3.2 Counter-current Models comparison.....	45
4.4 Comparison of the Models	46
5 RECOVERING NATURAL GAS LIQUIDS IN ATLANTIC CANADA’S OFFSHORE PETROLEUM PRODUCTION PROJECTS.....	48
5.1 Crude Oil and Natural Gas in Atlantic Canada	49
5.2 Process Description	49
5.3 Connection between HYSYS and MATLAB	51
5.4 Membrane Process Analysis	53
5.5 Analysis of Recovery of Propane plus components (C ₃ ⁺).....	55
5.5.1 Pressure Effect.....	55
5.5.2 Effect of Gas Composition.....	57
5.5.3 Effect of Flow Patterns.....	60
5.5.4 Effect of Stream Temperature	61
5.5.5 Location Effect.....	62
5.6 Analysis of Recovery of Ethane Plus Components (C ₂ ⁺).....	65
5.6.1 Pressure Effect.....	65
5.6.2 Effect of Gas Composition.....	67
5.6.3 Effect of Flow Patterns.....	70

5.6.4 Effect of Stream Temperature	70
5.6.5 Location Effect	72
5.7 Conclusion.....	75
6 PROCESS CASE STUDIES WITH RECYCLE STREAMS	76
6.1 Three-stage Crude oil Separation Process4.....	76
6.2 Alternatives processes with membranes	79
6.2.1 Case 1: Membrane after the high-pressure separator	79
6.2.2 Case 2: Membrane after the medium-pressure separator	82
6.2.3 Case 3: Membrane at the overhead of the low-pressure separator.....	86
6.2.4 Case 4: Membranes after each separator.....	89
6.2.5 Case 5: Four membranes: membranes after each separator and one treating all the residue streams	93
6.2.6 Case 6: Membranes after MP separator with recycle from LP separator	97
6.2.7 Case 7: Membrane after MP separator with recycle from LP separator	100
6.2.8 Case 8: Membrane after MP separator with recycle from LP separator	104
6.2.9 Case 9: Membrane after LP separator recycling the permeate to feed the MP separator	108
6.2.10 Case 10: Membrane after LP separator recycling the permeate to feed the LP separator.....	112
6.2.11 Case 11: Membrane after HP separator recycling the permeate to feed process.....	115

6.2.12 Case 12: Two membranes: one after HP separator recycling the permeate to feed process; and other membrane after MP separator, which receives a recycle from LP separator, and its permeate feeds the MP separator	119
6.3 Analysis and comparison of the twelve cases presented in the previous section	123
7 CONCLUSIONS	126
7.1 Summary	126
7.2 Conclusion.....	127
7.3 Future work	130
REFERENCES	132
APPENDIX A	137
A.1 Co-current Model	137
A.1.1 C-ocurrent model with differential equation	137
A.1.2Cocurrent model with discrete equations	142
A.2 Countercurrent Model	145
A.2.1 Countercurrent model with differential equation	145
A.2.1 Countercurrent model with differential equation	150
APPENDIX B	155
APPENDIX C	168

LIST OF FIGURES

Figure 2.1: Schematic flowsheet of a basic External Refrigeration process.....	8
Figure 2.2: Schematic flowsheet of a basic Turbo expander.....	10
Figure 2.3: Schematic flowsheet of a basic Absorption process.....	12
Figure 2.4: Schematic of a membrane.....	15
Figure 3.1: Hollow-fibre separator assembly.....	21
Figure 3.2: Spiral-wound elements and assembly.....	22
Figure 3.3: Local gas flow paths for spiral-wound separator.....	23
Figure 4.1: Single permeation stage of the co-current model.....	30
Figure 4.2: Module divided into N sections representing a co-current flow.....	35
Figure 4.3: Single permeation stage of the counter-current model.....	38
Figure 4.4: Module divided into N sections representing a counter-current flow.....	38
Figure 4.5: Co-current flow for the differential equation model.....	43
Figure 4.6: Co-current flow for the discrete model.....	44
Figure 4.7: Counter-current flow for the differential model.....	45
Figure 4.8: Counter-current flow for the discrete model.....	46
Figure 5.1: Three-stage crude oil separation.....	50
Figure 5.2: Conceptual schematic of a connection between MATLAB and HYSYS using a spreadsheet.....	52
Figure 5.3: Location of membranes in this analysis.....	54
Figure 5.4: Comparison of recovery for Positions 1 and 2.....	56

Figure 5.5: Comparison of recovery for Positions 3 and 4.....	57
Figure 5.6a: Comparison of recovery for Positions 4 and 5 for wide range of areas...	59
Figure 5.6b: Comparison of recovery for Positions 4 and 5 for small areas.....	59
Figure 5.7: Permeate molar flow rates for C_3^+ and methane in Position 2 for Co- and Counter-current models.....	61
Figure 5.8: Permeate molar flow rates for C_3^+ in Positions 2 when the temperature of the “Wellhead” stream is 30, 35 and 40 °C.....	62
Figure 5.9a: Permeate molar flows of C_3^+ and methane in Positions 2, 4, and 5 for a wide range of areas.....	64
Figure 5.9b: Permeate molar flows of C_3^+ and methane in Positions 2, 4, and 5 for small areas.....	64
Figure 5.10: Separation Factor with respect to methane for C_3^+ in Positions 2, 4, and 5.....	65
Figure 5.11: Comparison of recovery for Positions 1 and 2.....	66
Figure 5.12: Comparison of recovery for Positions 3 and 4.....	67
Figure 5.13a: Comparison of recovery for Positions 4 and 5 for wide range areas.....	69
Figure 5.13b: Comparison of recovery for Positions 4 and 5 for small areas.....	69
Figure 5.14: Permeate molar flow rates for C_2^+ and methane in Position 2 for Co- and Counter-current models.....	70
Figure 5.15: Permeate molar flow rates for C_2^+ in Positions 2 when the temperature of the “Wellhead” stream is 30, 35 and 40 °C.....	71
Figure 5.16a: Permeate molar flows of C_3^+ and methane in Positions 2, 4, and 5.....	73

Figure 5.16b: Permeate molar flows of C_3^+ and methane in Positions 2, 4, and 5.....	73
Figure 5.17: Separation Factor with respect to methane for C_3^+ in Positions 2, 4, and 5.....	74
Figure 6.1: Three-stage crude oil separation process.....	77
Figure 6.2: Case 1: Membrane located after high-pressure separator.....	79
Figure 6.3: Phase envelopes for the stream entering the medium pressure separator (“to MP stage” stream).....	81
Figure 6.4: Case 2: Membrane located after medium-pressure separator.....	83
Figure 6.5: Phase envelopes for the stream entering to the medium pressure separator (“to MP stage”).....	85
Figure 6.6: Case 3: Membrane located after low-pressure separator.....	86
Figure 6.7: Phase envelopes for the stream “Crude Oil Product” for both processes...	88
Figure 6.8: Case 4: Membranes located after each separator.....	90
Figure 6.9: Phase envelopes for the stream “Crude Oil Product” for both processes...	92
Figure 6.10: Case 5: Four membranes, three membranes located after each separator and one treating all the residual streams.....	94
Figure 6.11: Phase envelopes for the stream “Crude Oil Product” for both processes.	96
Figure 6.12: Case 6: Membrane after MP separator with recycle from LP separator...	97
Figure 6.13: Phase envelopes for the stream “Out Oil LP” for both processes.....	99
Figure 6.14: Case 7: Membrane after MP separator with recycle from LP separator...	100
Figure 6.15: Phase envelopes for the stream “Crude Oil Product” for both processes.	103
Figure 6.16: Case 8: Membrane after MP separator with recycle from LP separator...	105

Figure 6.17: Phase envelopes for the stream “Crude Oil Product” for both processes.	107
Figure 6.18: Case 9: Membrane after LP separator recycling the permeate to feed the MP separator.....	109
Figure 6.19: Phase envelopes for the stream “Crude Oil Product” for both processes.	111
Figure 6.20: Case 10: Membrane after LP separator recycling the permeate to feed the LP separator.....	112
Figure 6.21: Phase envelopes for the stream “Crude Oil Product” for both processes.	114
Figure 6.22: Case 11: Membrane after HP separator recycling the permeate to feed process.....	116
Figure 6.23: Phase envelopes for the stream “Crude Oil Product” for both processes.	118
Figure 6.24: Case 12: Two membranes: one after HP separator recycling the permeate to feed process; and other membrane after MP separator, which receives a recycle from LP separator, and its permeate feeds the MP separator.....	120
Figure 6.25: Phase envelopes for the stream “Crude Oil Product” for both processes.	122

LIST OF TABLES

Table 4.1: General conditions for the example	42
Table 4.2: Feed mole fractions and the permeance.....	42
Table 5.1: Conditions of input and output streams.....	51
Table 5.2: Conditions of input streams in each position shown in Figure 5.3.....	53
Table 5.3: Methane loss and C ₃ ⁺ recovery data for positions 4 and 5 for a small range of area	60
Table 6.1: Mass fractions and mass flow rates for the streams specified for the base process.....	78
Table 6.2: Crude oil production of the base process.....	78
Table 6.3: Mass fractions and mass flow rates for the streams specified for Case 1....	80
Table 6.4: Crude oil production of the process of Case 1.....	82
Table 6.5: Mass fractions and mass flow rates for the streams specified for Case 2....	83
Table 6.6: Crude oil production of the process of Case 2.....	86
Table 6.7: Mass fractions and mass flow rates for the streams specified for Case 3....	87
Table 6.8: Crude oil production of the process for Case 3.....	89
Table 6.9: Mass fractions and mass flow rates for the streams specified for of Case 4	91
Table 6.10: Crude oil production of the process of Case 4.....	93
Table 6.11: Mass fractions and mass flow rates for the streams specified for Case 5...	95
Table 6.12: Crude oil production of the process of Case 5.....	97
Table 6.13: Mass fractions and mass flow rates for the streams specified for Case 6	98

Table 6.14: Crude oil production of the process of Case 6.....	100
Table 6.15: Mass fractions and mass flow rates for the streams specified for Case 7...	102
Table 6.16: Crude oil production of the process of Case 7.....	104
Table 6.17: Mass fractions and mass flow rates for the streams specified for Case 8...	106
Table 6.18: Crude oil production of the process of Case 8.....	108
Table 6.19: Mass fractions and mass flow rates for the streams specified for Case 9...	110
Table 6.20: Crude oil production of the process of Case 9.....	112
Table 6.21: Mass fractions and mass flow rates for the streams specified for Case 10.	113
Table 6.22: Crude oil production of the process of Case 10.....	115
Table 6.23: Mass fractions and mass flows for the streams specified for the process of Case 11.....	117
Table 6.24: Crude oil production of the process of Case 11.....	119
Table 6.25: Mass fractions and mass flows for the streams specified for the process of Case 12	121
Table 6.26: Crude oil production of the process of Case 12.....	123
Table 6.27: Comparison of the twelve cases.....	124

NOMENCLATURE

Units

bbls/d: barrels/day

STDm³/d: standard cubic meters per day

mol/s: mol per seconds

Letters

A: membrane area (m²)

A_t: total membrane area (m²)

ΔA_k: area available for mass transfer on stage k (m²)

B_{j,k}, C_{j,k}, and D_{j,k}: coefficients of a matrix for component j on stage k

C₂⁺: ethane plus components

C₃⁺: propane plus components

C₅⁺: pentane plus components

F: flow rate on the feed (high-pressure) stream (mol/s)

F_f: feed flow rate stream (mol/s)

F_o: reject flow rate stream (mol/s)

f: dimensionless flow rate on the feed (high-pressure) stream

f_o: dimensionless flow rate stream at the outlet

G: flow rate on the permeate (low-pressure) stream parallel to the feed stream (mol/s)

g: dimensionless flow rate on the permeate stream

L : permeating length of the hollow fibres in the module (m)
 L_k : total feed flow rate
 $l_{j,k}$: feed flow rates of a component j leaving a stage k
 $m_{i,k}$: mass flow of component j leaving stage k due to permeation
 N : stages in the axial direction
 N_f : number of fibres in the module
 n : number of components
 P_h : pressure on the feed side
 P_h : pressure on the permeate side
 P_L : feed pressures
 P_V : permeate pressures
 Q : permeability
 q : ratio of permeability
 R_o : outer radius (m) of the hollow fibre
 s : dimensionless membrane area
 s_t : dimensionless total membrane area
 V_k : total permeate flow rate
 $v_{j,k}$: permeate flow rates of a component j leaving a stage k
 x : mole fractions of the gas component in the feed stream
 x_f : mole fractions of the gas component in the feed stream at the inlet
 x_o : mole fractions of the gas component in the feed stream at the outlet
 y : mole fractions of the gas component in the permeate stream
 y_p : mole fractions of the gas component in the permeate stream at the outlet

Greek

γ : pressure ratio, P_l/P_h

δ : thickness of membrane

θ : stage cut

Subscripts

i, j: component indication

k: stage

m: base component

CHAPTER 1

INTRODUCTION

In light of the emissions associated with fossil fuel combustion and associated health and environmental impacts, natural gas is becoming increasingly attractive when compared with other fuels. Natural gas is a mixture of methane and other gases, which may include heavier-than-methane hydrocarbon constituents (C_2^+) or natural gas liquids (NGL), water vapour, inert gases, carbon dioxide, and hydrogen sulphide. NGL includes ethane, propane, butanes and heavier hydrocarbons. The NGL fraction represents a valuable product when separated from the natural gas. Constituents that make up NGL are an important source of feedstock for a number of petrochemical processes. In addition, the removal of NGL results in less toxic emissions when the gas is flared due to the inability to recover the gas (e.g. offshore stranded gas). The recovery of NGL is commonly carried out in onshore oil and gas industries where space and weight are not critical design parameters. The limited space on offshore platforms makes NGL recovery a challenge.

1.1 Stranded gas

Stranded gas refers to gas resources located at far distances from a market, or where its recovery/storage/transportation is not favourable as a result of technical or economical challenges. Most of the discovered gas reserves around the world are

considered stranded, and it is suggested that half of them are offshore [1]. Newfoundland and Labrador has an estimated offshore reserve of 280 billion standard cubic meters (10 trillion standard cubic feet) of natural gas [2] with an estimated market value of \$50 billion. Due to the distance from shore (>300 km) and high iceberg traffic, these reserves are classified as stranded. The produced associated gas also contains high levels of NGL. Currently, this gas is re-injected, used for power on the platforms, and some is flared. The produced gas is not recovered as storage and transportation is difficult to the platforms remote location. Transporting the gas by means of pipelines is technically challenging and presently cost-prohibitive. In spite of this difficulty, Newfoundland and Labrador presents a strategic location due to the proximity to solid markets like the United States and Europe [3]. The NGL is a very valuable product of petroleum production and especially during the high oil price periods and relatively stable gas markets could significantly add value to all natural gas and crude oil production facilities.

1.2 Environmental Risk of the Emissions in Offshore Newfoundland

Flaring is used to dispose of waste hydrocarbon gas generated in the production process and in the event of an operational problem. Under optimum gas:air ratios, temperature, and mixing and no hydrocarbon liquids (NGL), the gas would combust to CO₂ and H₂O. However, the NGL combined with meteorological conditions at the flare tip results in incomplete combustion. The type of emission depends on several factors such as flare design, operation conditions, and composition of waste gases. The incomplete combustion results in products such as olefins, acetylenes and aromatics. As

the amount of liquid hydrocarbons is increased in the gas flared, combustion efficiency is reduced from 82 to 62 [4].

In general, typical emission components from flares are BTEX (benzene, toluene, ethylbenzene, and xylene), NDP (naphthalene, phenanthrene and dibenzothiophene), and PAH (polycyclic aromatic compounds represented by the 16 EPA PAH) [5]. The concentration of these compounds in the flared gas increases with increasing NGL, hydrogen sulphide, and other contaminants in the flared gas. The gas flared offshore Newfoundland and Labrador has high levels of NGL, between 12 and 21 % and therefore represents a potential source of these toxic compounds if flared.

PAHs can be transported in the atmosphere over large distances subsequently falling out on the water surface forming global hydrocarbon contamination of the marine environment [6]. In addition, some PAH particles can readily evaporate into the air from surface waters. PAHs can break down by reacting with sunlight and other chemicals in the air, over a period of days to weeks. In terms of human risk, PAH components are frequently associated with human cancers of the skin, lungs, and bladder; however, not all the PAH components are carcinogenic. Lower molecular weight aromatics are less toxic to aquatic organism than higher molecular weight. The degree of toxicity is related with the ability of bioaccumulation of the compound. The bioaccumulation increases with molecular weight of the compound. Although some of PAHs toxicities may be low, their toxicities are additive and aquatic toxicity may occur when they are combined [7].

1.3 Objectives of Study

The purpose of this thesis is to propose an alternative process to recover NGL from the associated gas produced in Newfoundland and Labrador platforms. After evaluating different alternatives, membranes are proposed as a possible option to implement in this area. The intention of this research is to provide a clear understanding of the performance of membranes to recover NGL. In addition, separation of the NGL from the produced gas could be used to increase the crude oil production on offshore through the recovery of heavier hydrocarbons from the associated gas. Thus, membranes are introduced into a three-stage separation train of an offshore platform, and the efficiency of the process to improve the crude oil production is evaluated.

1.4 Scope of Study

Based on a recent study two companies were identified to have commercially implemented membranes for natural gas treatment offshore: Membrane Technology and Research Inc. (MTR) [8] and Borsig Membrane Technology [9]. The membranes are used for different applications such as separation of propane plus (C_3^+) components, decrease water dew point and hydrocarbon dew point, prevent liquids in pipelines, reach pipeline gas specifications, and Fuel Gas Conditioning (FGC) for Gas Engines and Turbines [8-9]. Limited information is presented about the performance of the membrane in the previous applications mentioned. MTR proposes membranes to improve the crude oil production; however, they do not provide detailed information. This research intends to provide a complete overview of the efficiency of the membranes to recover heavier hydrocarbons from associated gas. Due to the unavailability of membrane data, some assumptions need

to be considered. The permeabilities of all components are assumed constant along the membrane as they either do not significantly influence results and/or the data are not published as it is the case pentanes and heavier hydrocarbons (C_5^+). For the same reason, the variability of the permeabilities of the components with respect to pressure is not included in the analyses. In addition, as the selected membrane material is more attractive to heavier hydrocarbons, it can be assumed that the permeabilities of the heavier hydrocarbons are significantly larger than the permeability of butanes (we assumed a factor of ten times the permeability of butane for all heavier than butane components).

1.5 Thesis Outline

The thesis is divided into seven chapters. Chapter 1 provides an introduction to the situation in the Newfoundland and Labrador offshore with respect to the NGL recovery. In Chapter 2, several alternative processes to recover NGL such as turbo-expander, absorption, adsorption, external refrigeration and membranes are reviewed and evaluated. After evaluating the main advantages and disadvantages of each of recovery techniques, membranes separation technologies are proposed as a possible alternative to implement in Newfoundland and Labrador offshore. In Chapter 3, a general introduction to membranes is given. The different arrangements adopted by the membranes are presented, and also the most common membrane materials used are discussed. In Chapter 4, four membrane models are presented; two co-current and two counter-current models. The main characteristics of each model are explained. Both co-current models as well as counter-current models are compared. In this chapter, the models based on discrete equations are recommended. In Chapter 5, membranes were introduced into a typical separation train

on an offshore platform to determine the efficiency of the membranes to recover NGL. The recovery of NGL is evaluated as a function of pressure, composition, feed process temperature, flow pattern (co- vs. counter-current) and location within the process. These effects are studied for the recovery of C_3^+ as well as ethane plus components (C_2^+). In Chapter 6, the analysis is extended to evaluate the impact of the membranes on the production of crude oil. Membranes are located at various locations within the process, and their permeates and/or residue streams are recycled. Twelve alternative configurations of the original process are investigated in this chapter. In Chapter 7, summaries of the thesis together with the conclusions reached are presented. In addition, recommendations for future work are provided.

CHAPTER 2

ALTERNATIVES TO OFFSHORE NGLS RECOVERY

In this chapter, the feasibility of recovering NGLs in Newfoundland's offshore platforms using different technologies including turbine expansion, adsorption, refrigeration, and membranes is investigated. The type of technology is limited by the space on the platform, chemical and operating requirements, and environmental impacts. After evaluating the main advantages and disadvantages of the different processes, membranes separation technologies are proposed as a possible process for offshore NGL recovery.

2.1 External Refrigeration/Cryogenic Processes

2.1.1 General Characteristics

In external refrigeration, natural gas is partially liquefied by means of a refrigerant. The liquid generated and the gas are separated in a later stage. In order to recover high levels of ethane and propane (deep-cut recovery), very low temperatures (below $-50\text{ }^{\circ}\text{C}$) are required. For this, cascade refrigeration or mixed refrigerant systems is required. A mixture of refrigerants such as propane and ethane or propane and ethylene is used instead of single pure refrigerant in cascade systems. Deep-cut systems can typically reach a minimum of 50 to 60% recovery for C_2^+ and in excess of 85 to 95% of C_3^+

this process involves several pieces of equipment, which requires a high maintenance cost and a high utility requirement. Propane refrigeration becomes inappropriate for feed throughputs of less than 25 million standard cubic feet per day (MMSCFD) [8].

For deep-cut recovery purposes, the amount of CO₂ in the feed must be as low as temperatures of the process can cause freezing of CO₂. In addition, if the feed gas contains a large amount of inert components, the efficiency of process will be reduced due to the interference of the inert.

2.2 Turbine expansion

2.2.1 General Characteristics

A turbo expander reduces the pressure of a gas stream by means of expansion. As a result, the temperature as well as the enthalpy of the gas is reduced. Work is obtained as a by-product, which can be used to compress the gas in a later stage.

The temperature drop results in condensation of the heavier hydrocarbons. The condensate recovery is a function of the composition of the gas, and final pressure and temperature. Depending on the inlet pressure of the gas, a turbo expander can reach cryogenic temperatures, close to -65.6 °C or even lower. These low temperatures permit recovery of about 75 to 80 % of ethane [13]. The gas flow rates can be up to 8.5 or 11.33 million standard cubic meters per day (MMSCMD) (300 or 400 MMSCFD) at 3,550/4,250 kPa. The compression horsepower requirement can vary from a few to several thousands horsepower.

In a typical turbo expander process, the inlet gas is cooled with the residue gas or with the liquids in the reboiler of the de-methanizer tower [13]. The cooled gas is

Variation in pressure and composition of the gas can significantly affect the operation of the turbo expander [12]. Another disadvantage of this process is the height required for the de-methanizer tower. The installation of an elevated tower is extremely difficult on offshore plants and could also present operational problems due to the common strong winds in the sea, especially in the Atlantic Canada. When ethane is not recovered, the height of the tower is reduced. Another drawback is the lack of tolerance to wet gas in the feed since it can damage the mechanical system. Nevertheless, a certain amount of liquid can be managed in the exit of the equipment. Another important limitation of the turbo expander is the elevated maintenance cost. In addition, the operation of this equipment represents a major issue in terms of safety.

2.3 Absorption

2.3.1 General Characteristics

Lean oil absorption is one of the processes to separate the heavy components from natural gas. A liquid hydrocarbon solvent (oil) retains the heavy hydrocarbon components in an absorber column. The lean oil is sent to a distillation column to recover the NGL components and recycle the oil. In order to improve propane recovery, lean oil and natural gas are chilled before entering the absorber. Recovery is enhanced by low temperature, high pressure, and low molecular weight oil [13]. Figure 2.3 outlines a typical absorption process.

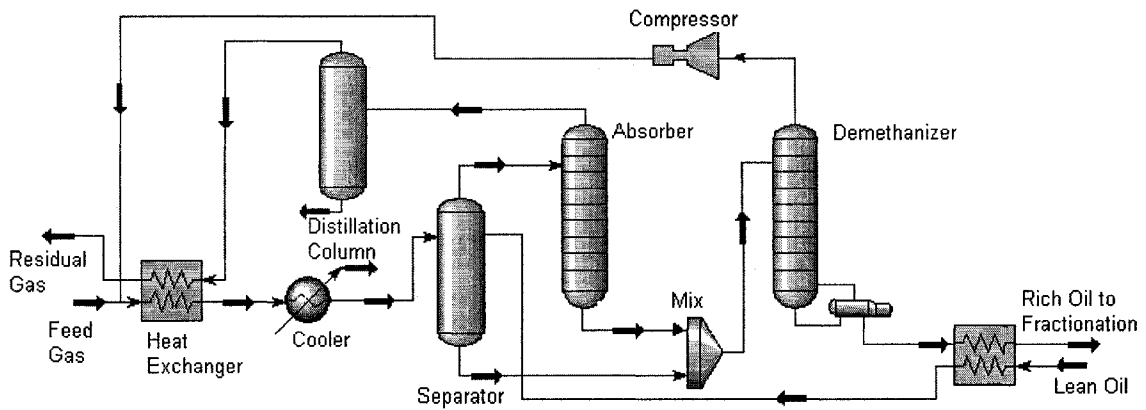


Figure 2.3: Schematic flowsheet of a basic Absorption process

2.3.2 Advantages and drawbacks

This process is selective to propane, and a low ethane recovery is achieved. The process can be used for feed gases containing CO_2 since the minimum temperature within the process is above the freezing point of even pure CO_2 . Inert gases in the feed gas do not interfere with the process of the absorption of the hydrocarbon and pre-treatment of the gas is not needed. This is also true for feed gas with water.

For offshore applications, the height of the distillation column must be restricted because wind in open sea can cause serious damage. Some areas are extremely windy, and this factor needs to be considered in the design of the equipment on platform. For the case of associate gas treatment, this process is rarely used [13]. There are also the possible environmental impacts of chemical use including spills, storage of virgin/waste oil, etc.

For feed pressures below 2,800 kPa absorption systems operate well, but for higher pressures a dual pressure absorber column with high and low pressure sections is

required. Above 8,500 kPa the efficiency of the absorption system will be reduced. The efficiency of the absorption process is improved with rich gases. In the cases of lean gases solvent make up is required due to solvent evaporation. The absorption systems also suffer from the high-energy costs needed to run solvent circulating pumps and also regeneration of oil.

2.4 Adsorption

2.4.1 General Characteristics

In this process, heavy hydrocarbons are removed by means of the adsorption over a solid. In general, silica gel is used as the adsorbent. The heavy components of the natural gas are adsorbed and condensed over the surface of the silica gel. Heated recycled or bypass gas is employed to regenerate the solid at temperatures around 250-280 °C. After that the adsorbent is cooled to ambient temperature for later use. The heavy hydrocarbons are recovered after cooling in a separator.

2.4.1 Advantages and drawbacks

An adsorption process requires enormous amount of energy due to the regeneration process. In addition, the equipment involved is heavy and expensive, which is unattractive for offshore plants. Safety is a considerable issue for this process since the high temperature with the hydrocarbon solids could produce a fire or related accident.

2.5 Membranes Separation Technologies

2.5.1 General Characteristics

Gas separation membranes are made of polymeric materials. Membranes separate gas mixtures due to the different permeate rates of the components. The driving forces for the separation are the difference in the partial pressure of the components over feed and permeate side of the membrane.

The basis of membrane separation is in the differences in dissolution and diffusion of the gases through the membrane. In glassy polymers (rigid polymers), the gas diffusion coefficients determine the selectivity of the membrane; thus, these membranes permeate small molecules and reject higher hydrocarbons. In rubbery polymer membranes the separation is a function of solubility. Thus, gas solubility coefficients determine the selectivity in rubbery membranes, permeating higher hydrocarbons and rejecting methane and small molecules. Figure 2.4 outlines gas flow in a membrane.

In the separation of heavy hydrocarbons from light gases (methane), rubbery polymer membranes are used. The heavy hydrocarbons are collected over the low-pressure side of the membrane (permeate) and the light gases remain on the high-pressure side (residue). The main applications of this separation are: NGL recovery, dew-point control for associated natural gas, and fuel gas conditioning for engines [8]. In the case of processing associated gas from oil production facilities, the incorporation of membrane into the process could increase the oil production up to 5 % by re-injecting the NGLs back into oil with only small compression requirements [8]. However, membranes separation processes are adequate for small to medium size production, around 10 to 100

MSCFD, since beyond these values the cost of the membranes process becomes prohibitive.

The selectivity of the membrane (ratio of permeabilities) together with operating conditions (temperature, pressure, flow rate), determine the efficiency of the separation of gas components.

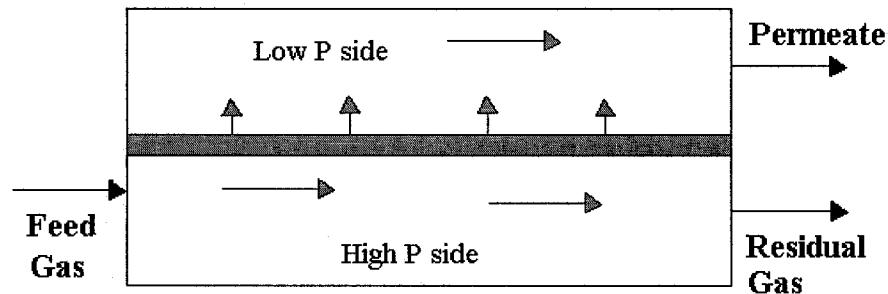


Figure 2.4: Schematic of a membrane

2.5.2 Advantages and drawbacks

Membranes require smaller space and are relatively light, which are desired characteristics for offshore applications. In addition, membranes typically have lower installation, operation, and maintenance costs compared with other technologies. For example, the installed cost to treat 10 MMSCFD of lean gas (3.9 GPM, 1185 Btu/SCF) for a membrane system is \$1.1 million while for propane refrigeration system is \$1.6 million. In addition, the relative processing cost (which includes capital cost) for membranes compared to propane refrigeration is 0.594 [8]. Additionally, membranes are operationally simple and do not require additional separation agents. The principal operating cost is the replacement of the polymeric membrane element [14]. Another advantage of membrane is the flexibility of its operations. This means production

conditions can be modified, and the membrane process can be easily adapted to it. The membranes are arranged in modules, which can be orientated in horizontal or vertical positions. However, the membrane separation technologies are appropriate for small to medium production, around 10 to 100 MSCFD since beyond these values the cost is prohibit.

2.6 Comparison of the Alternatives and Possibilities of installation in Newfoundland's Offshore

To study the possibility of recovering NGL components in Atlantic Canada's production platforms several processes were analyzed including: turbo-expander, absorption, adsorption, external refrigeration and membranes.

The criteria used to select a possible process to be implemented to recover NGL's on offshore included the following: inlet gas heavier hydrocarbon content in the gas, inlet gas pressure, gas flow rate, product recovery percentages, CO₂ content in the feed gas, space occupied for the equipment, process equipment weight, equipment maintenance, utilities required, and capital and operational costs.

The selection of the process is also affected if ethane is to be recovered. When ethane recovery is not feasible due to low levels in the feed gas, some processes become more attractive than others. For example, absorption processes have high selectivity to propane components and poor selectivity to ethane. In addition, for propane plus (C₃⁺) recovery, CO₂ freezing will not be a problem since the temperatures are above the freezing point.

Since the natural gas present in Newfoundland is relatively rich in heavier hydrocarbons (C_2^+) (see Appendix C for a typical gas composition in this area) with low amount of inert gases and moderate amount of CO_2 (between 1 and 2 %), NGL recovery can be significant. The amount of ethane plus (C_2^+) that can be recovered at the Hibernia production platform is 1,382 m^3/d .

The objective of this work is to recover propane plus hydrocarbons. In general the reservoir pressures in Newfoundland are high. The recovery of ethane plus requires distillation processes, and in general this conduces to a large facility, which produces a large cost. In the case of the Hibernia platform, the well pressure is around 39 MPa (5,700 psia), which is one of the highest in this area, and the flow rate of the associate gas is approximately 290 MMSCFD [15]. Considering these conditions and the composition of the natural gas in this area, absorption and adsorption processes are not suitable. These two processes occupy a large area, consume large amounts of energy, and operations are difficult in offshore.

The high inlet pressure of the gas favours the use of the turbo expander process; however, turbo expanders are more efficient for lean rather than rich gases. As the amount of heavy hydrocarbons C_5^+ increases the turbo expander process becomes less attractive [16]. The application of external refrigeration on platforms is less attractive due to the large area, heavy weight and large energy consumption. Although membranes are new technologies and they have not been proved extensively in the offshore, they present some attractive features. When membranes are compared to other separation technologies advantages such as low energy consumption, mild operating conditions, no environmental pollution, process continuity and flexibility, easy scalability, space saving and modular

plant design are apparent [17]. However, the long-term stability of the membranes and material is an issue, as permeabilities will vary in the long-term operation.

CHAPTER 3

APPLICATION OF MEMBRANES IN NATURAL GAS PROCESSING

In this chapter a brief description of membranes and their use in the natural gas processing industry, natural gas liquids (NGLs) recovery in particular, is given. Then, different membrane configurations are discussed including; flat membranes, hollow fiber membranes and spiral membranes. In this study, heavier hydrocarbons (NGL products) are separated from methane. In this application, nonporous membranes are required. Therefore, nonporous membranes are described in more detail and compared with porous membranes

3.1 Membrane description

A membrane is a thin barrier in contact with two phases, which could be two liquid phases; two gas phases; or a liquid and a gas phase. Driving forces such as pressure or concentration induce the transport of molecules through the membranes. For example, a differential pressure across the membrane can facilitate the separation of gases. The transport is a non-equilibrium process, and the separation of the components is due to different mass transfer rates through the membrane [18].

In general, polymeric membranes have been employed for gas separation in industrial applications. The factors that determine gas separation in polymeric membranes are: permeability and selectivity. Permeability and selectivity are described in the Equations 3.1 and 3.2, respectively. Permeability (P) is defined as the solubility (S) times the diffusivity (D). Selectivity (α), which is a thermodynamic parameter, provides a dimension of the penetrant sorbed in the membrane under equilibrium conditions. Diffusivity, which is a mass transfer parameter, provides information about how quickly the penetrant cross the membrane. [19]

$$P = S \times D \quad (3.1)$$

$$\alpha = \frac{\text{Permeability of component A}}{\text{Permeability of component B}} \quad (3.2)$$

3.2 Gas Membrane Systems

Different membrane arrangements are used in the industry. The most common are: flat membranes, spiral-wound membranes, and hollow-fibre membranes [19].

3.2.1 Flat membranes

The flat plate arrangement is not commonly applied in the industry because of the large surface required and resulting high costs. Flat membranes are used to determine permeabilities of membranes at laboratory scale.

3.2.2 Hollow fibre membranes

Hollow fibre membranes are membranes with very small diameters. The internal diameter is in the range of 100-500 μm and the external diameter in the range of 200-1000 μm . When the internal diameter of the fibre is very small, the chances of plugging

of a hollow fibre membrane are very high. The length of the fibre averages from 3 to 5 m. The packing density of a hollow fibre membrane is very high and membranes are arranged in a compact form, which produces a membrane area per unit volume of up to $10,000 \text{ m}^2/\text{m}^3$. Typically, an industrial permeator is 0.15 m in diameter and 3 m long with fibres of 200 μm and 400 μm internal and external diameter, respectively [19].

Typically the high pressure feed enters the shell side while the permeate gas inside the fibres flows counter-current to the shell side flow and is collected in a container where the fibres terminate. Figure 3.1 outlines a hollow fibre separator assembly.

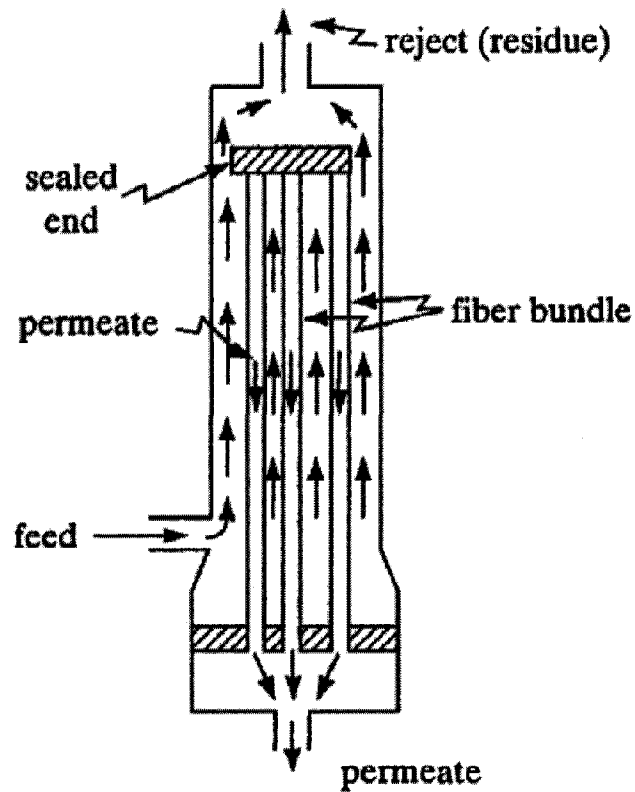


Figure 3.1: Hollow-fibre separator assembly [19]

3.2.3 Spiral membranes

The spiral membranes consist of four parallel sheets around a central perforated core. The sheets starts with a membrane, which is in contact with the central core, then a porous felt backing, followed by a membrane, and finally a top sheet of an open separator grid for the feed channel. The spiral-wound element has a diameter between 100 to 200 mm in diameter and a longitude about 1 to 1.5 m. The sizes of the sheets are about 1-1.5 m by about 2-2.5 m, and the space between the membranes is close to 1 mm. A metal shell recovers the spiral [19].

The feed gas enters at the left side of the spiral and then flows to the other end. The permeate flows perpendicular to the membrane, and it is collected in the perforated tube located in the center of the spiral. Figure 3.2 outlines a spiral-wound element and assembly. In addition, Figure 3.3 outlines the local gas flow paths for the spiral-wound separator.

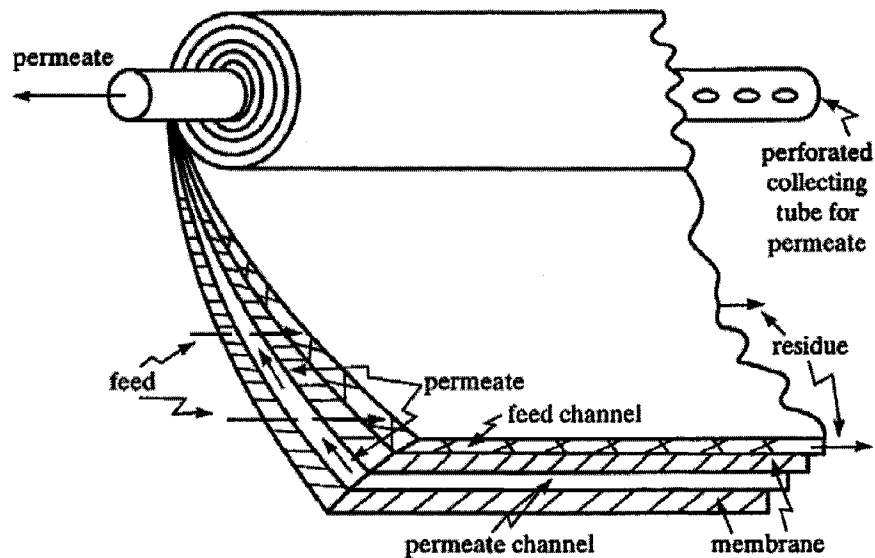


Figure 3.2: Spiral-wound elements and assembly [19]

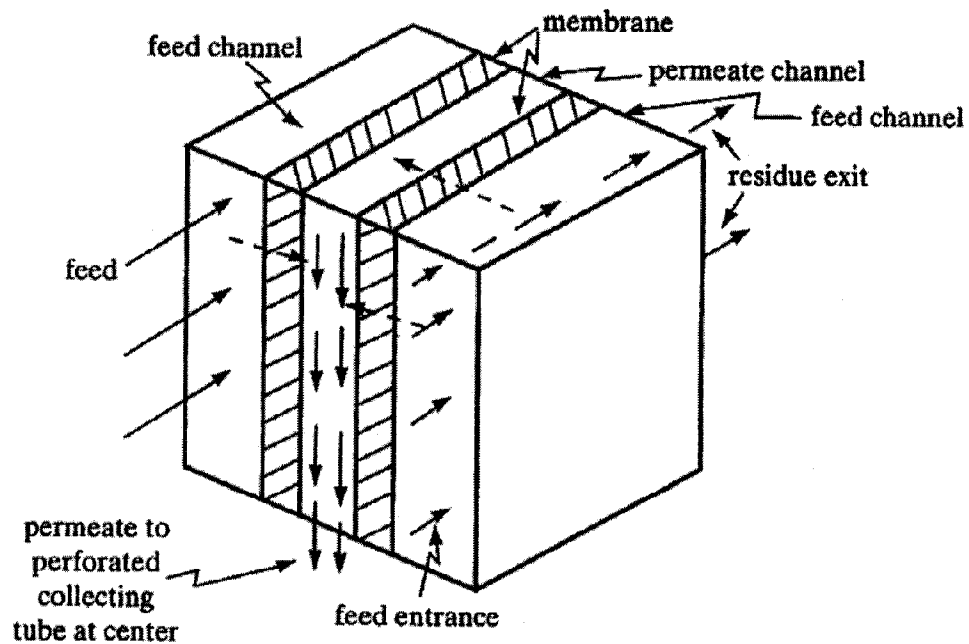


Figure 3.3: Local gas flow paths for spiral-wound separator [19]

3.3 Classification of membranes

Membranes fall into two classes: porous and nonporous. Porous membranes act as an ordinary filter; as a result, molecules are separated by micro-porous membranes according to their sizes. The separation is a function of the permeate and the membrane properties (i.e. molecule size, and pore size and distribution). These membranes are described by the average pore diameter, the membrane porosity, and the tortuosity of the membrane.

Nonporous membranes separate the gas components according to the solubility in, and diffusion through the membrane. Molecules of similar size can be separated by means of nonporous membranes. The main characteristic of nonporous membranes is their high selectivity but the permeate (recovery) rates are low.

The objective of this work is to recover the heavy hydrocarbon components of the natural gas (NGLs) from methane. Nonporous membranes are selected for this application due to the similarity in size of some of the components of the natural gas (i.e. methane and ethane), which cannot be separated by means of porous membranes. In addition, some specific nonporous membranes have a high solubility to heavy hydrocarbons. Thus, heavy hydrocarbons cross the membrane to the low-pressure side leaving methane and the lighter gases on the high-pressure side. This is convenient since the methane will remain at high pressures allowing transport as a compressed natural gas at lower cost.

3.4 Transport of gases through nonporous membranes

The transport of gases through a nonporous or dense polymeric membranes is by the solution-diffusion mechanism [18]. The permeate dissolves into the membrane on the high-pressure side, and flows through the membrane to the low-pressure side. Separations are a result of the different thermodynamic activities of the components and membrane and permeate interaction forces. Thus, a concentration gradient is formed between both sides of the membrane.

The solution-diffusion mechanism occurs in three steps [18]:

- 1) absorption or adsorption at the high pressure side boundary,
- 2) dissolution and diffusion of the components sorbed through the membrane,
- 3) desorption or evaporation of the components on the low-pressure side of the membrane.

This model assumes that the pressure inside the membrane is homogeneous, and that the chemical gradient transverse to the membrane is a concentration gradient.

3.5 Nonporous membrane materials

The membrane material chosen is critical for the efficient separation of the heavier hydrocarbons from methane. Materials may suffer from: a weak selectivity of the polymers to individual hydrocarbons, a degradation of the mechanical properties of the material with time (plasticization of the material), and a reduction in selectivity due to the heavier hydrocarbons condensation on the membrane surface [20].

In general, for this type of application rubbery or glassy polymers are used. Rubbery polymers permeability coefficients increase with molecular weight, while glassy polymer permeabilities decrease with molecular weight. For example, if having methane on the permeate stream is necessary, glassy polymers are used. The differences in gas permeabilities may be small depending on the selected membrane material and therefore proper selection is key.

The general transport mechanisms for rubbery and most glassy polymers are similar. In general, the mixed gas selectivity is lower than the pure gas selectivity. The pure gas selectivity is the ratio of the permeabilities of the pure components with respect to a specific material, while the mixed gas selectivity is the ratio of the permeabilities of mixed components in the mixture. The solubility coefficients govern the separation for mixtures. The reason is due to the swelling of the silicones when vapours are sorbed, which reduces the attraction between the chains resulting in an increase in the free volume. Consequently, the species find a lower transport resistance through the polymer. In other words, when butane or other larger species are sorbed into the polymer, the free volume is increased, and methane or other small molecule transportation through the rubbery polymer is favoured [21].

Common types of membrane materials are described below:

Polysiloxanes copolymers (Silar and carbosil) polymeric membranes: It is a rubbery polymer with a higher permeability for heavier hydrocarbons compared to methane. A study with these materials indicated a dependence of the permeability coefficients of the heavier hydrocarbons on pressure. As pressure increases so does the permeability to heavier hydrocarbons while permeability of methane remains constant [20].

Polyphenyleneoxide (POP) and PPO-based copolymers: These materials are glassy based polymers, and they are appropriate for separation of alkanes and alkenes. The permeability difference is based on the different diffusion coefficients. Alkanes have larger diffusion coefficients than alkenes in the PPO-based polymers [22].

Polyoctylmethylsiloxane (POMS): This material is a silicone derivative from PDMS (Polydimethylsiloxane) where some of the methyl-groups have been changed by C₈-side-chains. A study Schultz and Peinemann showed that POMS is one of the most selective rubbery polymers to separate butane from methane. However, the permeability is highly dependent on the total feed pressure, especially for heavy hydrocarbons. The permeability is reduced as the total feed pressure increases. Further as the pressure increases swelling is induced in POMDs, which reduces the transport resistance. At the same time, due to the softness of the material, the compression increases the density resulting in an increase in transport resistance. Clearly, compression is the predominant of these two effects [21].

Polytrimethylsilylpropyne (PTMSP): It is a glassy polymer but it differs from the typical behaviour of glassy polymers. This polymer has a high selectivity for large and condensable hydrocarbons in the presence of low molecular weight gases such as methane or nitrogen. This particular behaviour is due to the fact that PTMSP has a large fractional free volume, above 25 %, and it results in unusual gas permeation properties [23].

PTMSP has the highest n-butane permeability and the highest n-butane/methane selectivity compared to any other known polymer [23]. It has been observed that the total feed pressure does not affect the permeability [21]. Instead, the temperature affects permeability coefficients; as temperature increase the permeability coefficients [24].

In a study by Schultz and Peinemann [21], a binary mixture of butane and methane was separated using this membrane material. As the fraction of butane in the feed increased the selectivity of butane with respect to methane increased. The possible reason could be due to a plugging of the pore by the condensed butane. PTMSP is one of the polymers that show the highest selectivities and permeabilities with respect to heavy hydrocarbons. The disadvantage of this polymer is that permeability decreases by one order of magnitude in the three first months and then it stabilizes [21].

Polydimethylsiloxane (PDMS): This material has satisfactory vapour/gas selectivity for several applications. Also, it has good chemical resistance and can be fabricated into thin film composite membranes. An investigation by Pinnau [25], using n-butane/methane and hydrocarbon/hydrogen mixtures, studied the influence of feed composition and temperature on permeation properties. In this study, as the proportion of heavy

hydrocarbons increase at constant feed pressure and temperature, the permeabilities of all components also increases. The vapour components produce a swelling of the polymer, which resulted in higher diffusion coefficients of all penetrants. As the component size of the penetrant increases, the permeability increases. As a result, the selectivity increases when the vapour concentration in the feed is larger [25].

AF1600: This is a glassy copolymer composed of 65 % mol of 2,2-bis(trifluoromethyl)-4,5-difluoro-1,3-dioxole (BDD) and 35 % mol tetrafluoroethylene (TFE). As any glassy polymer, the permeability coefficients decrease as the size of the penetrant molecule increases. In addition, the permeability of the hydrocarbons varies with the pressure except for lighter gases, which are independent of the pressure. As the number of carbons increases a strong dependence with the pressure is observed starting at ethane. The temperature also affects the permeabilities with an increase in temperature producing an increase in permeation rates of all the components except carbon dioxide (CO₂) [24].

Polypermethylsilalkylenes: This is new polycarbosilane polymer that results from different substitutions at the silicon atom. This material separates hydrocarbon mixtures according to solubility-control mechanism [26].

CHAPTER 4

COMPARISON OF MEMBRANE SEPARATION MODELS

In this chapter, different steady state models are compared for two flow patterns: co-current and counter current flows. Two co-current flow models are presented, and compared. Then, two counter-current flow models are presented and explained. The advantages and disadvantages of each model are presented in terms of computational difficulty and the most appropriate model is determined.

4.1 Co-current Flow Models

4.1.1 Model based on differential equations

The first co-current (steady state) flow model is based on the set of differential equations derived for a membrane module for multi-component gas separation. For this set of equations the following assumptions apply: the rates of permeation follow Fick's law, the effective membrane thickness is constant, concentration gradients in the permeation direction are negligible, pressure drops of the feed and permeate gas streams are negligible, and plug flow exists in the feed and permeate streams. Figure 4.1 outlines a single permeation stage for this model [27].

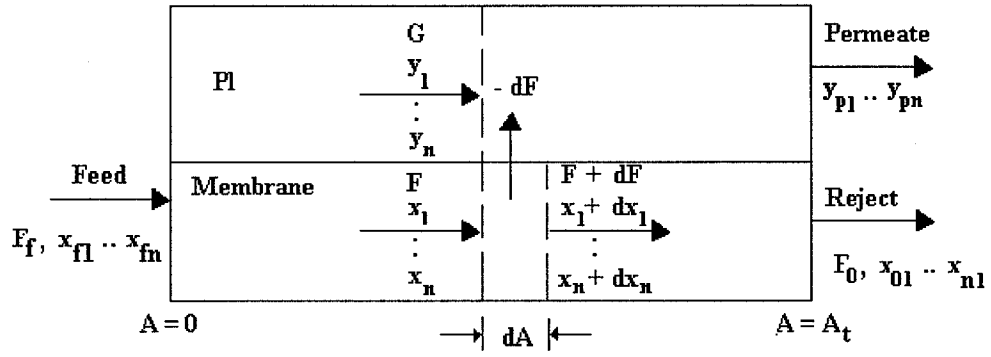


Figure 4.1: Single permeation stage of the co-current model [27]

The overall material balance is generated over a differential area dA , and it corresponds to Equations 4.1 and 4.2 as follows:

$$-dF = dG \quad (4.1)$$

$$-dF = dA \sum_{k=1}^n \frac{Q_k}{\delta} (P_h x_k - P_l y_k) \quad (4.2)$$

The material balance for component “ i ” is indicated in Equations 4.3 and 4.4:

$$-d(x_i F) = d(y_i G) \quad (4.3)$$

$$-d(x_i F) = dA \frac{Q_i}{\delta} (P_h x_i - P_l y_i) \quad (4.4)$$

Where, F is the flow rate on the feed (high-pressure) stream; G is the flow rate on the permeate (low-pressure) stream parallel to the feed stream; n is the number of gaseous components; P_h and P_l are the pressure on the feed side and the permeate side, respectively; Q_i is the permeability of component i ; δ is the membrane thickness; and x_i and y_i are the mole fractions of component i on the feed side and the permeate side,

respectively. Based on material balances the mole fractions are calculated from Equations 4.5 and 4.6:

$$\sum_{k=1}^n x_k = 1 \quad (4.5)$$

$$\sum_{k=1}^n y_k = 1 \quad (4.6)$$

By combining Equations 4.2 through to 4.4:

$$dx_i = \frac{-dA}{F} \left[\frac{Q_i}{\delta} (P_h x_i - P_l y_i) - x_i \sum_{k=1}^n \frac{Q_k}{\delta} (P_h x_k - P_l y_k) \right] \quad (4.7)$$

If Equations 4.1 and 4.3 are integrated from the input point to an arbitrary point, the flow rate and the fraction of “*i*” in the permeate stream are obtained:

$$G = F_f - F \quad (4.8)$$

$$y_i = \frac{x_{fi} F_f - x_i F}{F_f - F}, \quad G \neq 0 \quad (4.9)$$

Where, F_f is the feed flow rate at the input, and x_{fi} is the feed mole fraction of component *i*.

$$y_i = \frac{\frac{Q_i}{\delta} (P_h x_i - P_l y_i)}{\sum_{k=1}^n \frac{Q_k}{\delta} (P_h x_k - P_l y_k)}, \quad G = 0 \quad (4.10)$$

In order to calculate the permeate mole fraction y_i at $G = 0$ (or $A = 0$), the permeate flow rate G is considered zero when the value of the area is zero. Thus the mole

fractions are estimated by the L'Hospital rule as $F \rightarrow F_f$. Solving Equation 4.10 simultaneously for every component, the mole fractions on the permeate stream at $G = 0$ can be estimated.

The mole fraction ratio of two components is expressed in Equation 4.11, and solving for y_j gives Equation 4.12.

$$\frac{y_i}{y_j} = \frac{Q_i(P_h x_i - P_l y_i)}{Q_j(P_h x_j - P_l y_j)} \quad (4.11)$$

$$y_j = \frac{x_j Q_j / Q_i}{P_l / P_h \{(Q_j / Q_i) - 1\} + (x_i / y_i)} \quad (4.12)$$

Replacing the expression of y_j from Equation 4.12 into Equation 4.6 results in:

$$\sum_{k=1}^n \frac{x_k Q_k / Q_i}{P_l / P_h \{(Q_k / Q_i) - 1\} + (x_i / y_i)} = 1 \quad (4.13)$$

Dimensionless variables are indicated in the following equations:

$$s = A \frac{Q_m P_h}{F_f \delta} \quad s_t = A_t \frac{Q_m P_h}{F_f \delta} \quad (4.14)$$

$$f = F / F_f \quad f_o = F_o / F_f \quad (4.15)$$

$$\theta = 1 - f_o \quad (4.16)$$

$$g = G / F_f \quad (4.17)$$

$$\gamma = P_l / P_h \quad (4.18)$$

$$q_i = Q_i / Q_m \quad (4.19)$$

Where, Q_m is the permeability of the base component, usually the most permeable component; F_0 is the flow rate of the reject stream; and θ is the stage cut.

Based on the dimensionless variables the set of equations that describe the co-current flow are obtained from Equations 4.2, 4.5 to 4.9, 4.12 and 4.13.

$$\frac{df}{ds} = -\sum_{k=1}^n q_k (x_k - \gamma_k) \quad (4.20)$$

$$\frac{dx_i}{ds} = -\frac{q_i}{f} (x_i - \gamma_i) + \frac{x_i}{f} \sum_{k=1}^n q_k (x_k - \gamma_k) \quad (i = 1, \dots, n-1) \quad 4.21$$

$$x_n = 1 - \sum_{k=1}^{n-1} x_k \quad (4.22)$$

$$g = 1 - f \quad (4.23)$$

$$y_i = \frac{x_{if} - x_i f}{1 - f}, \quad g \neq 0 \quad (i = 1, \dots, n-1) \quad (4.24)$$

$$\sum_{k=1}^n \frac{x_k q_k / q_i}{\gamma \{(q_k / q_i) - 1\} + (x_i / y_i)} = 1, \quad g = 0 \quad (4.25)$$

$$y_j = \frac{x_j q_k j / q_i}{\gamma \{(q_j / q_i) - 1\} + (x_i / y_i)}, \quad g = 0 \quad (j \neq i, n) \quad (4.26)$$

$$y_n = 1 - \sum_{k=1}^{n-1} y_k \quad (4.27)$$

The co-current model for multi-component flow can be calculated using Equation 4.20 to 4.27. If the feed mole fractions of the components (x_{fi}), q_i , γ , and s_i are known, the mole fractions of the components on the feed and permeate stream at the output (x_{oi} and

y_{oi}) and θ can be calculated. For that, the initial conditions required for these calculations are set are as follow:

$$f = 1, \quad x_i = x_{fi} \quad (i = 1, \dots, n-1) \quad \text{at } s = 0$$

4.1.2 Model based on discrete equations

This is a multi-component (steady state) model that provides a quick solution of the differential mass and pressure distribution in a hollow-fibre gas separation contactor. The numerical solution involves a discretization of the membrane instead of integration through the membrane. The model is based on the following assumptions: negligible pressure changes in the shell and bore side; the hollow fibre consists of a very thin membrane layer on a porous support, all mass-transfer resistance is confined to the membrane or the total membrane wall; there is no axial mixing of the shell or lumen side gases in the direction of bulk gas flow; the gas on the shell side of the hollow fibres and in the lumen is plug flow; the calculation are for a single hollow fibre, and then the results are scaled in proportion to the number of fibres to consider the total gas flow and membrane area; all fibres are of uniform radius and thickness; and the membrane module is operated at steady state. Figure 4.2 outlines a schematic of a module membrane divided into N sections implemented in this model [28].

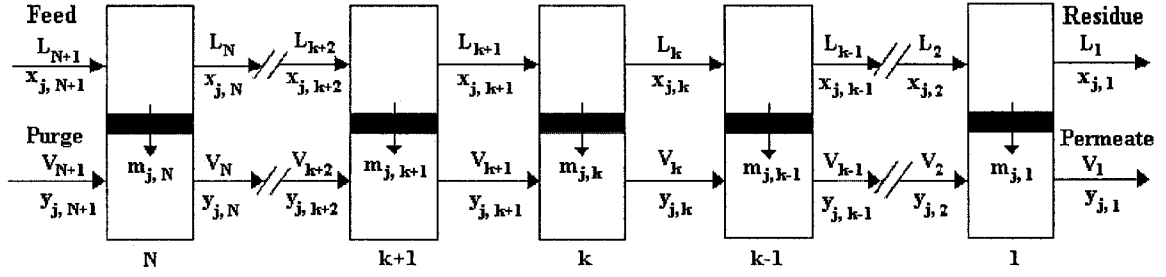


Figure 4.2: Module divided into N sections representing a co-current flow [28]

The hollow fibre is divided into a series of N stages in the axial direction and mass balances are established in each section:

$$\Delta A_k = \frac{2 \pi R_o L N_f}{N} \quad (4.28)$$

where ΔA_k is the area for increment “ k ”, L is the permeating length of the hollow fibres in the module (m), N_f is the number of fibres in the module, and R_o is the outer radius (m) of the hollow fibre.

The feed and permeate flow rates ($l_{j,k}$ and $v_{j,k}$, respectively) of a component j leaving a stage k are given by Equations 4.29 and 4.30:

$$l_{j,k} = x_{j,k} L_k \quad (4.29)$$

$$v_{j,k} = y_{j,k} V_k \quad (4.30)$$

Where L_k and V_k are the total feed and permeate flow rates respectively, and $x_{j,k}$ and $y_{j,k}$ are the mole fractions of component j in the feed and permeate side.

Thus, the total feed and permeate flow rates on stage k are the sum of the component flow rates indicated in Equations 4.31 and 4.32:

$$L_k = \sum_{j=1}^R l_{j,k} \quad (4.31)$$

$$V_k = \sum_{j=1}^R v_{j,k} \quad (4.32)$$

Where, R is the number of components.

A mass balance on stage k for an ideal co-current flow is shown in Equation 4.33:

$$l_{j,k} + v_{j,k} - l_{j,k+1} - v_{j,k+1} = 0 \quad (4.33)$$

The mass flow of component j leaving stage k due to permeation is indicated in Equation 4.34:

$$m_{j,k} = l_{j,k+1} - l_{j,k} = Q_j \Delta A_k \left(P_L \frac{l_{j,k}}{L_k} - P_V \frac{v_{j,k}}{V_k} \right) \quad (4.34)$$

Equation 4.34 is arranged to display an expression for the permeate flow of component j leaving stage k , and this new expression is indicated in Equation 4.35:

$$v_{j,k} = \left(\frac{V_k}{Q_j \Delta A_k P_V} + \frac{P_L V_k}{P_V L_k} \right) l_{j,k} - \frac{V_k}{Q_j \Delta A_k P_V} l_{j,k+1} \quad (4.35)$$

Combining Equations 4.33 with 4.35, it can be obtained an expression for the residue flow of component j leaving stage k .

$$l_{j,k} = \frac{v_{j,k+1} + \left(1 + \frac{V_K}{Q_j \Delta A_k P_V}\right) l_{j,k+1}}{1 + \left(\frac{V_K}{Q_j \Delta A_k P_V} + \frac{P_L V_k}{P_V L_k}\right)} \quad (4.36)$$

The calculation starts at the feed module (stage N) and continues stage to stage until the end of the permeator. The calculations of the flow rates of each component on each stage from Equation 4.36 required estimation of the total flow rate. Therefore, the calculation is repeated until the change in component flow rates is within a defined tolerance limit. The limit established is that the differences in the change in the total permeate flow from one iteration to the next does not exceed 10^{-8} .

4.2 Counter-current Flow Models

4.2.1 Model based on differential equations

Figure 4.4 outlines a single permeation stage of this model. The following equations are obtained integrating Equations 4.1 and 4.3 from an arbitrary point to the output, using dimensionless variables [27].

$$g = f - (1 - \theta) \quad (4.37)$$

$$y_i = \frac{x_i f - x_{oi}(1 - \theta)}{f - (1 - \theta)}, \quad g \neq 0 \quad (4.38)$$

This model (steady state) uses almost the same set of equations as in Section 4.1.1 but with some minor differences. Equations 4.20 to 4.22 and 4.25 to 4.27 are used, while

Equations 4.23 and 4.24 are replaced by Equations 4.37 and 4.38. The procedure to solve this model is to guess the residue fraction and θ and integrate from $s = s_t$ to $s = 0$, then the feed fractions and f at $s = 0$ are compared with their actual values. If these values disagree, a new guess is required. This sequence is repeated as many times as required in order to match the values.

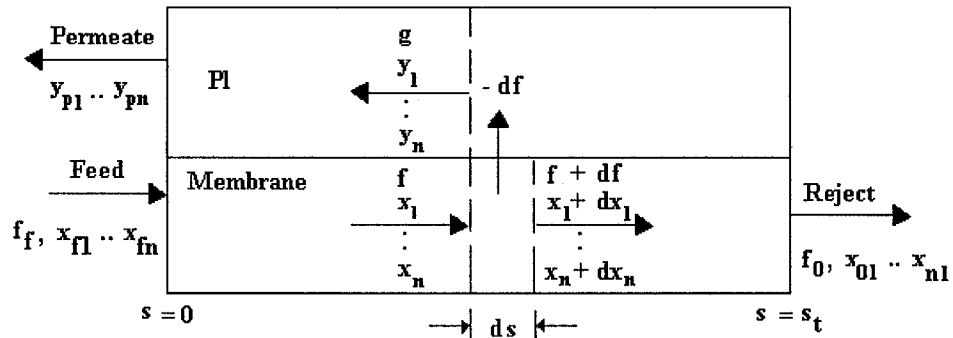


Figure 4.3: Single permeation stage of the counter-current model [27]

4.2.2 Model with discrete equations

This model (steady state) is similar to the model outlined in Section 4.1.2. In this case, the counter-current model involves a more complicated system of equation [28].

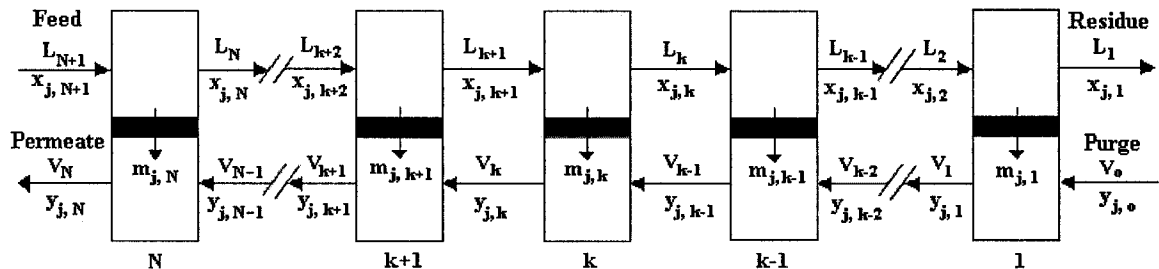


Figure 4.4: Module divided into N sections representing a counter-current flow [28]

A mass balance on stage k for an ideal counter-current flow is shown in Equation 4.39:

$$l_{j,k+1} - l_{j,k} + v_{j,k-1} - v_{j,k} = 0 \quad (4.39)$$

The mass flow of component j across the membrane on stage k due to permeation is indicated in Equation 4.40.

$$m_{j,k} = l_{j,k+1} - l_{j,k} \quad (4.40)$$

The mass flow rate was determined by Barrer et al. [29], Ghosal and Freeman [30], and Graham [31] and it is indicated in Equation 4.41:

$$m_{j,k} = Q_j \Delta A_k (P_L x_{j,k} - P_V y_{j,k}) \quad (4.41)$$

where Q_j is the permeance (permeability divided by active layer membrane thickness) of component j given in unit $kmol/(m^2 s Pa)$, ΔA_k is the area available for mass transfer on stage k (m^2) and P_L and P_V are the feed and permeate pressures.

Rearrangement of the equation produces an expression for the permeate flow rate for component j on stage k , and it is indicated in Equation 4.42.

$$v_{j,k} = \frac{-V_k}{Q_j \Delta A_k P_V} \left[l_{j,k+1} - \left(1 + \frac{Q_j \Delta A_k P_L}{L_k} \right) l_{j,k} \right] \quad (4.42)$$

This equation is combined with Equation 4.39 to eliminate $v_{j,k}$ and $v_{j,k-1}$ and this expression is given in Equation 4.43.

The total feed side flow rate is obtained from Equation 4.31; therefore, the permeate side flow rate at each stage can be calculated by means of a mass balance:

$$V_k = V_{k-1} + L_{k+1} - L_k \quad (4.48)$$

After calculating the flow rate, the coefficients of the matrices are recalculated with these new values. This procedure continues until the flow rates have similar values according to the following criteria:

$$\left| \frac{\Delta L_1}{L_1} \right| < 10^{-8} \quad (4.49)$$

$$\left| \frac{\Delta V_1}{V_1} \right| < 10^{-8} \quad (4.50)$$

where ΔL_1 and ΔV_1 are the difference of the values of total residue flow and total permeate flow from one iteration to the next.

An initial guess of the component flow rates on each stage is required in order to obtain the initial values of coefficients of the matrices. For this initial estimation, a cross flow model is used. In a cross flow model the composition of gas produced on a stage depends only on the upstream compositions, permeances, and upstream and downstream pressures. The cross flow models applied to obtain the initial guesses are Shindo et al. [27], and Geankoplis [33]

4.3 Example for Comparison of the Models

The models were compared to determine both the accuracy and capacity to obtain a solution using software such as MATLAB. The general conditions of the example are illustrated in Table 4.1, and the feed mole fractions and the permeance of the three components are illustrated in Table 4.2.

Table 4.1: General conditions for the example

Conditions	Values
Feed flow rate (m ³ STP/h)	283.2
Area (m ²)	37.7
Feed side pressure (Pa)	1,000,000
Permeate side pressure (Pa)	100,000

Table 4.2: Feed mole fractions and the permeance

Component	Fraction	Permeance (GPU)
a	0.3333	500
b	0.3333	100
c	0.3334	10

* 1 GPU = $10^{-6} \text{ cm}^3(\text{STP})/(\text{cm}^2 \cdot \text{s} \cdot \text{cmHg}) = 7.501 \times 10^{-12} \text{ m}^3(\text{STP})/(\text{m}^2 \cdot \text{s} \cdot \text{Pa}) = 3.346 \times 10^{-13} \text{ kmol}/(\text{m}^2 \cdot \text{s} \cdot \text{Pa})$.

Similar results were obtained between the two-co-current models and between the two counter-current models. The differences lie in the mathematical complexity of each model, the requirement of initial conditions, the method used to calculate the parameters, and in the flexibility of the models.

4.3.1 Co-current Models comparison

In Figures 4.5 and 4.6 the change of the feed and permeated molar fractions along the membrane for co-current flow patterns for the two models presented in sections 4.1.1 and 4.1.2 are shown. From these figures, it can be observed that similar results are obtained with the two models presented; they differ in terms of mathematical complexity.

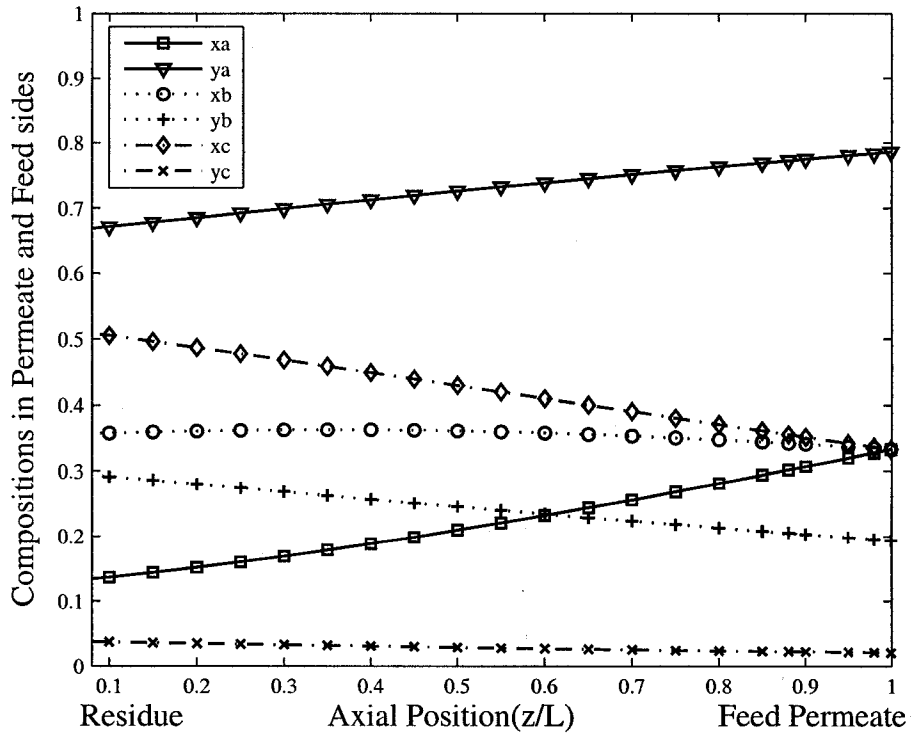


Figure 4.5: Co-current flow for the differential equation model

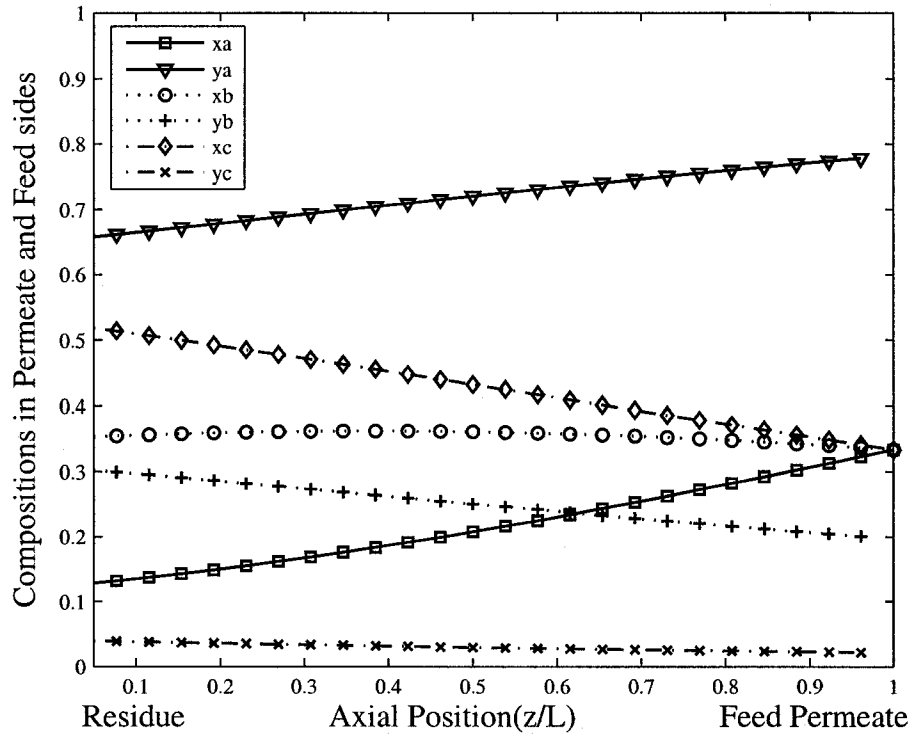


Figure 4.6: Co-current flow for the discrete model

4.3.2 Counter-current Models comparison

In Figures 4.7 and 4.8 the change of the feed and permeated molar fractions along the membrane for counter-current flow patterns for the two models presented in sections 4.2.1 and 4.2.2 are compared. From these figures, it can be observed that similar results are obtained with the two models presented; they differ in terms of mathematical complexity.

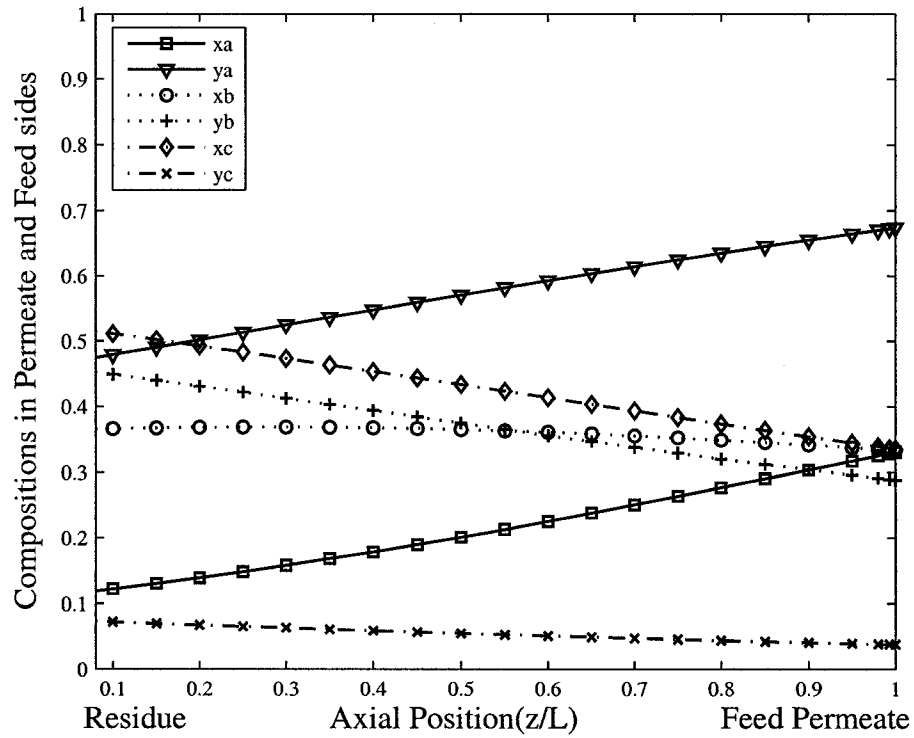


Figure 4.7: Counter-current flow for the differential model

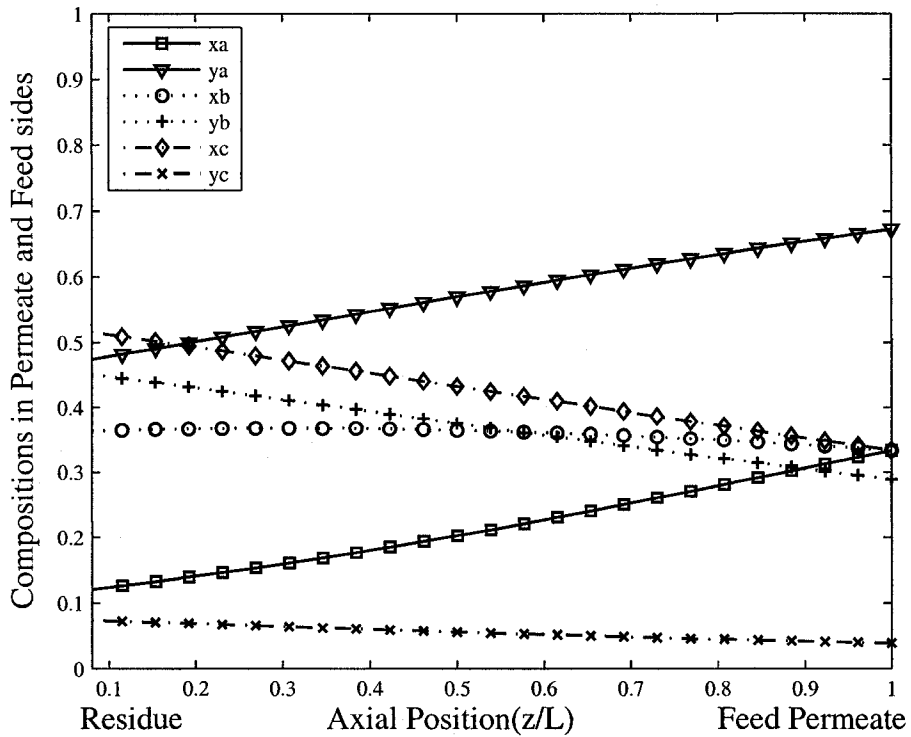


Figure 4.8: Counter-current flow for the discrete model

4.4 Comparison of the Models

The differential equation models are a more complex system of equations, and this is reflected in the mathematical codes for the simulations (see Appendix A). The model requires initial conditions, and for the counter-current model not all of the initial conditions are known. The “guess” required to run the iteration, which must be close to the actual value or the iteration, could give an initial condition that is not correct. This trial and error iteration could result in long and/or variable simulation times. The co-current differential model has similar simulation times as the discrete model. The use of

dimensionless variables presents a problem when a parameter such as area needs to be changed in terms of the simulation code.

The model that proposes discrete equations to solve the membrane performance is a relatively less complex system of equations, and this is reflected in the mathematical codes (see Appendix A). The initial conditions for this model are not as critical as in the previous model, since across the iterations the model converges at the same value. For example, the model simulation was run with initial values obtained from a cross flow model recommended in the literature [27]. Then, the initial feed and permeate flow rate values were assigned with arbitrary values. These arbitrary values were generated by splitting the feed flow rate of the membrane (L_f) into N equal fractions, where N is the number of stage adopted. Therefore, each fraction was the feed and permeate rate for each stage. As a result, the exact same values were obtained in both cases differing only in the number of iterations not in the simulation time. In addition, the solution of the system of equations requires a numerical method such as the Thomas method, but it is simpler in terms of programming than the RungeKutta method used to solve the differential equations. The Thomas method uses an iteration procedure, and it stops the calculation when the difference between two consecutive simulations is within the tolerance. Additionally, this model has good flexibility to changes.

CHAPTER 5

RECOVERING NATURAL GAS LIQUIDS IN ATLANTIC CANADA'S OFFSHORE PETROLEUM PRODUCTION PROJECTS

The recovery of NGL from associated gas has two benefits: recovery of propane plus (C_3^+) and enrichment of the produced oil. Recovery of natural gas liquids (NGL) from natural gas is common in natural gas processing. In some regions, large quantities of the gas produced from crude oil are routinely flared. By recovering the NGL from the produced gas, the toxicity of the flared gas is significantly reduced (ARC paper), as NGL is a valuable product can provide economic benefits [34]. Typically NGL is recovered from natural gas to: produce transportable gas, meet sales gas specifications, or maximize liquid recovery [35]. As outlined in Chapter 2, membranes are an economically feasible option for NGL recovery. The position of the membrane within the separator train will impact the recovery of the NGL and the enrichment of the oil. The purpose of this chapter is to place the membranes in different positions and compare the performance.

This chapter starts with a general description of crude oil and associated gas produced in Hibernia platform. Then, the efficiency of the membranes to recover NGL and optimize oil is evaluated as function of pressure, composition, temperature, flow pattern (co- vs. counter-current) and location of the membrane into the process. These

effects are studied for the recovery of C_3^+ as well as ethane plus components (C_2^+). In order to analyse the efficiency of the membranes into the process, two types of software are used: a process simulator (HYSYS) and a computing tool (MATLAB).

5.1 Crude Oil and Natural Gas in Atlantic Canada

The location selected for this study is the Hibernia platform located offshore of the province of Newfoundland and Labrador. In this area, the natural gas is very rich in NGL (12 to 21 %), does not contain hydrogen sulphide, and contains 1-2% and 0.2% of carbon dioxide and nitrogen, respectively. Oil is produced at 1.955×10^5 bbls/d ($31,084$ $STDm^3/d$) and produced gas is at 290 MMSCFD ($8,184 \times 10^3$ $STDm^3/d$); this translates into approximately 10,968 bbl/d ($1,744 \times 10^3$ $STDm^3/d$) of NGL (C_2^+) [15].

5.2 Process Description

A typical separation train on an offshore platform consists of a series of two- and three-phase separators at different pressures. Figure 5.1 outlines a typical flowsheet for this process. The pressure and temperature of the crude oil before entering the process are based on industry data [8] and set at 6,998 kPa and 35 °C, respectively. The crude oil passes through three separation stages to optimize crude recovery. In the first stage, the crude enters a high-pressure separator (V-100), and gas exiting this separator is rich in methane (~85%). The pressure of the liquids exiting is reduced to typically around 1,700-1,800 kPa and sent to a second separator. In this medium pressure separator (V-101), the associated gas released is still rich in methane (about 72%). A third separator at a lower pressure (V-102) (400-500 kPa) is used to further separate the remaining hydrocarbon

liquids. Our HYSYS simulation indicates that the gas in this stage contains relatively higher concentration of NGL (C_2^+) when compared with previous stages. The composition of methane is smaller compared with the previous two streams, and the molar flow is considerably smaller. In Table 5.1, the base conditions of the input and output streams are shown. The relative percentage of each stream with respect to the initial molar flow of the feed to the first separator (“Wellhead” stream) is shown in brackets. The pressures indicated in the Table 5.1 were selected in order to have a compression ratio for each stage of compression of no more than 4. If the compression ratio exceeds 4 the temperature of the stream could be too high and special material would be required. In most compression applications the maximum compressor discharge temperature that can be reached without causing any operational problem is 150 °C; interstage cooling is provided to bring the temperature back to near ambient before the gas enters the next stage.

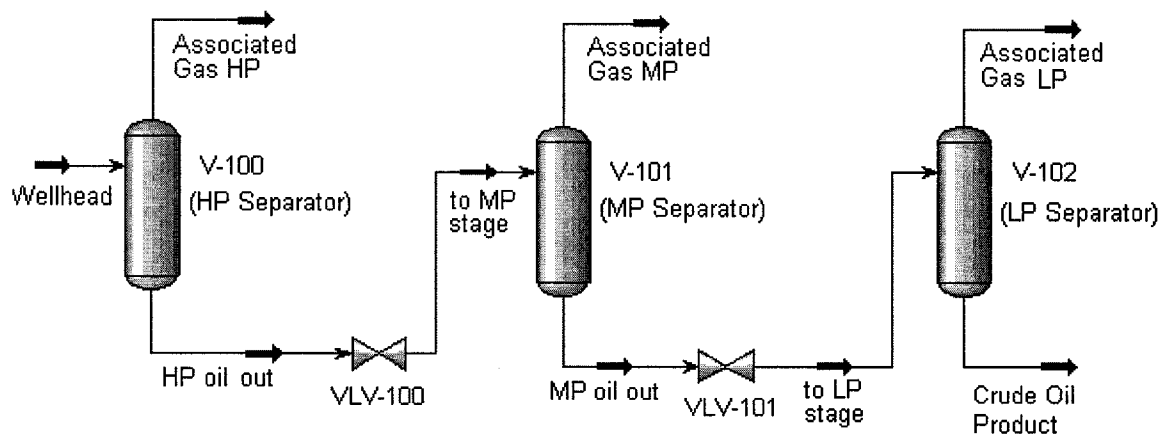


Figure 5.1: Three-stage crude oil separation

Table 5.1: Conditions of input and output streams of the process

Streams	Temp. °C	Pressure kPa	Total Molar Flow kgmole/h	Methane Molar Flow kgmole/h	Ethane Molar Flow kgmole/h	C3+ Molar Flow kgmole/h
“Wellhead” stream	35	6,998	19,979 (100%)	11,349 (100%)	1,273 (100%)	7,145 (100%)
“Associated Gas HP”	42	6,998	11,433 (57%)	9,680 (85.3%)	793 (62.3%)	804 (11.25%)
“Associated Gas MP”	40	1,724	1,868 (9.35%)	1,353 (11.9%)	231 (18.15%)	250 (3.5%)
“Associated Gas LP”	38	414	658 (3.3%)	275 (2.42%)	142 (11.15%)	226 (3.16%)
“Out Oil LP”	38	414	6,020 (30.13%)	41 (0.363%)	107 (8.37%)	5,865 (82%)

5.3 Connection between HYSYS and MATLAB

HYSYS process simulator was used to simulate the crude production and the proposed NGL recovery processes. MATLAB programs linked to HYSYS were developed to predict the membrane efficiency in separating hydrocarbon components out if separated gas in crude stabilization train discussed previously. Process simulators are critical in achieving cost and timesaving during design stages. Simulators such as HYSYS can be used to design and optimize processes systems using well-established routines available within the software package. Computing tools such as MATLAB can be used to model new technologies or modify existing ones. However, MATLAB lacks the extensive thermophysical property and equipment database. The connection between these two software packages leads to an powerful integrated simulation tool for the study of new processes. A simple method to perform a connection of these two powerful programs is through the spreadsheet, which is a unit operation within HYSYS. The

spreadsheet allows complete access to all process variables, and it is extremely powerful with many applications in HYSYS. In general, the spreadsheet is used to perform calculations that are not provided by HYSYS the unit operation such as calculation of pressure drop during dynamic operation of a Heat Exchanger. The spreadsheet has access to any variable by importing them. Any variable in the simulation may be imported virtually into the Spreadsheet. In the same way, a cell's value, such as a calculation result, can be exported to any specifiable input field in the simulation. As a result, all the variables needed for the MATLAB program code can be imported to the spreadsheet. This simplifies the task of reading the variables from MATLAB since the routes toward the variables are not always clear (i.e., number of plates in a distillation column). Figure 5.2 outlines a conceptual schematic of a connection between MATLAB and HYSYS using a spreadsheet [36]. (For further information about the connection of these two programs refer to Appendix B)

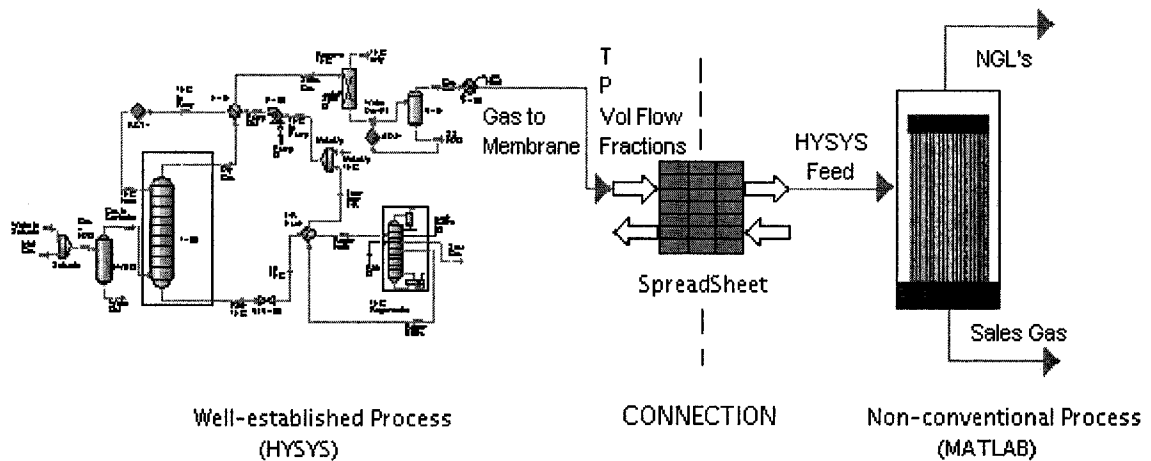


Figure 5.2: Conceptual schematic of a connection between MATLAB and HYSYS using a spreadsheet

5.4 Membrane Process Analysis

The objective of this study is to investigate the optimal configuration of recovery of NGL from the associated gas by means of membranes.

A typical rubbery polymeric membrane, polypermethysilalkylenes, is selected as the membrane material [26]. This material presents a greater permeability for heavier hydrocarbons compared to methane [20]. Thus, the permeate stream of the membrane (low pressure stream) is rich in NGL components, and the residue stream (high pressure stream) is rich in methane.

In order to analyze the efficiency of the process for recovering NGL, membranes are placed in different locations in the separation train, and the results are compared. In Figure 5.3, the locations of the membranes are shown. Each position is studied independently from the others. The temperature and pressure of the feed stream to the membrane in each position are indicated in Table 5.2.

Table 5.2: Conditions of input streams in each position shown in Figure 5.3.

	Position 1	Position 2	Position 3	Position 4	Position 5
Temperature (°C)	38	38	40	40	42
Pressure (kPa)	414	1,690	1,724	6,966	6,998
ΔP membrane	310	1,276	1,310	5,242	5,274

3. Permeate molar flow.

The recovery rates of NGL (C_3^+) are calculated as follows:

$$\text{Recovery } \% = \frac{C_3^+ \text{ amount in permeate stream}}{C_3^+ \text{ amount in "Wellehad" stream}} \times 100 \quad (5.1)$$

The separation factor is calculated as follow:

$$\alpha = \frac{[RH]_p/[CH_4]_p}{[RH]_o/[CH_4]_o} \quad (5.2)$$

where “RH” is any hydrocarbon except methane and “CH₄” refers to methane, while subscripts “o” and “p” refer to the *feed* and the *permeate* of the membrane, respectively.

5.5 Analysis of Recovery of Propane plus components (C_3^+)

5.5.1 Pressure Effect

In the “Associated Gas LP” stream the membrane is placed in Position 1 and the results are compared with those generated where the membrane is in Position 2. In this comparison composition, temperature, and molar flow rates remain constant. In Figure 5.4, the recoveries (%) of C_3^+ and methane loss are plotted against membrane area (which essentially indicates cost and space required for the membrane) for Positions 1 and 2. Methane loss (C_1 loss) refers to the amount of methane that permeates through the membrane (low-pressure side). Since the NGL are concentrated in the low-pressure side

of the membrane the minimum amount of methane is desired to pass through the membrane. The curves of the Figure 5.4 have the same pattern in both positions but are shifted. Thus, for a given recovery of C_3^+ , a larger area is required in Position 1 compared to Position 2. In these two positions the recovery (%) of C_3^+ are higher than the methane loss. Recovery of C_3^+ increases quickly for small areas, and then is constant, while methane loss increases linearly with the area.

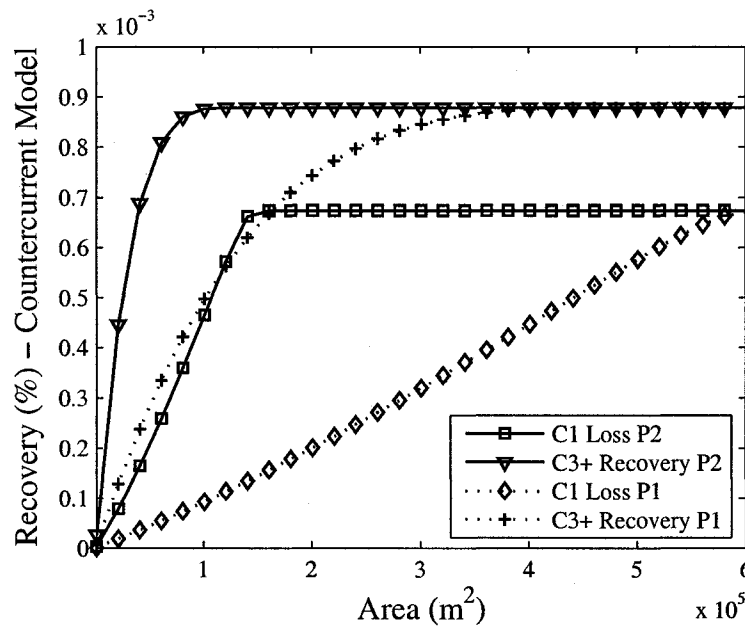


Figure 5.4: Comparison of recovery for Positions 1 and 2

In the “Associated Gas MP” stream the membrane is placed in Position 3 and its results are compared with Position 4. As in the previous case all the parameters except the pressure remain constant. In Figure 5.5, the recoveries (%) of the C_3^+ and methane loss are presented for Positions 3 and 4. The recovery (%) curves for Position 3 are the same shape as the curves for Positions 4 are shifted. Thus, the curves in both positions reach the

same final values but with different areas. The curves of the recovery of C_3^+ and methane loss (with respect to the “Wellhead” stream) are very close for small areas in both positions. As the pressure increases, the loss of methane increases drastically overshadowing the recovery of C_3^+ for large areas, greater than $1 \times 10^5 \text{ m}^2$ and $0.3 \times 10^5 \text{ m}^2$ for Positions 3 and 4, respectively. The recovery (%) curves of C_3^+ also increase relatively quickly for small areas and then approach a constant value for large areas.

These two simulations indicate the pressure increases the mass transfer through the membrane but it does not affect the maximum possible recovery of C_3^+ .

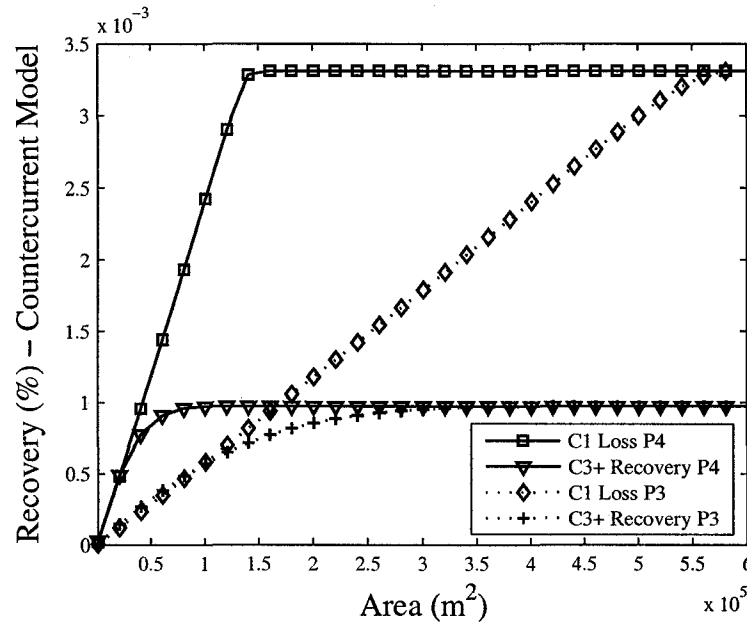


Figure 5.5: Comparison of recovery for Positions 3 and 4

5.5.2 Effect of Gas Composition

In order to evaluate the effect of gas composition, Positions 4 and 5 are compared since their conditions are almost the same, except for the composition and the flow rate.

The recovery (%) curves for C_3^+ and methane loss with respect to “Wellhead” stream for these two positions are presented in Figure 5.6a for a wide range of areas and Figure 5.6b for smaller range of areas. In Position 5, the loss of methane is higher than the C_3^+ recovery for all the area values considered. In Position 4, the recoveries of methane and C_3^+ are similar for small areas, but then for large areas the recovery of methane becomes higher. The shape of the curves for the recovery is similar for both positions. Methane recovery increases linearly until it reaches a constant value, and the C_3^+ curve increases exponentially for small areas and then it reaches a constant value.

The methane loss curves for these two positions are similar for small area values. When the area is close to 15×10^4 m² the methane loss curve for Position 4 reach a constant value, which is the maximum methane loss possible. Instead, the methane loss curve of Position 5 keeps growing after this point since the flow rate in this position is higher than the flow rate of Position 4.

For areas smaller than 8×10^4 m², the recovery (%) of C_3^+ for Position 4 is higher than recovery of (%) of C_3^+ for Position 5, while both positions show the same methane recovery (%). After this point, the recovery (%) of C_3^+ of Position 5 keeps increasing due to the higher molar flow, but the recovery (%) of C_3^+ of Position 4 remains constant, since it is the maximum C_3^+ recovery possible in this position. As a result, a higher concentration in C_3^+ produces a better recovery of them. For example, for an area of 30,000 m² the recovery of C_3^+ and methane for Positions 4 and 5 are 0.6×10^{-3} and 0.35×10^{-3} , respectively.

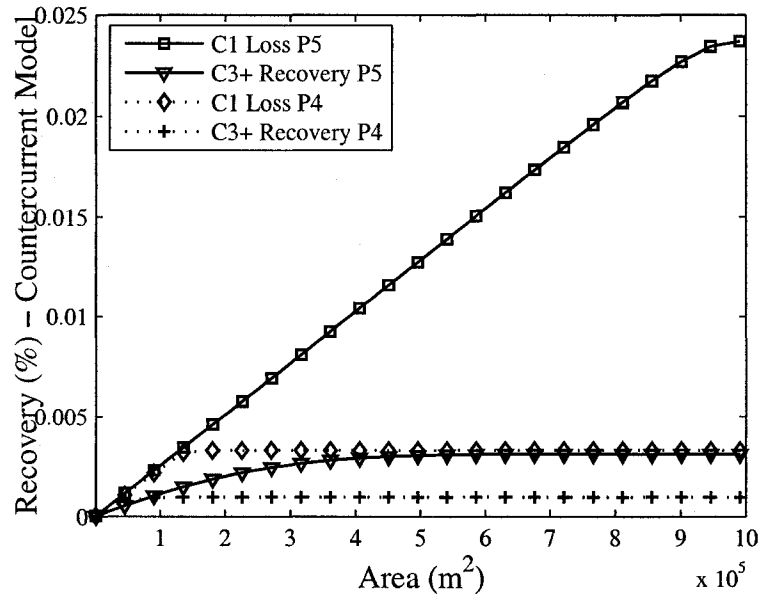


Figure 5.6a: Comparison of recovery for Positions 4 and 5 for wide range of areas

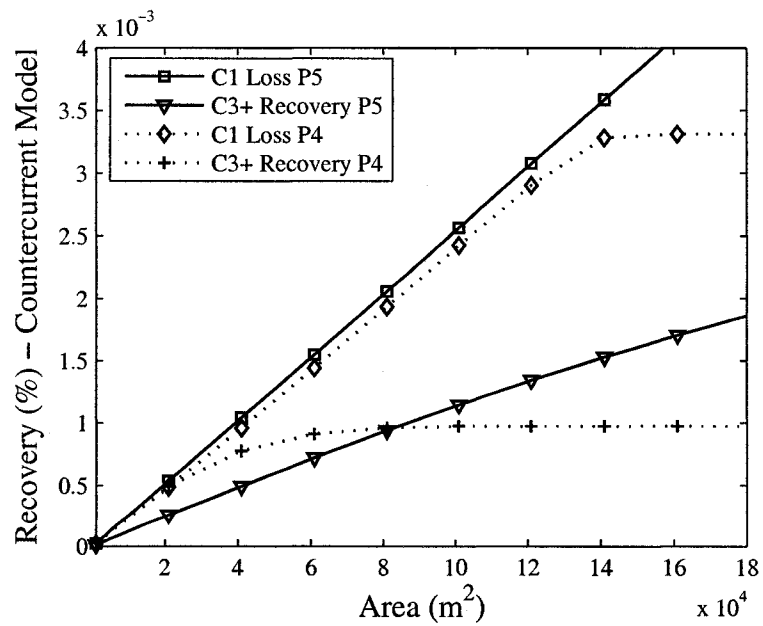


Figure 5.6b: Comparison of recovery for Positions 4 and 5 for small areas

In Table 5.3, the methane loss and C_3^+ recovery data for positions 4 and 5 are indicated for a range of area from 0 to 10,000 m^2 .

Table 5.3: Methane loss and C_3^+ recovery data for positions 4 and 5 for a small range of area

Area (m^2)	Position 4		Position 5	
	C_1 Loss (%)	C_3^+ Recovery (%)	C_1 Loss (%)	C_3^+ Recovery (%)
1000	0.0000	0	0	0
11000	0.0003	0.00028	0.0003	0.0001
21000	0.0005	0.00048	0.0005	0.0003
31000	0.0007	0.00065	0.0008	0.0004
41000	0.0010	0.00077	0.0010	0.0005
51000	0.0012	0.00085	0.0013	0.0006
61000	0.0014	0.0009	0.0015	0.0007
71000	0.0017	0.00094	0.0018	0.0008
81000	0.0019	0.00095	0.0021	0.0009
91000	0.0022	0.00097	0.0023	0.0010
101000	0.0024	0.00097	0.0026	0.0011

5.5.3 Effect of Flow Patterns

In Figure 5.7, permeate molar flow rates for co- and counter-current models are compared for Position 2. For all the cases considered, the counter-current model is more efficient since permeate molar flows of C_3^+ are larger except for very large membrane areas, while permeate molar flow of methane is similar compared to those produced with co-current model.

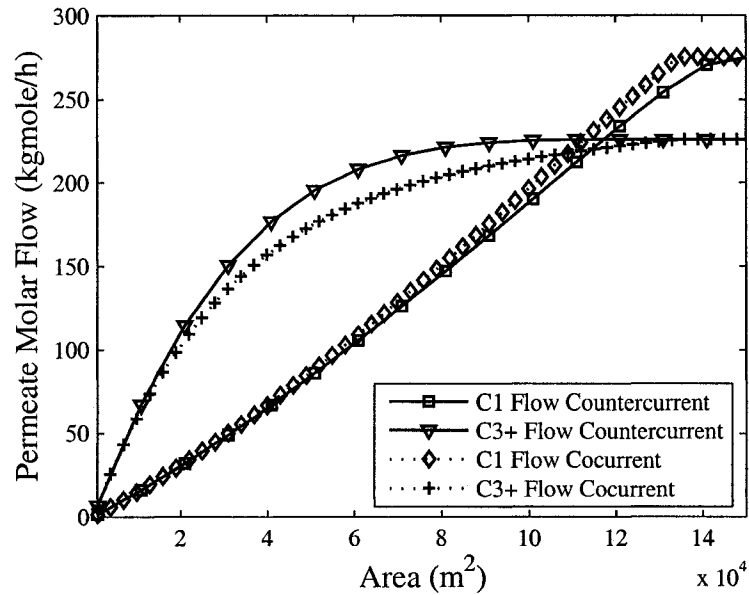


Figure 5.7: Permeate molar flow rates for C_3^+ and methane in Position 2 for Co- and Counter-current models

5.5.4 Effect of Stream Temperature

The input temperature of the process (“Wellhead” stream) is varied to examine the change of the composition of the associated gas generated in the three separators into the process, which will affect the performance of the membranes in the positions selected. The input temperature of the process is varied at: 30 °C, 35 °C and 40 °C. The input temperatures of the membranes in Positions 2 and 4 remain the same as the preceding cooler sets their value. As the input temperature of the process increases the recovery of C_3^+ also increases, while the recovery of methane remains constant. The effect of the temperature is shown only for the Position 2 in Figure 5.8 since all the other positions show similar behaviour. In this figure, permeate molar flow rates of C_3^+ are shown for the

three different temperatures. The recovery of C_3^+ and methane was not greatly affected by the change in feed.

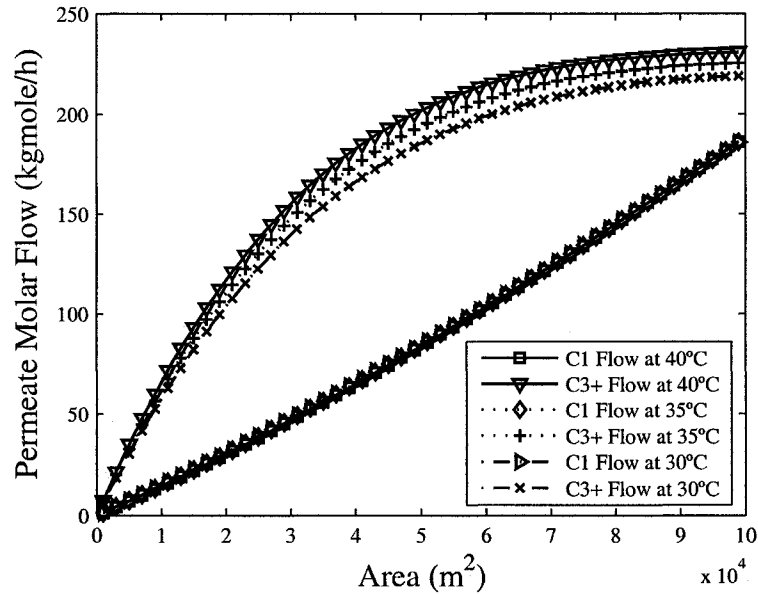


Figure 5.8: Permeate molar flow rates for C_3^+ in Positions 2 when the temperature of the “Wellhead” stream is 30, 35 and 40 °C

5.5.5 Location Effect

Ultimately, the purpose of the membrane is to maximize recovery of C_3^+ while minimizing methane content, which in turn is a function of position. Positions 1 and 3 are not considered in this case since the difference between position 1 and 2, and 3 and 4 is the area required; that is positions 1 and 3 required more area than positions 2 and 4. Thus, permeate molar flow rates of C_3^+ and methane as function of the membrane areas are compared for positions 2, 4 and 5 in Figure 5.9. From this figure it can be seen that for Positions 4 and 5 permeate molar flow of methane is greater than the permeate molar

flow of C_3^+ . For position 2, permeate molar flow of methane is lower than permeate molar flow of C_3^+ for areas smaller than $1.2 \times 10^5 \text{ m}^2$. For larger membranes the permeate flow of methane keeps increasing until reaching a constant value of 275 kmole/h at an area of $1.5 \times 10^5 \text{ m}^2$, which is the total amount of methane entering the membrane. This means that if the area of the membrane is very large, all the components will cross the membrane after some time. Thus, it is necessary to choose an area that permits a great recovery of C_3^+ with the minimum amount of methane in the permeate stream.

Separation factors for C_3^+ with respect to methane are also compared in the three positions selected. In Position 2, the separation factor for small areas is larger than for Positions 4 and 5 due to the higher concentration of heavy hydrocarbons. Position 2 shows a higher separation factor for small areas since the feed of the membrane is richer in C_3^+ compared to the feed of the membranes in Positions 4 and 5. The increment of C_3^+ in the feed of the membrane improves the separation of the C_3^+ components from methane. The separation factor of Position 4 is larger than the separation factor of Position 5 only for small area, and then it decreases similarly to the separation factor of Position 2. For moderate to large area values, the separation factor for Position 5 is larger since the amount of flow rate treat in this position is several times larger than the flow rates treated in the other two positions. The separation factor for Position 2, 4 and 5 are shown in Figure 5.9.

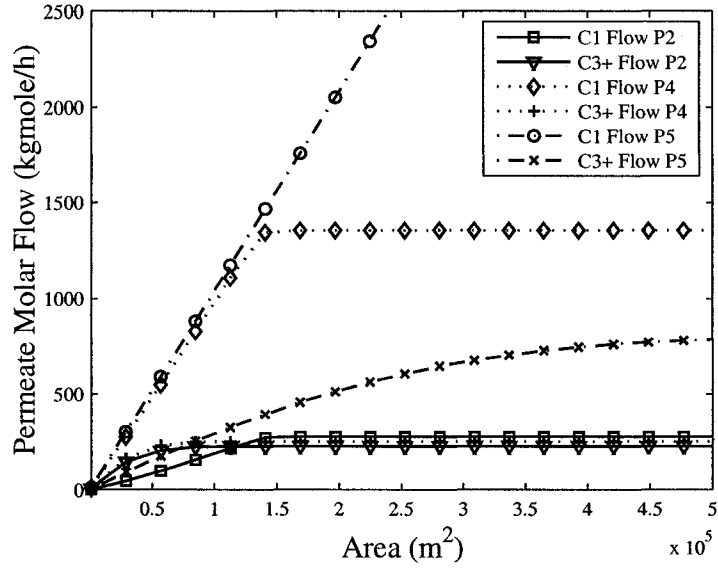


Figure 5.9a: Permeate molar flows of C_3^+ and methane in Positions 2, 4, and 5 for a wide range of areas

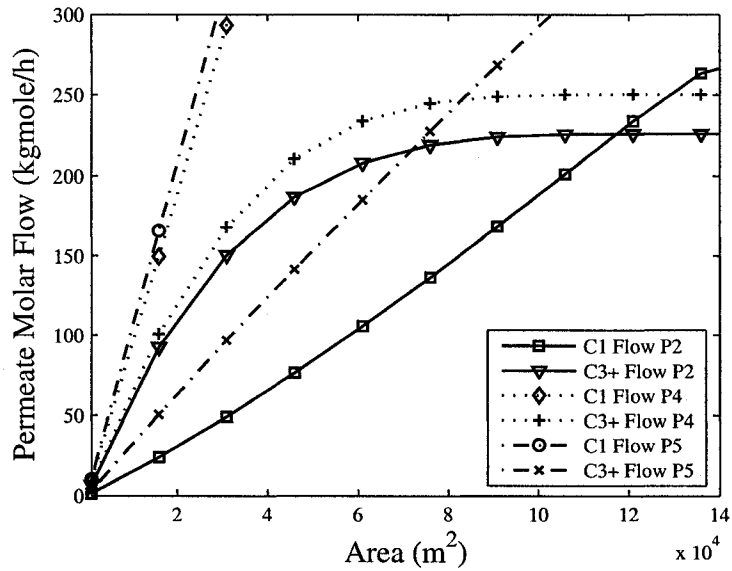


Figure 5.9b: Permeate molar flows of C_3^+ and methane in Positions 2, 4, and 5 for small areas

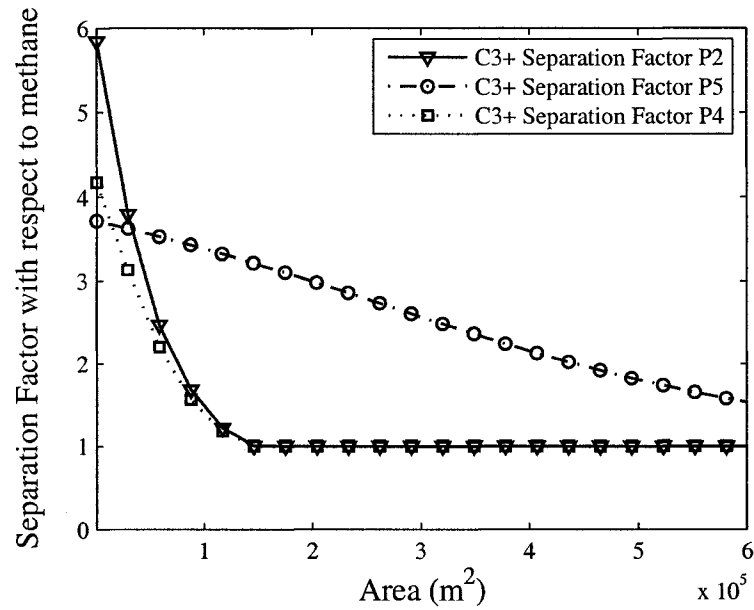


Figure 5.10: Separation Factor with respect to methane for C_3^+ in Positions 2, 4, and 5

5.6 Analysis of Recovery of Ethane Plus Components (C_2^+)

5.6.1 Pressure Effect

In the “Associated Gas LP” stream the membrane is placed in position 1 and the results are compared with those generated when the membrane is in position 2. In this comparison composition, temperature, and molar flow rates remain constant. In Figure 5.11, the recoveries (%) of C_2^+ and methane loss are plotted against membrane area for positions 1 and 2. The same behaviour as in the case of C_3^+ is observed. The maximum recovery percentage of C_2^+ is larger than the maximum recovery percentage of C_3^+ . The curves have the same pattern in both positions, but the curves are shifted. Thus, for a

given recovery of C_2^+ , a larger area is required in position 1 compared to position 2. In these two positions the recovery (%) of C_2^+ are higher than the methane loss. Recovery of C_2^+ increases quickly for small areas, and then is constant, while methane loss increases linearly with the area.

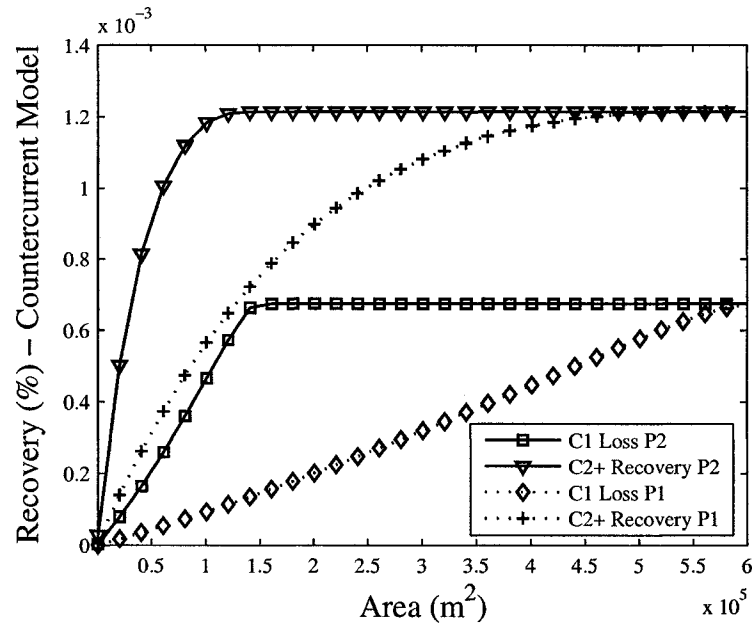


Figure 5.11: Comparison of recovery for Positions 1 and 2

In the “Associated Gas MP” stream the membrane is placed in the position 3 and compared with position 4. As in the previous case, all the parameters except the pressure remain constant. In Figure 5.12, the recoveries (%) of the C_2^+ and methane loss are shown for Positions 3 and 4. The recovery (%) curves for Position 3 are the same shape as the curves for Position 4 but shifted.. For both positions, the recovery of C_2^+ is higher than methane losses for small areas. When these curves are close to maximum recovery, methane loss curves overshadow the C_2^+ recovery curves. As in the case described before,

the recovery (%) curves of C_2^+ also increase relatively quickly for small areas and then approach a constant value for large areas, while methane loss curves increase linearly with the area until reaching their maximum value.

After locating the membrane at different pressures, it can be concluded that the pressure increase the mass transfer through the membrane but it does not affect the maximum possible recovery of C_2^+ .

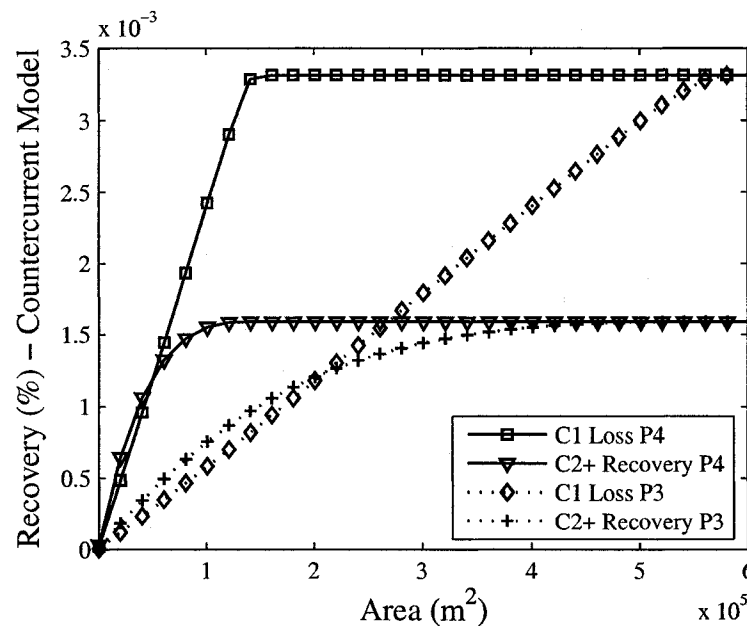


Figure 5.12: Comparison of recovery for Positions 3 and 4

5.6.2 Effect of Gas Composition

In order to evaluate the effect of gas composition, Positions 4 and 5 are compared since their conditions are almost the same, except for the composition. The recovery (%) curves for C_2^+ and methane loss with respect to “Wellhead” stream for these two positions are presented in Figure 5.13. In this Figure, part “a” indicates the curves for a

large range of area values, and part “b” indicates the curves for small area values. In Position 5, the recovery of methane is higher than the C_2^+ recovery for all the area values considered. In Position 4, the recoveries of methane and C_2^+ are higher for considerably small areas, but then for large areas the recovery of methane becomes higher. The shape of the curves for the recovery is similar for both positions. Methane recovery increases linearly until it reaches a constant value, and the C_2^+ curve increases exponentially for small areas and then it reaches a constant value.

For areas smaller than $1 \times 10^5 \text{ m}^2$, the recovery (%) of C_2^+ for Position 4 is higher than recovery of (%) of C_2^+ for Position 5, while both positions show similar methane recovery (%). After this point, the recovery (%) of C_2^+ of Position 5 keeps increasing due to the higher molar flow, but the recovery (%) of C_2^+ of Position 4 remains constant, since it is the maximum C_2^+ recovery possible in this position. As a result, a higher concentration in C_2^+ produces a better recovery. For example, for an area of $30,000 \text{ m}^2$ the recovery of C_2^+ and methane for Positions 4 and 5 are $1.1 \times 10^{-3} \%$ and 0.7×10^{-3} , respectively.

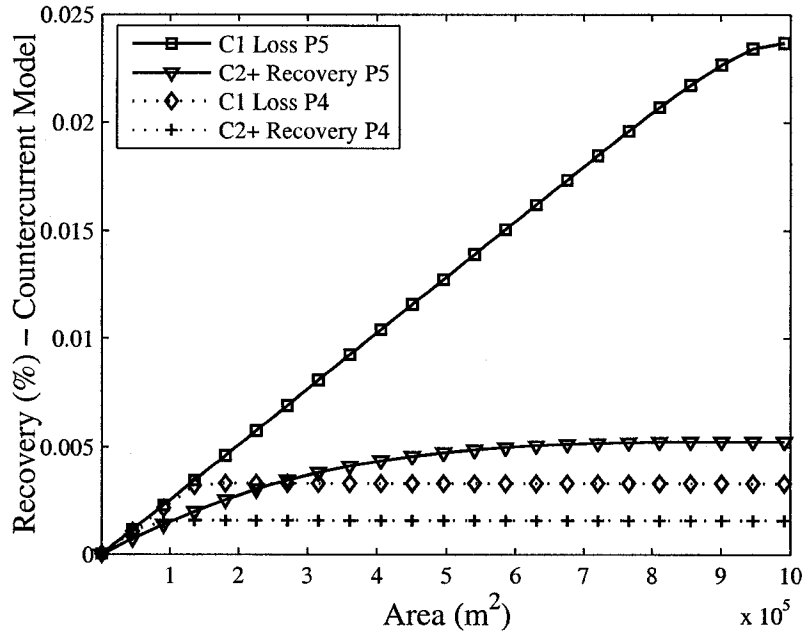


Figure 5.13a: Comparison of recovery for Positions 4 and 5 for wide range areas

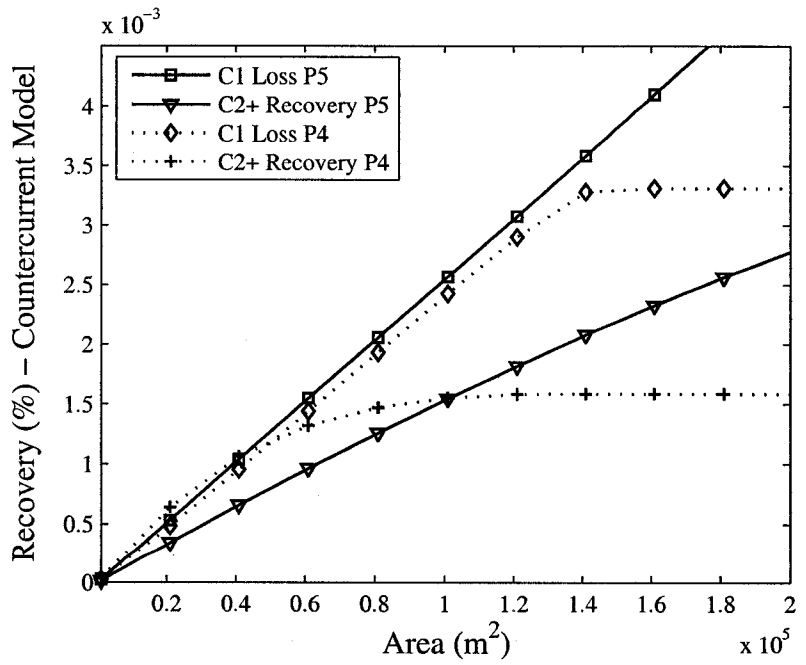


Figure 5.13b: Comparison of recovery for Positions 4 and 5 for small areas

5.6.3 Effect of Flow Patterns

In Figure 5.14, permeate molar flow rates for co- and counter-current models are represented for Position 2. For all the cases considered, the counter-current model is more efficient since permeate molar flows of C_2^+ are larger and permeate molar flow of methane is smaller compared to those produced with co-current model. These results show similitude with the previous mentioned study of C_3^+ recovery.

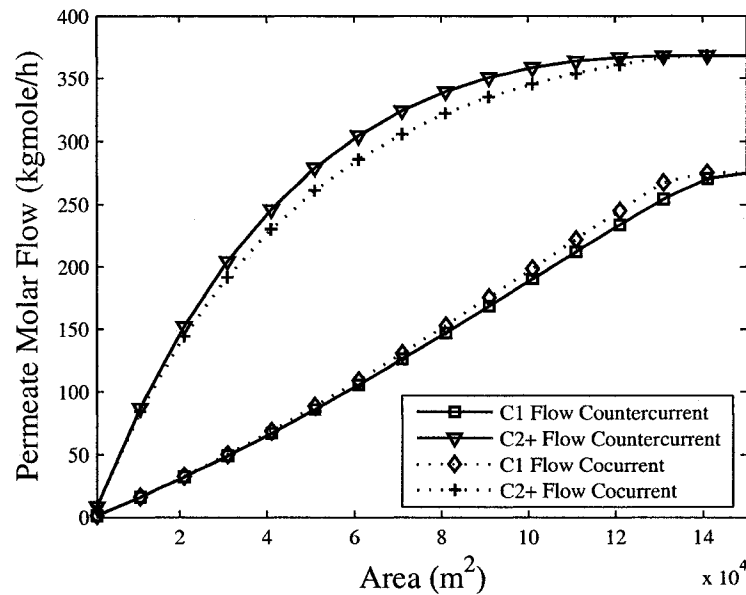


Figure 5.14: Permeate molar flow rates for C_2^+ and methane in Position 2 for Co- and Counter-current models

5.6.4 Effect of Stream Temperature

The input temperature of the process (“Wellhead” stream) is varied to examine the change of the composition of the associated gas generated in the three separators into the process. The input temperature set at three different values: 30 °C, 35 °C and 40 °C. The

input temperatures of the membranes in positions 2 and 4 are determined by the cooler and therefore are not varied. As the input temperature of the process increases the recovery of C_2^+ also increases, while the recovery of methane remains practically constant. The effect of the temperature is shown for the position 2 in Figure 5.15. In this figure, permeate molar flow rates of C_2^+ are shown for the three different temperatures. The recovery of C_2^+ and methane was practically not affected by change the feed temperature of the input of the process.

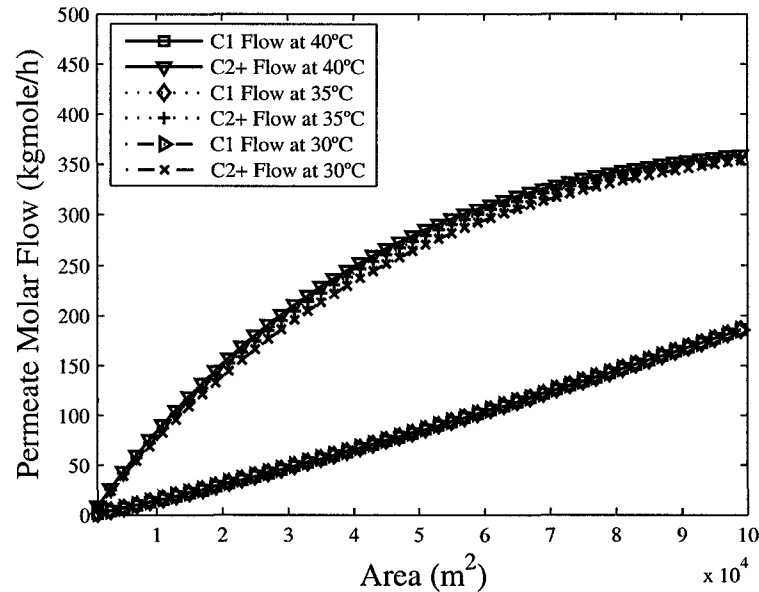


Figure 5.15: Permeate molar flow rates for C_2^+ in Positions 2 when the temperature of the “Wellhead” stream is 30, 35 and 40 °C

5.6.5 Location Effect

The objective is to recover as much C_2^+ as possible while minimizing methane content in the recovered stream. As mentioned before, the Positions 1 and 3 are not considered since the difference between Positions 1 and 2, and 3 and 4 is the area required; Positions 1 and 3 required more areas than Positions 2 and 4, respectively. Thus, permeate molar flow rates of C_2^+ and methane as function of the membrane areas are compared for these three positions in Figure 5.16. In part “a” of this figure, a wide range of area values is indicated, while in part “b” of this figure smaller area values are plotted. From these figures it can be seen that for Positions 5 permeate molar flow of methane is greater than the permeate molar flow of C_3^+ , while for Position 4 these permeate molar flow are similar for small areas and then permeate molar flow of methane overshadow C_2^+ permeate molar flow. For Position 2, permeate molar flow of methane is lower than permeate molar flow of C_2^+ for all the area values considered. However, the difference between these two molar flows become smaller from a area value of $1.4 \times 10^5 \text{ m}^2$, where both curves are constant representing the total amount of C_2^+ and methane entering the membrane. This means that if the area of the membrane is very large, all the components will eventually cross the membrane when the area is increased. Thus, it is necessary to choose an area that permits a great recovery of C_2^+ with the minimum amount of methane lost.

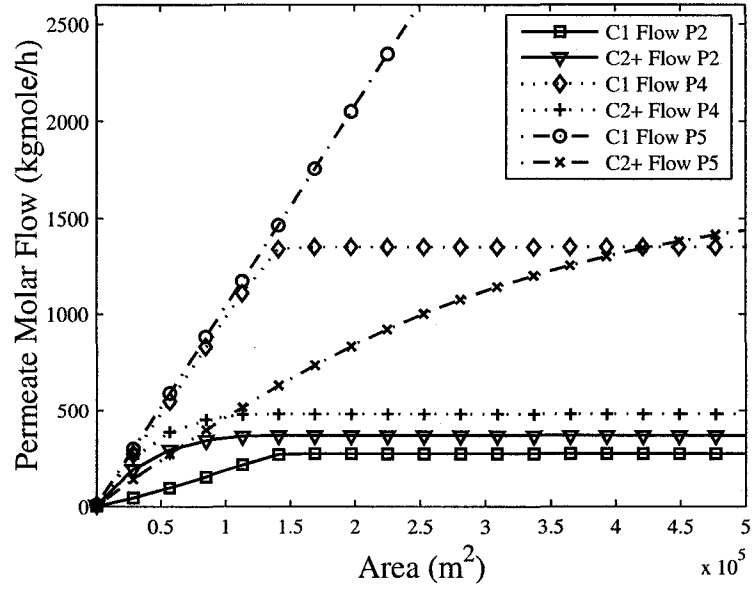


Figure 5.16a: Permeate molar flows of C₂⁺ and methane in Positions 2, 4, and 5

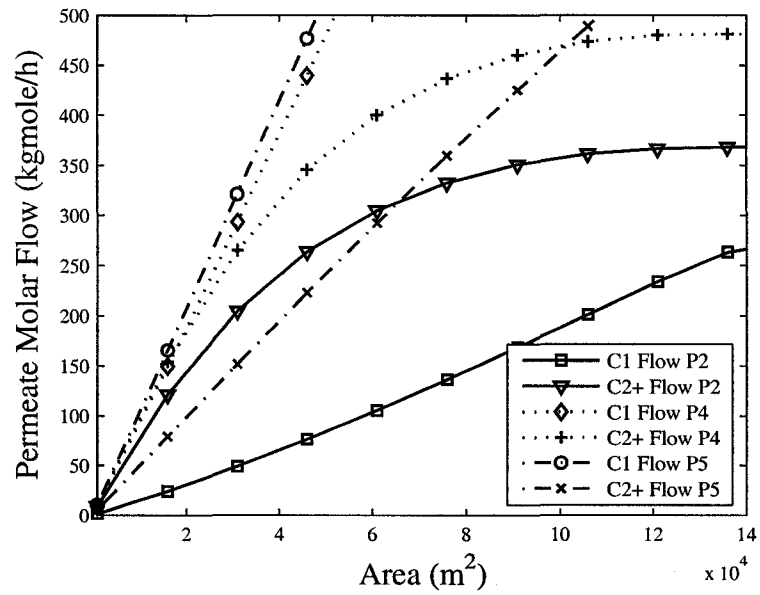


Figure 5.16b: Permeate molar flows of C₂⁺ and methane in Positions 2, 4, and 5

In addition, the separation factors of C_2^+ with respect to methane are also compared for the three selected positions. The separation factors indicate separation of heavy hydrocarbons from methane. As the separation factor increases, a greater separation is obtained. A separation factor equal to 1 means that the ratio of the concentration relation of heavy hydrocarbons/methane in permeates and in residue streams is the same. In Position 2, the separation factor for small areas is larger than for Positions 4 and 5 due to the higher concentration in heavy hydrocarbons. However, the separation factors of the three positions for C_2^+ recovery are lower compared to C_3^+ recovery. The reason is due to the fact that the structure of ethane is very similar to structure of methane, which makes it more difficult to establish an efficient separation. The separation factor for Position 2, 4 and 5 are shown in Figure 5.17.

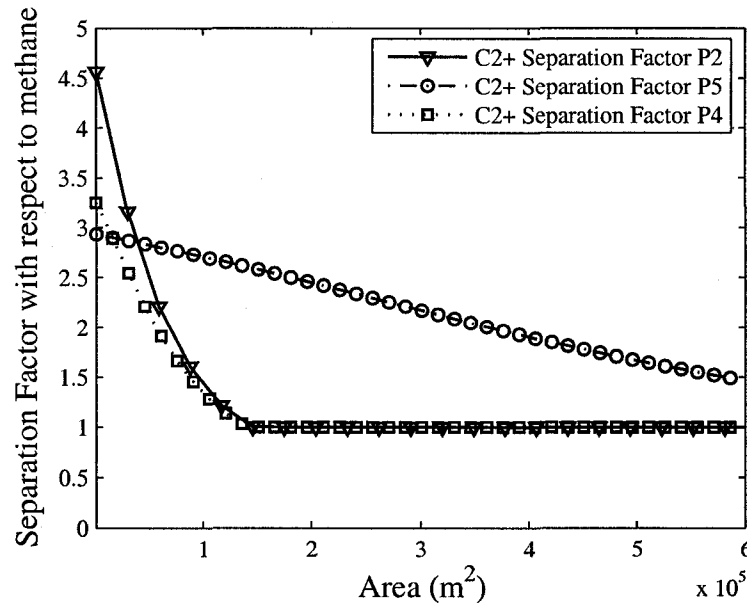


Figure 5.17: Separation Factor with respect to methane for C_2^+ in Positions 2, 4, and 5

5.7 Conclusion

In this chapter the recovery of NGL (C_3^+ , C_2^+) in offshore Newfoundland and Labrador was evaluated by means of membrane, which were placed at different positions in a three-stage separation train. The effects of pressure, composition, temperature, flow pattern and location on NGL recovery were evaluated. An increase in the pressure of the feed to the membrane produces a higher NGL recovery but also a higher methane loss. An increase in the feed temperature of the process (“Wellhead” stream temperature) results in a higher recovery of NGL while methane is unaffected. A higher concentration of NGL in the feed stream to the membrane resulted in an incremental mass transfer driving force, which translated into better separation. In addition, the counter-current model showed a better performance since a higher recovery of NGL with less methane could be reached in all cases studied.

The recovery of C_2^+ and C_3^+ showed similar behaviour in all simulations. However, C_3^+ recovery had higher separation factors with respect to methane, which indicates lower methane loss in the permeate stream.

For the studied cases, the best location for the membrane was concluded to be on the low pressure associated gas stream after compression since the recovery of NGL was higher than the methane loss in the permeate stream. Nevertheless, for a complete analysis of the system, it is necessary to include a recycle in the process to return permeate back to feed a separator. Thus, the effect of the introduction of membrane into the process to the crude oil production can be studied. It is believed that the incorporation of the recycles will notably improve the recovery of NGL. This further analysis is considered in the Chapter 6.

CHAPTER 6

PROCESS CASE STUDIES WITH RECYCLE STREAMS

In the previous chapter, membranes were introduced into a typical separation train on an offshore platform to determine the efficiency of the membranes to recover NGL. In this chapter, the analysis is extended to evaluate the impact of the membranes on the production of crude oil base. For that the permeate and or the residue streams are recycle into different part of the process. Twelve alternative configurations of the original process are investigated in this chapter. The purpose of this chapter is to investigate how the recycling of different streams of the process improve the production of crude oil

6.1 Three-stage Crude oil Separation Process⁴

The crude oil separation train considered for this analysis consists of three separation stages, which work at different pressures. The first separator operates at 7,000 kPa, the second one at 1,724 kPa, and the third one at 413.7 kPa. Each separator flashes the lighter gases through the top and concentrates the heavier hydrocarbons in the bottom. More details of this process are provided in the previous chapter (refer to Chapter 5 Section 5.2). Figure 6.1 outlines the process flow. For the base case, the mass fractions and mass flow rates of each component are shown for six streams in Table 6. These six streams are the three associated gas streams leaving each separator, the two streams

entering the medium and low-pressure separators, and the stream leaving the low-pressure separator. In addition in Table 6.2, the production of Ethane Plus components (C_2^+), Propane Plus components (C_3^+), and Pentane Plus components (C_5^+) in mass and volumetric units are shown. The recovery percentage indicated in Table 6.2 refers to the recovery of the components with respect to the input of the process. Also, the value of the Reid Vapour Pressure (RVP) is presented for the stream where crude oil is concentrated (“Crude Oil Product”). The ideal value for RVP is 12 psia, and for values close to this ideal value it is safe to store crude oil at atmospheric conditions. For example, if the value of RVP exceeds the ideal value, the crude may flash vapours in storage or transportation, increasing explosion and over-pressure risks. The RVP value obtained in the crude oil product is not necessary high considering that this oil goes to other facilities for further processing. The oil is treated to break the emulsions at near ambient pressure; therefore, gas is going to be flashed, which is going to reduce the RVP value.

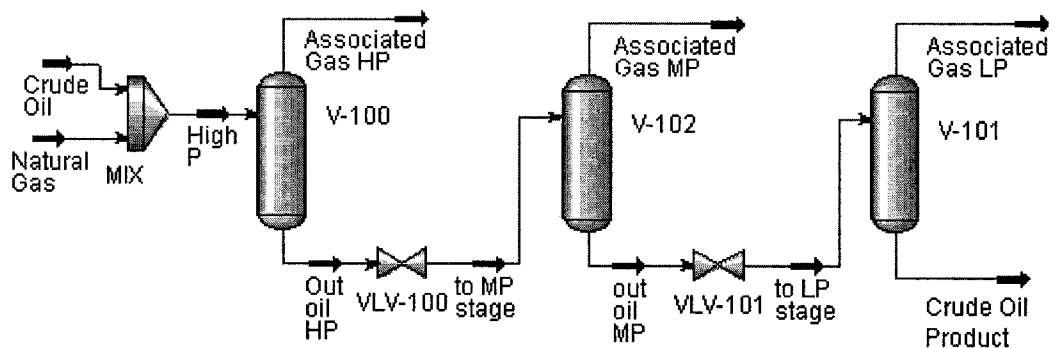


Figure 6.1: Three-stage crude oil separation process

Table 6.1: Mass fractions and mass flow rates for the streams specified for the base process

	Associated Gas HP		To MP stage		Associated Gas MP		To LP stage		Associated Gas LP		Crude Oil Product	
	Mass Frac.	Mass Flow (kg/h)	Mass Frac.	Mass Flow (kg/h)	Mass Frac.	Mass Flow (kg/h)	Mass Frac.	Mass Flow (kg/h)	Mass Frac.	Mass Flow (kg/h)	Mass Frac.	Mass Flow (kg/h)
Total	1.000	209,329	1.000	1,243,978	1.000	36,500	1.000	1,207,478	1.000	17,056	1.000	1,190,423
Methane	0.746	156,061	0.021	25,980	0.571	20,853	0.004	5,126	0.259	4,413	0.001	713
Ethane	0.112	23,494	0.012	14,794	0.183	6,675	0.007	8,119	0.255	4,343	0.003	3,776
Propane	0.083	17,462	0.023	28,385	0.159	5,795	0.019	22,590	0.333	5,677	0.014	16,913
i-Butane	0.008	1,726	0.004	5,398	0.015	546	0.004	4,852	0.035	594	0.004	4,258
n-Butane	0.016	3,294	0.011	13,804	0.028	1,025	0.011	12,779	0.067	1,142	0.010	11,637
i-Pentane	0.002	429	0.003	3421	0.003	117	0.003	3,304	0.008	130	0.003	3,173
n-Pentane	0.002	373	0.003	3,788	0.003	99	0.003	3,689	0.006	110	0.003	3,579
Hexane	0.000	76	0.001	1,788	0.000	17	0.001	1,772	0.001	18	0.001	1,754
CO2	0.025	5,321	0.002	2,231	0.036	1,308	0.001	923	0.036	621	0.000	302
N2	0.005	1,024	0.000	67	0.002	62	0.000	5	0.000	5	0.000	0
C7+	0.000	69	0.920	1,144,323	0.000	4	0.948	1,144,319	0.000	3	0.961	1,144,316
C3 Plus	0.112	23,429	0.965	1,200,907	0.208	7,602	0.988	1,193,305	0.450	7,674	0.996	1,185,631
C5 Plus	0.005	946	0.927	1,153,320	0.006	236	0.955	1,153,084	0.015	261	0.968	1,152,823

Table 6.2: Crude oil production of the base process

	Mass Flow (kg/h)	Recovery (%)	RVP (psia)	Volume Flow	
				(m ³ /h)	(bbl/day)
Total	1,190,423	81.91	19.878	1,365	206,152
Methane	713	0.39	-	-	-
Ethane Plus	1,189,407	94.20	-	1,364	205,935
Propane Plus	1,185,631	96.84	-	1,358	205,009
C5+	1,152,823	99.87	-	1,307	197,318

6.2 Alternatives processes with membranes

In the following sections, twelve different alternatives of the three-stage crude oil separation process are presented and compared to the base process.

6.2.1 Case 1: Membrane after the high-pressure separator

In Case 1, a membrane is placed after the first separator (V-100 in Figure 6.1 at 7,000 kPa). The heavier hydrocarbons are concentrated on the low-pressure side of the membrane (1,724 kPa), while the lighter gases are retained on the high-pressure side of the membrane. Thus, the “Permeate from HP” stream is rich in heavier hydrocarbons and is mixed with the crude oil coming from the bottom of the separator after reducing its pressure to 1,724 kPa

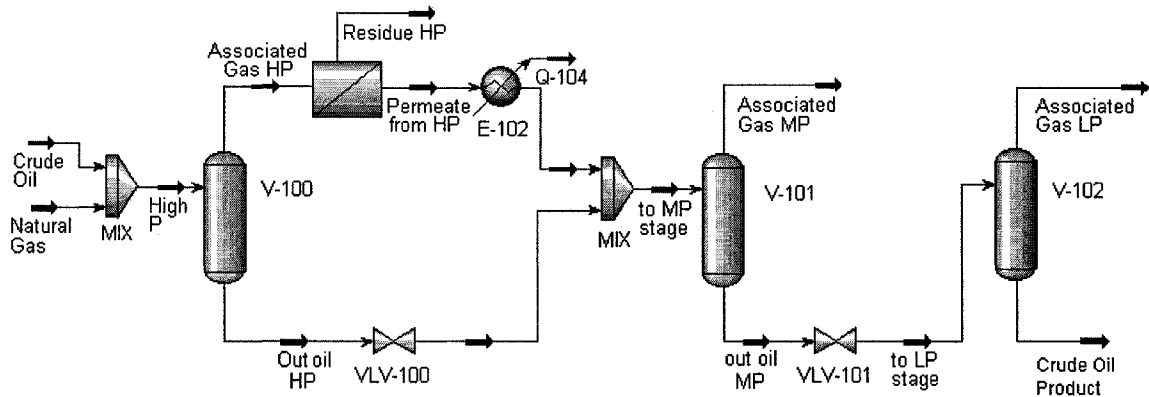


Figure 6.2: Case 1: Membrane located after high-pressure separator

In Table 6.3, the mass fractions and mass flow rates downstream of the “MIX” block are outlined.

Table 6.3: Mass fractions and mass flow rates for the streams specified for Case 1

	To MP stage			Associated Gas MP			To LP stage			Associated Gas LP			Crude Oil Product		
	Mass Frac.	Mass Flow (kg/h)	(%)*	Mass Frac.	Mass Flow (kg/h)	(%)*	Mass Frac.	Mass Flow (kg/h)	(%)*	Mass Frac.	Mass Flow (kg/h)	(%)*	Mass Frac.	Mass Flow (kg/h)	(%)*
Total	1.000	1,256,178	1.01	1.000	48,088	1.32	1.000	1,208,090	1.00	1.000	17,122	1.00	1.000	1,190,968	1.00
Methane	0.026	32,691	1.26	0.573	27,546	1.32	0.004	5,145	1.00	0.259	4,430	1.00	0.001	715	1.00
Ethane	0.013	16,864	1.14	0.182	8,764	1.31	0.007	8,099	1.00	0.253	4,335	1.00	0.003	3,764	1.00
Propane	0.024	30,649	1.08	0.161	7,737	1.34	0.019	22,912	1.01	0.337	5,763	1.02	0.014	17,149	1.01
i-Butane	0.005	5,687	1.05	0.015	733	1.34	0.004	4,954	1.02	0.035	607	1.02	0.004	4,346	1.02
n-Butane	0.011	14,353	1.04	0.029	1,371	1.34	0.011	12,982	1.02	0.068	1,161	1.02	0.010	11,820	1.02
i-Pentane	0.003	3,494	1.02	0.003	156	1.33	0.003	3,338	1.01	0.008	132	1.01	0.003	3,206	1.01
n-Pentane	0.003	3,849	1.02	0.003	131	1.33	0.003	3,717	1.01	0.006	111	1.01	0.003	3,607	1.01
Hexane	0.001	1,803	1.01	0.000	22	1.32	0.001	1781	1.01	0.001	18	1.01	0.001	1763	1.01
CO2	0.002	2,374	1.06	0.032	1,546	1.18	0.001	828	0.90	0.033	557	0.90	0.000	270	0.90
N2	0.000	83	1.23	0.002	78	1.26	0	5	0.96	0.000	5	0.96	0.000	0	0.95
C7+	0.911	1,144,334	1.00	0.000	5	1.32	0.947	1,144,329	1.00	0.000	3	1.00	0.961	1,144,327	1.00
C3 Plus	0.959	1,204,168	1.00	0.211	10,155	1.34	0.988	1,194,013	1.00	0.455	7,795	1.02	0.996	1,186,217	1.00
C5 Plus	0.918	1,153,479	1.00	0.007	314	1.33	0.955	1,153,166	1.00	0.015	263	1.01	0.968	1,152,902	1.00

- With respect to the same stream in the base proces

Comparing the base process with the process of Case 1, the stream that enters the medium pressure separator (“To MP stage”) has a higher concentration of lighter gases as well as heavier components. At the MP separator the composition of the bottom stream (“To LP stage”) is similar in composition to the base process.

The composition differences in the stream “To MP stage” are also reflected in the phase envelopes. The envelopes for both processes are shown in Figure 6.3. The dew point curves of these processes are similar; however, the bubble point curve of the process of Case 1 is above the bubble point of the base process. The reason is that the “to MP stage” stream is richer in lighter hydrocarbons, which expands the two-phase region of the envelope towards lower bubble point temperatures.

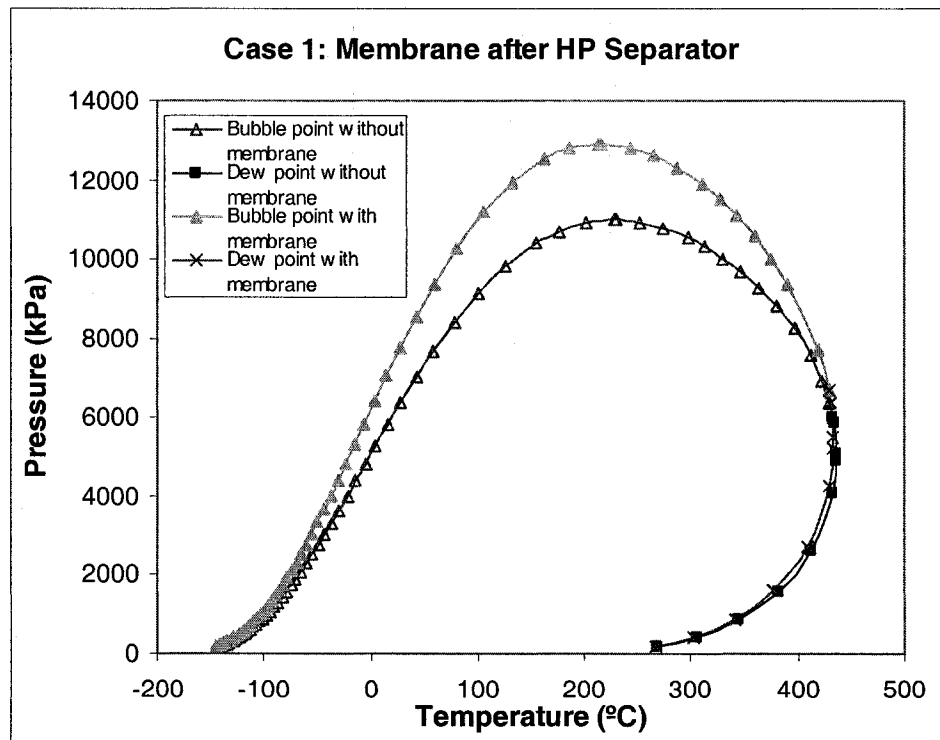


Figure 6.3: Phase envelopes for the stream entering the medium pressure separator (“to MP stage” stream).

In Table 6.4, the concentration of NGLs in the final crude oil product and RVP are shown. The recovery of heavier hydrocarbons is slightly improved when compared with the base process without membrane, while the amount of methane in this stream remains constant. The RVP value is similar to that of the base process, which is an acceptable value. The process of Case 1 does not result in a considerable increase of crude oil production. In addition, if the cost of the membrane is added, this process will not be feasible.

Table 6.4: Crude oil production of the process of Case 1

	Mass Flow (kg/h)	Recovery (%)	RVP (psia)	Volume Flow	
				(m ³ /h)	(bbl/day)
Total	1,190,968	81.95	19.977	1,366	206,287
Methane	715	0.39	-	-	-
Ethane Plus	1,189,982	94.25	-	1,365	206,071
Propane Plus	1,186,217	96.89	-	1,359	205,147
C5+	1,152,902	99.88	-	1,307	197,335

6.2.2 Case 2: Membrane after the medium-pressure separator

In Case 2, a membrane is placed at the overhead of the second separator (V-101 in Figure 6.4 at 1,724 kPa). Before entering the membrane, the associated gas is compressed to 7,000 kPa and then cooled to increase the efficiency of the membrane. The heavier hydrocarbons are concentrated on the low-pressure side of the membrane (1,724 kPa), while the lighter gases are retained on the high-pressure side of the membrane. The “Permeate from MP” stream is then mixed with the crude oil coming from the second separator after reducing its pressure to 413.7 kPa. These two mixed streams are the new feed to the third separator (low pressure separator, 413.7 kPa).

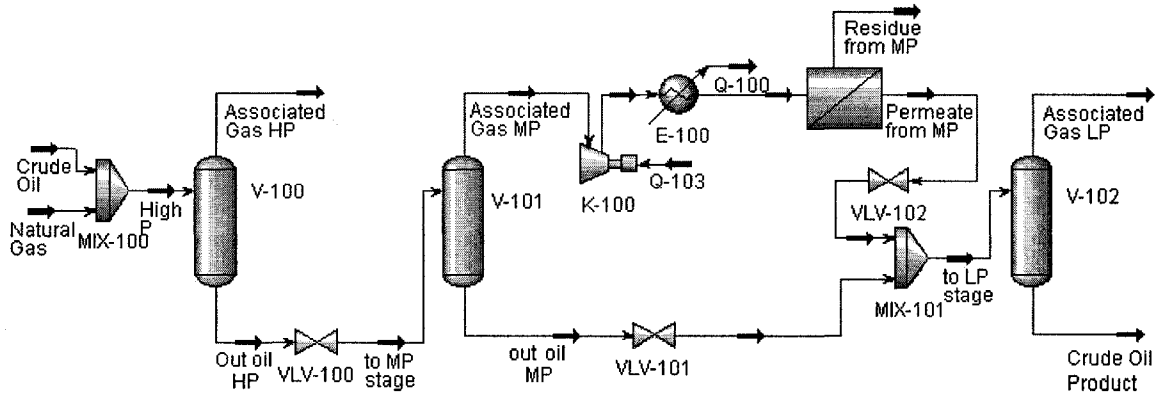


Figure 6.4: Case 2: Membrane located after medium-pressure separator

In Table 6.5, the mass fractions and mass flows of each component are shown for those streams that differ from the base process.

Table 6.5: Mass fractions and mass flow rates for the streams specified for Case 2

	To LP stage			Associated Gas LP			Crude Oil Product		
	Mass Frac.	Mass Flow (kg/h)	(%)*	Mass Frac.	Mass Flow (kg/h)	(%)*	Mass Frac.	Mass Flow (kg/h)	(%)*
Total	1.000	1,223,360	1.01	1.000	35,183	2.06	1.000	1,188,177	1.00
Methane	0.009	11,310	2.21	0.299	10,523	2.38	0.001	787	1.10
Ethane	0.010	11,721	1.44	0.237	8,344	1.92	0.003	3,377	0.89
Propane	0.022	26,823	1.19	0.319	11,209	1.97	0.013	15,614	0.92
i-Butane	0.004	5,339	1.10	0.035	1,225	2.06	0.003	4,114	0.97
n-Butane	0.011	13,689	1.07	0.067	2,366	2.07	0.010	11,323	0.97
i-Pentane	0.003	3,409	1.03	0.008	274	2.10	0.003	3,135	0.99
n-Pentane	0.003	3,776	1.02	0.007	231	2.10	0.003	3,545	0.99
Hexane	0.001	1,788	1.01	0.001	37	2.11	0.001	1,751	1.00
CO2	0.001	1,174	1.27	0.027	957	1.54	0.000	216	0.72
N2	0.000	12	2.39	0.000	12	2.45	0.000	0.000	1.13
C7+	0.935	1,144,319	1.00	0.000	5	2.05	0.963	1,144,314	1.00
C3 Plus	0.980	1,199,144	1.00	0.436	15,347	2.00	0.996	1,183,796	1.00
C5 Plus	0.943	1,153,293	1.00	0.000	547	2.10	0.970	1,152,746	1.00

* With respect to the same stream in the base process

From Table 6.5, the composition of the stream “To LP stage” in Case 2 is much richer in methane (CH_4) and nitrogen (N_2) compared with this stream in the base process. The amount of Liquid Petroleum Gases (LPG) components (butanes and propane) also increases but not to the same extent. This behaviour is also reflected in the phase envelope of the “To LP stage” stream for both processes. The increase in lighter hydrocarbons again results in the bubble point curve shifting upwards and to the left. Although the dew point curves remain similar for both processes the resulting two-phase area of the stream of Case 2 is significantly larger.

The new concentration of the components entering the low-pressure separator affects its efficiency and the bottom stream (“Crude Oil Product”), where crude oil is further stabilized. The oil leaving this separator shows a higher concentration of CH_4 and N_2 , and a lower concentration in LPG components when compared to the base process. Instead, the associated gas produced in this separator is richer in heavier hydrocarbons when compared with the base process without the implementation of membranes.

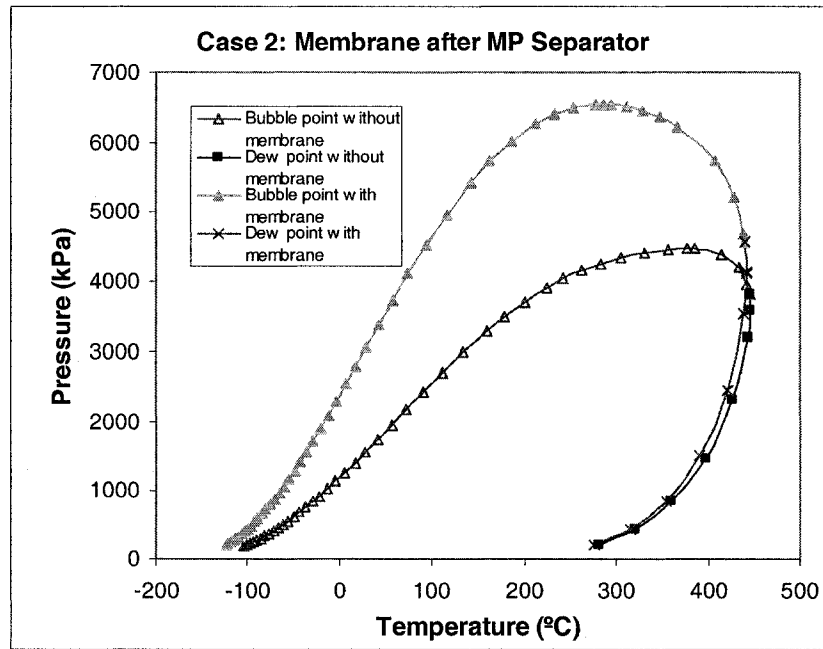


Figure 6.5: Phase envelopes for the stream entering to the medium pressure separator (“to MP stage”)

In Table 6.6, the concentration of NGLs in the oil product is shown along with the RVP value. The recovery of heavier hydrocarbons is lower than the base process while the amount of methane in the oil is higher. Thus, the efficiency of the process is reduced when a membrane is placed at this location. The RVP value is lower than the base process, which means that is less volatile at atmospheric condition. Since this alternative process presents a lower recovery of heavier hydrocarbons than the base process, this alternative is offering no great advantage over the base process.

Table 6.6: Crude oil production of the process of Case 2

	Mass Flow (kg/h)	Recovery (%)	RVP (psia)	Volume Flow	
				(m ³ /h)	(bbl/day)
Total	1,188,176	81.76	18.827	1,362	205,635
Methane	787	0.43	-	-	-
Ethane Plus	1,187,173	94.02	-	1,360	205,401
Propane Plus	1,183,796	96.69	-	1,355	204,573
C5+	1,152,746	99.87	-	1,307	197,301

6.2.3 Case 3: Membrane at the overhead of the low-pressure separator

In Case 3, a membrane is placed at the overhead of the third separator (V-102 in Figure 6.6) to treat the associated gas produced. Before entering the membrane, the associated gas is compressed to 1,724 kPa and then cooled to increase the efficiency of the membrane. The heavier hydrocarbons are concentrated on the low-pressure side of the membrane (413.7 kPa), while the lighter gases are retained on the high-pressure side of the membrane. The “Permeate from LP” stream is mixed with the crude oil coming from the bottom of the separator. The mixed stream is the crude oil product of the process.

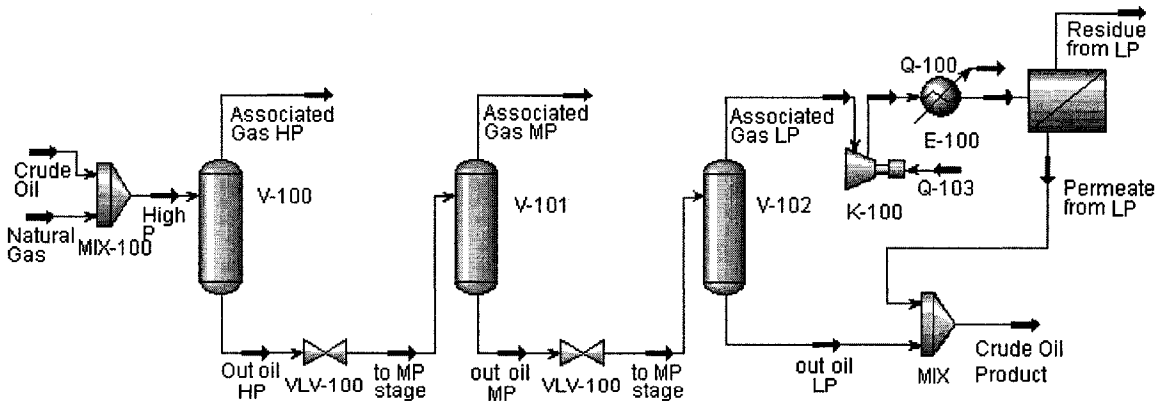


Figure 6.6: Case 3: Membrane located after low-pressure separator

In Table 6.7, the mass fractions and mass flow rates of each component are indicated for the stream leaving the third separator since this stream (“Crude Oil Product”) is the only one that differs from the base process.

Table 6.7: Mass fractions and mass flow rates for the streams specified for Case 3

	Crude Oil Product		
	Mass Frac.	Mass Flow (kg/h)	(%)*
Total	1.000	1,199,634	1.01
Methane	0.002	1,823	2.56
Ethane	0.005	5,938	1.57
Propane	0.017	20,964	1.24
i-Butane	0.004	4,791	1.13
n-Butane	0.011	12,662	1.09
i-Pentane	0.003	3,290	1.04
n-Pentane	0.003	3,679	1.03
Hexane	0.001	1,770	1.01
CO2	0.000	400	1.32
N2	0.000	1	3.93
C7+	0.954	1,144,316	1.00
C3 Plus	0.993	1,191,472	1.00
C5 Plus	0.961	1,153,056	1.00

* With respect to the same stream in the base process

The percentage of CH₄ and N₂ increase notably compared to the base process, which is a negative result in terms of the crude oil quality. The amount of ethane, propane, and butanes in the oil increases for Case 3 but not to the same extent as the lighter components. In addition, increase in heavier hydrocarbons is relatively small. This result is also observed in the comparison of the two-phase envelopes of both processes (see Figure 6.7). In this figure, the two-phase area is larger for the process with four membranes, which makes the stream more volatile.

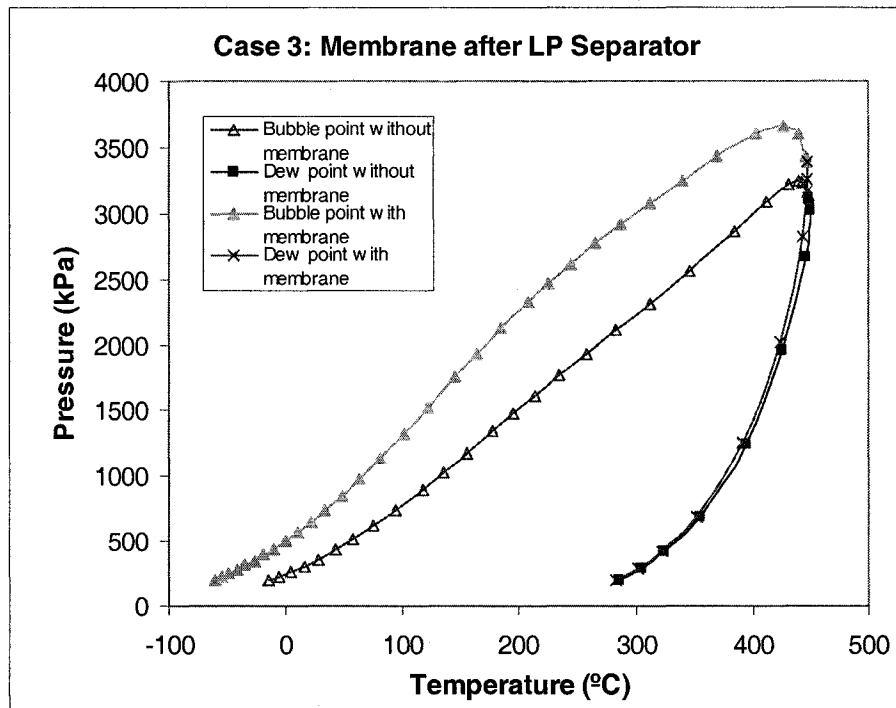


Figure 6.7: Phase envelopes for the stream “Crude Oil Product” for both processes

In Table 6.8, a description of the crude oil production for the process presented in Case 3 is indicated in mass and volumetric units together with the RVP value. Here, the recovery of heavier hydrocarbons is slightly higher than the base process without membrane, while the amount of methane is twice than that of in the base process. Therefore, the efficiency of the process is reduced when a membrane is placed at this location. Due to the excessive amount of methane in the output of the system, RVP value is larger than the base process. Under the storage and transport conditions (ambient temperature and atmospheric pressure) this high RVP will result in volatilization of vapours from the crude increasing pressure hazards and explosion risks. As a result, this process is not desirable

Table 6.8: Crude oil production of the process for Case 3

	Mass Flow (kg/h)	Recovery (%)	RVP (psia)	Volume Flow	
				(m ³ /h)	(bbl/day)
Total	1,199,633	82.55	29.261	1,380	208,428
Methane	1,823	1.00	-	-	-
Ethane Plus	1,197,410	94.84	-	1,377	207,865
Propane Plus	1,191,472	97.32	-	1,367	206,403
C5+	1,153,056	99.90	-	1,307	197,370

6.2.4 Case 4: Membranes after each separator

In Case 4, one membrane is placed after each separator. The first membrane treats the associated gas from V-100, and its permeate stream is mixed with the bottom stream of this separator previous reduction of its pressure (to 1,724 kPa). This mixed stream is the new feed to V-101. The second membrane treats the associated gas from the medium-pressure separator, and its permeate stream is mixed with the bottom stream of this separator after the reduction of its pressure to 413.7 kPa. This mixture enters V-102. The third membrane treats the associated gas coming from the low-pressure separator. The permeate stream is then mixed with the crude oil coming from the bottom of this separator. This last mixed stream is composed of the final crude oil product.

Before entering the membrane, the associated gases from the medium and low-pressure separators are compressed to 7,000 and 1,724 kPa, respectively, and then these streams are cooled, so they can be mixed with other streams. The heavier hydrocarbons are concentrated on the low-pressure side of the membranes, while the lighter gases are retained on the high-pressure side of the membrane. Figure 6.6 outlines the process flow.

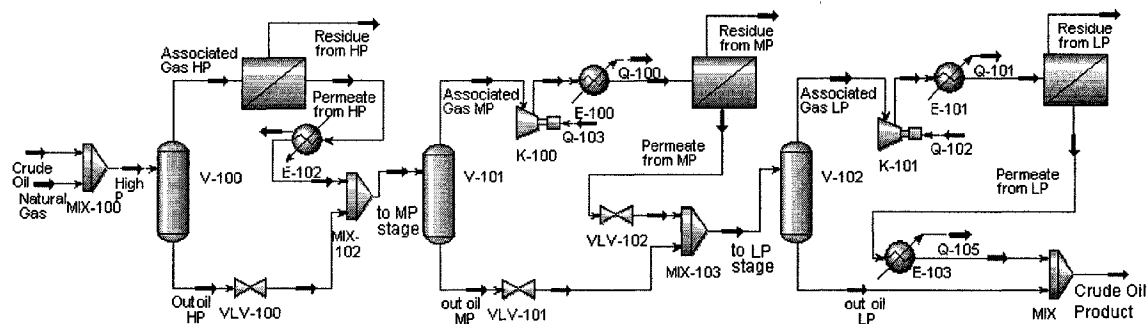


Figure 6.8: Case 4: Membranes located after each separator

In Table 6.9, the mass fractions and mass flow rates of each component are indicated for those streams that differ from the stream in the base process. These include: the three associated gas streams, the streams entering the second and third separators, and the stream “Crude Oil Product”.

Table 6.9: Mass fractions and mass flow rates for the streams specified for of Case 4

	To MP stage			Associated Gas MP			To LP stage			Associated Gas LP			Crude Oil Product		
	Mass Frac.	Mass Flow (kg/h)	(%)*	Mass Frac.	Mass Flow (kg/h)	(%)*	Mass Frac.	Mass Flow (kg/h)	(%)*	Mass Frac.	Mass Flow (kg/h)	(%)*	Mass Frac.	Mass Flow (kg/h)	(%)*
Total	1.000	1,256,178	1.01	1.000	48,088	1.32	1.000	1,224,741	1.01	1.000	35,684	2.09	1.000	1,199,127	1.01
Methane	0.026	32,691	1.26	0.573	27,546	1.32	0.0092	11,311	2.21	0.295	10,528	2.39	0.002	1,921	2.69
Ethane	0.013	16,864	1.14	0.182	8,764	1.31	0.0097	11,845	1.46	0.237	8,448	1.95	0.005	5,430	1.44
Propane	0.024	30,649	1.08	0.161	7,737	1.34	0.0225	27,572	1.22	0.324	11,570	2.04	0.017	20,480	1.21
i-Butane	0.005	5,687	1.05	0.015	733	1.34	0.0045	5,515	1.14	0.036	1,272	2.14	0.004	4,947	1.16
n-Butane	0.011	14,353	1.04	0.029	1,371	1.34	0.0115	14,032	1.10	0.068	2,440	2.14	0.011	12,941	1.11
i-Pentane	0.003	3,494	1.02	0.003	156	1.33	0.0028	3,457	1.05	0.008	280	2.14	0.003	3,332	1.05
n-Pentane	0.003	3,849	1.02	0.003	131	1.33	0.0031	3,818	1.03	0.007	235	2.14	0.003	3,713	1.04
Hexane	0.001	1,803	1.01	0.000	22	1.32	0.0015	1,798	1.01	0.001	38	2.14	0.001	1,781	1.02
CO2	0.002	2,374	1.06	0.032	1,546	1.18	0.0009	1,048	1.14	0.024	856	1.38	0.000	248	0.82
N2	0.000	83	1.23	0.002	78	1.26	0.0000	11	2.23	0.000	11	2.30	0.000	1	2.68
C7+	0.911	1,144,334	1.00	0.000	5	1.32	0.9343	1,144,334	1.00	0.000	5	2.07	0.954	1,144,333	1.00
C3 Plus	0.959	1,204,168	1.00	0.211	10,155	1.34	0.9802	1,200,525	1.01	0.444	15,840	2.06	0.994	1,191,526	1.00
C5 Plus	0.918	1,153,479	1.00	0.007	314	1.33	0.9418	1,153,407	1.00	0.016	558	2.14	0.962	1,153,159	1.00

* With respect to the same stream in the base process

When the permeate streams are mixed with the bottom streams of the separators to feed the next separator, the amount of CH₄ and N₂ increase notably. The amount of heavier hydrocarbons also increases but to a much lesser extent. As a result of the implementation of three membranes into the process, the quality of the crude oil is reduced since it is richer in lighter hydrocarbons. This result is also reflected in the comparison of the two-phase envelopes of the output stream for both processes in Figure 6.9.

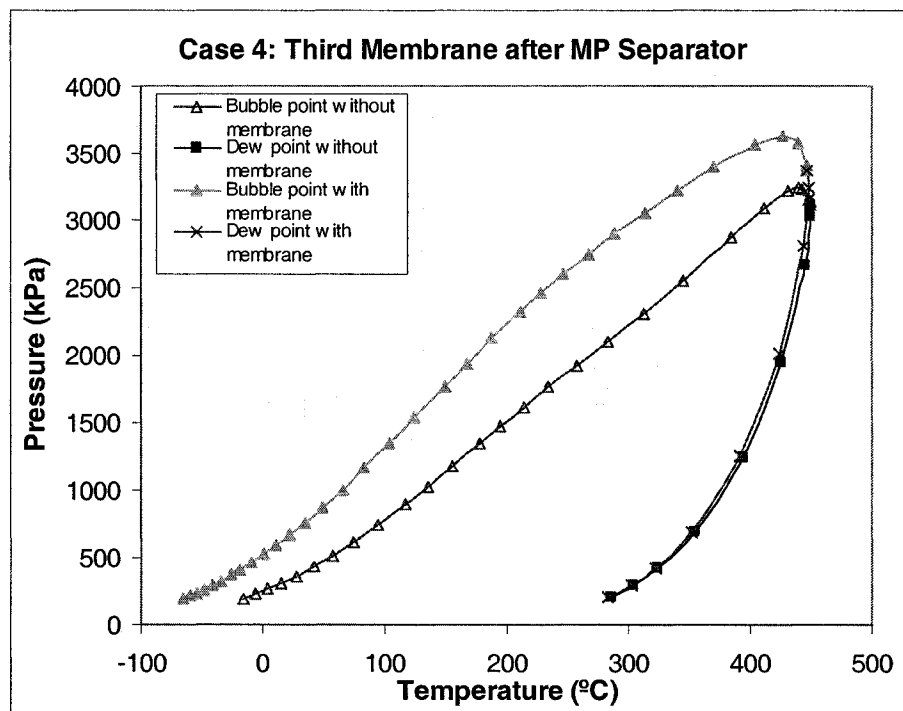


Figure 6.9: Phase envelopes for the stream “Crude Oil Product” for both processes

In Table 6.10, a description of the crude oil production for Case 4 is outlined. As mentioned previously, the recovery of heavier hydrocarbons is slightly higher than the base process, while the amount of methane is three times the value of the base process.

Therefore, the efficiency of the process is reduced for this case. Due to the excessive amount of methane in the output of the system, RVP value is larger than the base process due to the large amount of methane, which makes less attractive.

Table 6.10: Crude oil production of the process of Case 4

	Mass Flow (kg/h)	Recovery (%)	RVP (psia)	Volume Flow	
				(m ³ /h)	(bbl/day)
Total	1,199,126	82.51	28.588	1,380	208,334
Methane	1921	1.06	-	-	-
Ethane Plus	1,196,957	94.80	-	1,376	207,748
Propane Plus	1,191,526	97.32	-	1,367	206,411
C5+	1,153,159	99.90	-	1,307	197,392

6.2.5 Case 5: Four membranes: membranes after each separator and one treating all the residue streams

In Case 5, four membranes are introduced into the process. Three membranes are arranged with the same configuration as in Case 4. A fourth membrane treats the residue streams of the three membranes together, which are at a pressure of 7,000 kPa (the permeate of the third membrane is compressed to reach this pressure). Then, the permeate stream of this membrane is mixed with the crude oil coming from the low-pressure separator simultaneously with the permeate coming from the membrane treating the associated gas from this separator. Thus, this new mixed stream forms the crude oil production of the process. Figure 6.10 outlines the process flow.

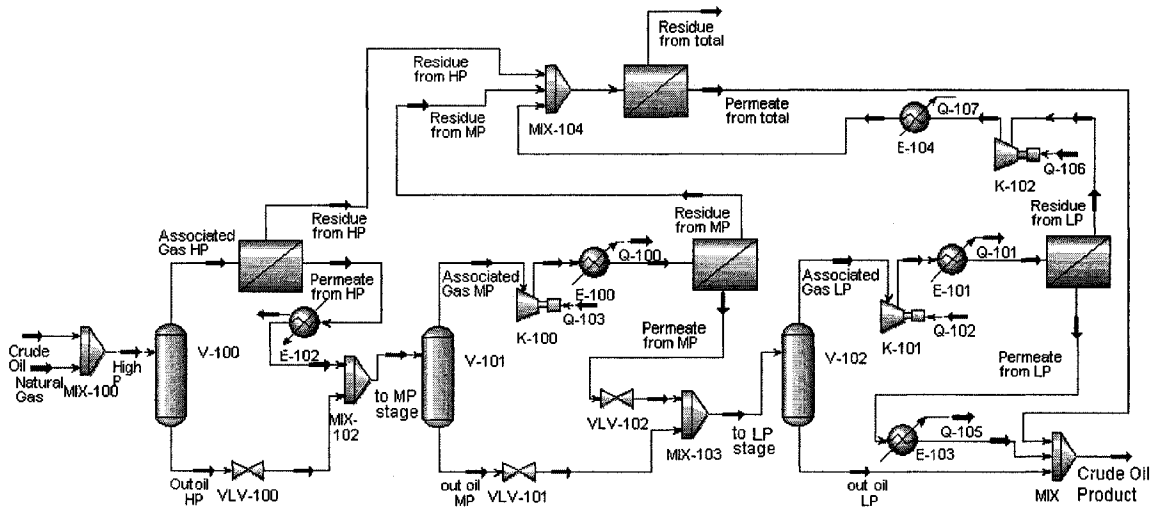


Figure 6.10: Case 5: Four membranes, three membranes located after each separator and one treating all the residual streams

In Table 6.11, the mass fractions and mass flow rates of each component are outlined for the output stream of the process (“Crude Oil Product”). This stream is constituted of the bottom stream leaving the low-pressure separator, the permeate stream from the third membrane, and the permeate stream of the fourth membrane.

Table 6.11: Mass fractions and mass flow rates for the streams specified for Case 5

	Crude Oil Product		
	Mass Frac.	Mass Flow (kg/h)	(%)*
Total	1.000	1,202,453	1.01
Methane	0.003	3,557	4.99
Ethane	0.005	6,062	1.61
Propane	0.018	21,215	1.25
i-Butane	0.004	5,029	1.18
n-Butane	0.011	13,098	1.13
i-Pentane	0.003	3,352	1.06
n-Pentane	0.003	3,730	1.04
Hexane	0.001	1,784	1.02
CO2	0.000	288	0.96
N2	0.000	4	16.33
C7+	0.952	1,144,335	1.00
C3 Plus	0.992	1,192,542	1.01
C5 Plus	0.959	1,153,201	1.00

* With respect to the same stream in the base process

The crude oil shows a considerable increase in the amount of N₂ and CH₄, which will reduce its quality. LPG components are in a larger proportion when compared with the base process. This effect is also shown in the phase diagrams (see Figure 6.11).

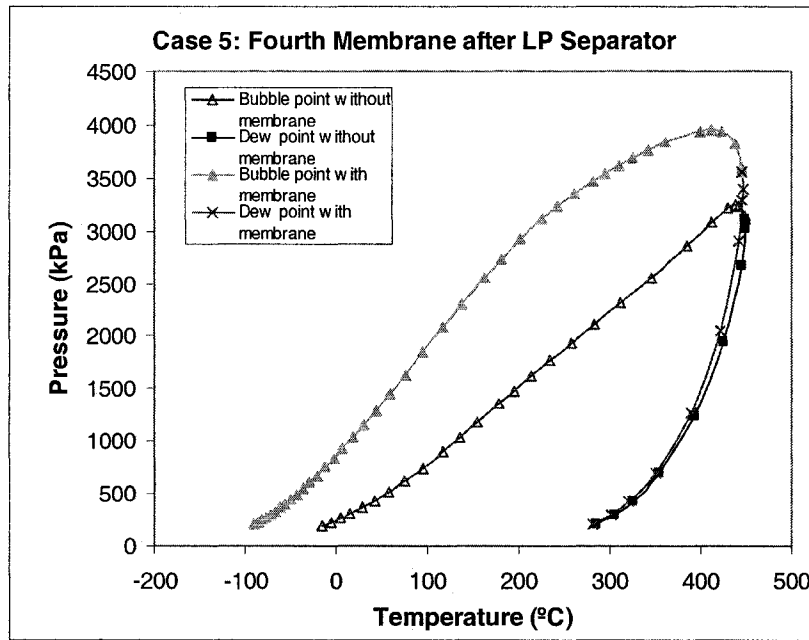


Figure 6.11: Phase envelopes for the stream “Crude Oil Product” for both processes

In Table 6.12, the crude oil composition for Case 5 is outlined. In this process, the recovery of heavier hydrocarbons is higher than the base process; however the amount of methane is remarkably larger than in crude oil of the base process.

The introduction of the membranes into the process accomplishes a high recovery of the heavier hydrocarbons but the amount of methane decreases the overall quality of the crude product. Therefore, this process is also rejected.

Table 6.12: Crude oil production of the process of Case 5

	Mass Flow (kg/h)	Recovery (%)	RVP (psia)	Volume Flow	
				(m ³ /h)	(bbl/day)
Total	1,202,452	82.74	36.026	1,386	209,245
Methane	3,557	1.95	-	-	-
Ethane Plus	1,198,604	94.93	-	1,379	208,149
Propane Plus	1,192,542	97.40	-	1,369	206,654
C5+	1,153,201	99.91	-	1,307	197,401

6.2.6 Case 6: Membranes after MP separator with recycle from LP separator

In Case 6, a membrane is placed after the second separator (V-101 at 1,724 kPa). The associated gas from V-102 is compressed to a pressure of 1,724 kPa. Then, this stream is mixed with the associated gas coming from V-101. Before entering to the membrane, these streams are compressed to 7,000 kPa and cooled. The heavier hydrocarbons are concentrated on the low-pressure side of the membrane (1,724 kPa), while the lighter gases are retained on the high-pressure side of the membrane. The “Permeate from MP” stream is mixed with the crude oil from V-102. Figure 6.4 outlines the process flow.

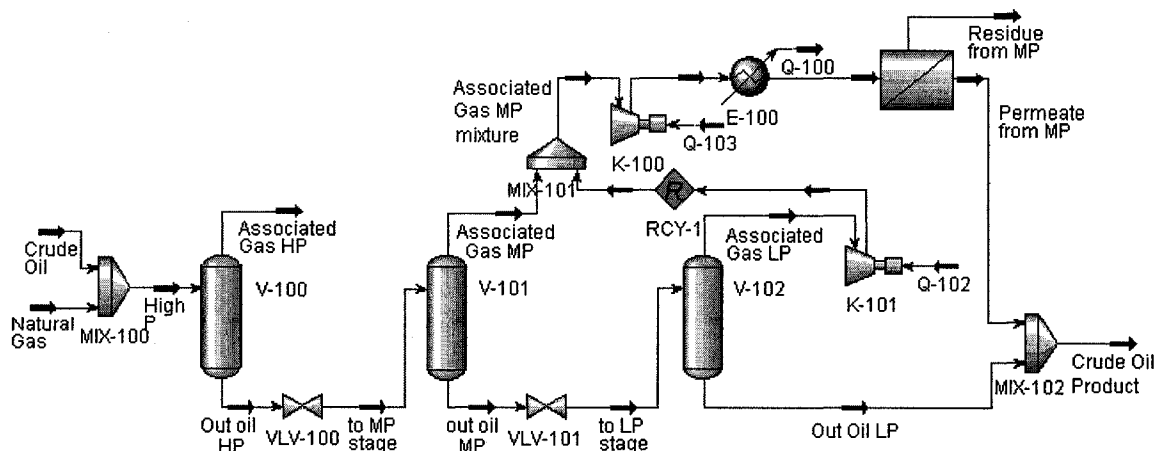


Figure 6.12: Case 6: Membrane after MP separator with recycle from LP separator

Table 6.13 outlines the concentrations and flow rates component are indicated for the associate gas from the low-pressure separator and the output stream of the process (“Crude Oil Product”), where the crude oil is concentrated.

Table 6.13: Mass fractions and mass flow rates for the streams specified for Case 6

	Associated Gas MP mixture			Crude Oil Product		
	Mass Frac.	Mass Flow (kg/h)	(%)*	Mass Frac.	Mass Flow (kg/h)	(%)*
Total	1.000	53,556	1.47	1.000	1,211,594	1.02
Methane	0.472	25,267	1.21	0.005	6,487	9.09
Ethane	0.206	11,018	1.65	0.007	8,643	2.29
Propane	0.214	11,472	1.98	0.020	24,112	1.43
i-Butane	0.021	1,140	2.09	0.004	5,171	1.21
n-Butane	0.040	2,167	2.11	0.011	13,372	1.15
i-Pentane	0.005	248	2.11	0.003	3,372	1.06
n-Pentane	0.004	209	2.11	0.003	3,747	1.05
Hexane	0.001	34	2.06	0.001	1,782	1.02
CO2	0.036	1,929	1.47	0.000	581	1.93
N2	0.001	67	1.08	0.000	6	23.45
C7+	0.000	6	1.69	0.944	1,144,323	1.00
C3 Plus	0.285	15,275	2.01	0.987	1,195,877	1.01
C5 Plus	0.009	497	2.10	0.952	1,153,222	1.00

* With respect to the same stream in the base process

From Table 6.13, two impacts can be observed. First, the mixture of the two associated gas streams from low and medium pressure separators produce a larger increase in the concentration of heavier hydrocarbons compared to the lighter gases. This will enhance membrane’s efficiency. The second impact is observed in the output stream of the process (“Crude Oil Product”). In this stream, the concentration of CH₄ and N₂ is much higher than the base case while the LPG concentration also increases but to a much lesser extent. As a result, the crude oil quality decreases. Figure 6.13 depicts the two-

phase envelopes of the output stream (“Crude Oil Product”). In this figure, the large increase in the two-phase region of the envelope is obvious.

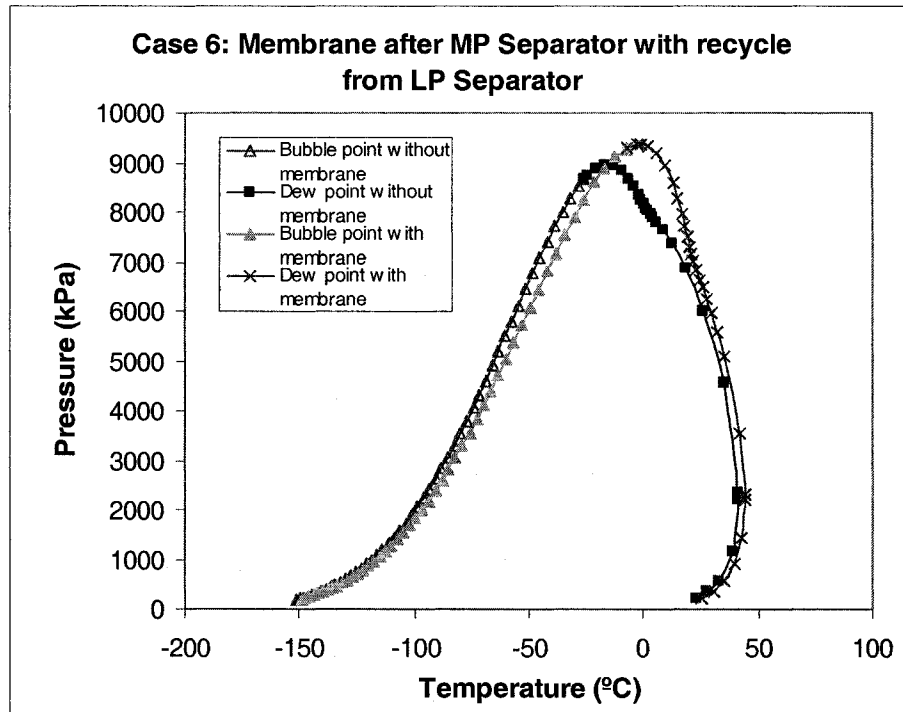


Figure 6.13: Phase envelopes for the stream “Out Oil LP” for both processes

Table 6.14 outlines the composition of the crude oil product for Case 6. In this process, the recovery of heavier hydrocarbons is higher than the base process; however the amount of methane in crude oil is also much larger. As with Case 5, the effect of mixing the permeate streams with the crude oil coming from the low-pressure separator adds a considerable amount of lighter gases to the crude oil reducing its quality. This is also demonstrated by the high RVP value, which is more than twice the base case’s value. Thus, this process is also rejected.

Table 6.15 outlines the mass fractions and mass flow rates for each streams that differ from the base process including: the associate gas MP mixture, the associated gas LP, and the bottom streams of the medium and low pressure separators, “To LP stage” and “Crude Oil Product”, respectively.

Table 6.15: Mass fractions and mass flow rates for the streams specified for Case 7

	Associated Gas MP mixture			To LP stage			Associated Gas LP			Crude Oil Product		
	Mass Frac.	Mass Flow (kg/h)	(%)*	Mass Frac.	Mass Flow (kg/h)	(%)*	Mass Frac.	Mass Flow (kg/h)	(%)*	Mass Frac.	Mass Flow (kg/h)	(%)*
Total	1.000	77,236	2.12	1.000	1,234,862	1.02	1.000	40,784	2.39	1.000	1,194,078	1.00
Methane	0.397	30,670	1.47	0.009	10,499	2.05	0.241	9,812	2.22	0.001	687	0.96
Ethane	0.220	16,971	2.54	0.011	14,188	1.75	0.253	10,312	2.37	0.003	3,876	1.03
Propane	0.264	20,388	3.52	0.027	33,428	1.48	0.359	14,625	2.58	0.016	18,803	1.11
i-Butane	0.027	2,092	3.83	0.005	6,332	1.30	0.038	1,549	2.61	0.004	4,783	1.12
n-Butane	0.051	3,905	3.81	0.013	15,541	1.22	0.071	2,884	2.53	0.011	12,657	1.09
i-Pentane	0.006	432	3.69	0.003	3,609	1.09	0.008	315	2.41	0.003	3,294	1.04
n-Pentane	0.005	362	3.66	0.003	3,945	1.07	0.006	263	2.39	0.003	3,682	1.03
Hexane	0.001	58	3.49	0.001	1,813	1.02	0.001	41	2.35	0.001	1,771	1.01
CO2	0.029	2,276	1.74	0.001	1,170	1.27	0.024	967	1.56	0.000	203	0.67
N2	0.001	72	1.16	0.000	10	1.88	0.000	9	1.93	0.000	0	0.84
C7+	0.000	10	2.62	0.927	1,144,328	1.00	0.000	6	2.36	0.958	1,144,322	1.00
C3 Plus	0.353	27,247	3.58	0.979	1,208,996	1.01	0.483	19,684	2.57	0.996	1,189,312	1.00
C5 Plus	0.011	861	3.65	0.934	1,153,695	1.00	0.015	625	2.40	0.966	1,153,070	1.00

* With respect to the same stream in the base process

The combination of the two associated gas stream creates a stream with a much larger proportion of heavier hydrocarbons, while the CO₂, N₂ and CH₄ proportions do not increase significantly. When the permeate stream is mixed with the bottom stream of the medium separator (“To LP stage”) the concentrations of all components increase but the lighter gases increase to a larger degree. In the low-pressure separator, the associated gas is twice the base value for almost all components. However, there is a lower concentration of lighter gases (CO₂, N₂ and CH₄) in the final oil product (“Crude Oil Product”) and the concentration of heavier hydrocarbons is slightly larger than the base case. This is reflected in the two-phase diagrams for both processes in Figure 6.15. In this figure, both processes possess similar bubble and dew point curves.

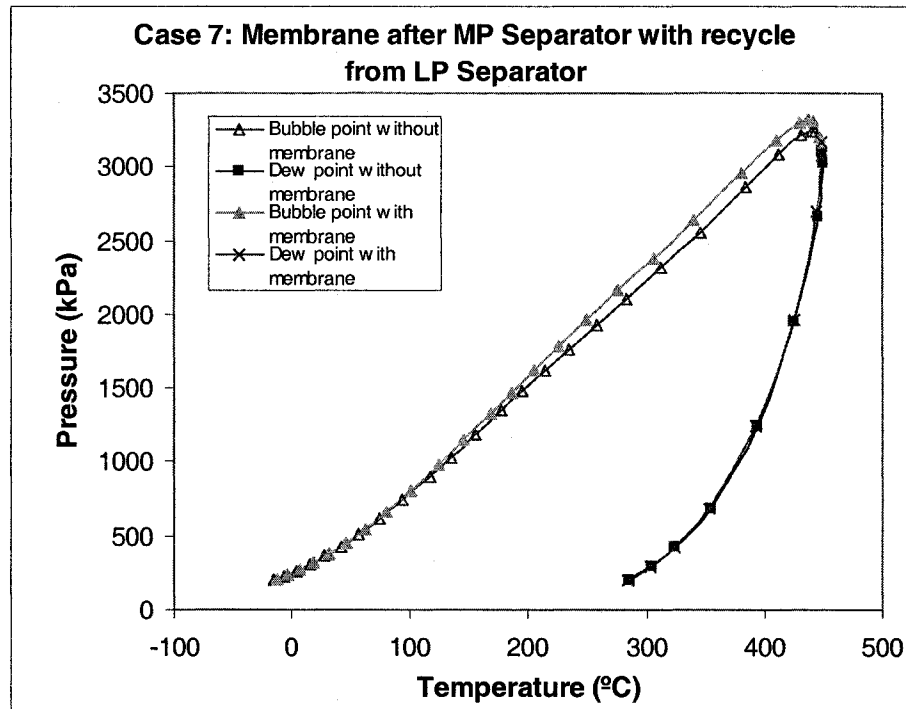


Figure 6.15: Phase envelopes for the stream “Crude Oil Product” for both processes

In Table 6.14, the crude oil production for Case 7 is outlined. This process possesses several advantages with respect to the other cases. The amount of methane is lower than the process, and at the same time the production of heavier hydrocarbons is larger. In addition the RVP value is closer to the base RVP value. Therefore, this process is more attractive than the base process.

Table 6.16: Crude oil production of the process of Case 7

	Mass Flow (kg/h)	Recovery (%)	RVP (psia)	Volume Flow	
				(m ³ /h)	(bbl/day)
Total	1,194,078	82.16	20.879	1,371	207,044
Methane	687	0.38	-	-	-
Ethane Plus	1,193,188	94.50	-	1,370	206,836
Propane Plus	1,189,312	97.14	-	1,364	205,882
C5+	1,153,070	99.90	-	1,307	197,372

6.2.8 Case 8: Membrane after MP separator with recycle from LP separator

In Case 8, a membrane is placed after the second separator (V-101). The associated gas from V-102 is compressed to 1,724 kPa and then mixed with associated gas from the medium-pressure separator. This mixture, called “Associated Gas MP mixture”, is the feed to the membrane. Before entering the membrane, the mix is compressed to 7,000 kPa, and then cooled to 35 °C. The permeate stream of the membrane is sent to feed the medium-pressure separator together with the bottom stream (“to MP stage”) coming from the high-pressure separator.

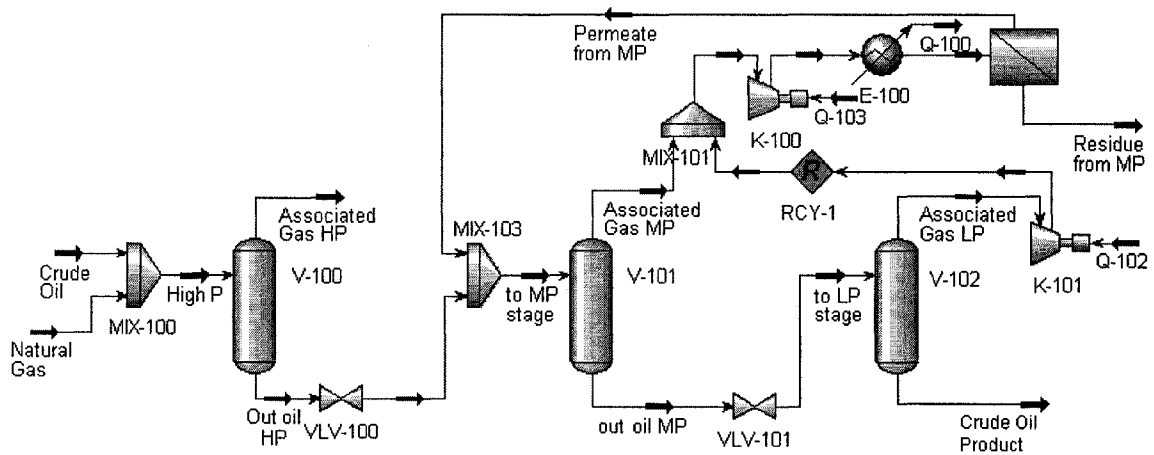


Figure 6.16: Case 8: Membrane after MP separator with recycle from LP separator

Table 6.17 outlines the mass fractions and mass flow rates of each component for those streams that differ from the base process including: the associate gas MP mixture, the associated gas LP, and the bottom streams of the medium and low pressure separators, “To LP stage” and “Crude Oil Product”, respectively.

Table 6.17: Mass fractions and mass flow rates for the streams specified for Case 8

	Associated Gas MP mixture			To LP stage			Associated Gas LP			Crude Oil Product		
	Mass Frac.	Mass Flow (kg/h)	(%)*	Mass Frac.	Mass Flow (kg/h)	(%)*	Mass Frac.	Mass Flow (kg/h)	(%)*	Mass Frac.	Mass Flow (kg/h)	(%)*
Total	1.000	72,511	1.99	1.000	1,217,361	1.01	1.000	21,082	1.24	1.000	1,196,279	1.00
Methane	0.426	30,855	1.48	0.004	4,986	0.97	0.207	4,369	0.99	0.001	617	0.87
Ethane	0.227	16,468	2.47	0.008	9,919	1.22	0.268	5,655	1.30	0.004	4,265	1.13
Propane	0.242	17,532	3.03	0.023	28,063	1.24	0.373	7,860	1.38	0.017	20,204	1.19
i-Butane	0.023	1,665	3.05	0.005	5,703	1.18	0.038	797	1.34	0.004	4,906	1.15
n-Butane	0.042	3,041	2.97	0.012	14,380	1.13	0.070	1,476	1.29	0.011	12,904	1.11
i-Pentane	0.005	328	2.81	0.003	3,484	1.05	0.008	160	1.22	0.003	3,324	1.05
n-Pentane	0.004	274	2.77	0.003	3,840	1.04	0.006	133	1.21	0.003	3,707	1.04
Hexane	0.001	44	2.67	0.001	1,796	1.01	0.001	21	1.19	0.001	1,775	1.01
CO2	0.031	2,222	1.70	0.001	860	0.93	0.029	605	0.98	0.000	255	0.85
N2	0.001	71	1.15	0.000	4	0.84	0.000	4	0.85	0.000	0	0.74
C7+	0.000	9	2.34	0.940	1,144,325	1.00	0.000	3	1.23	0.957	1,144,322	1.00
C3 Plus	0.316	22,894	3.01	0.987	1,201,592	1.01	0.496	10,449	1.36	0.996	1,191,142	1.00
C5 Plus	0.009	656	2.78	0.947	1,153,445	1.00	0.015	317	1.22	0.964	1,153,128	1.00

* With respect to the same stream in the base process

The process of Case 8 changes the proportion of the components in the medium and low-pressure separator output streams. As such, concentrations of all components increase in the associated gas of the medium-pressure separator when compared with to base process. The bottom stream of the low-pressure separator (V-102) contains a larger amount of heavy hydrocarbons and lower amounts of CH₄, CO₂, N₂.

The phase envelopes for the process of Case 8 and for the base process are shown in Figure 6.17.

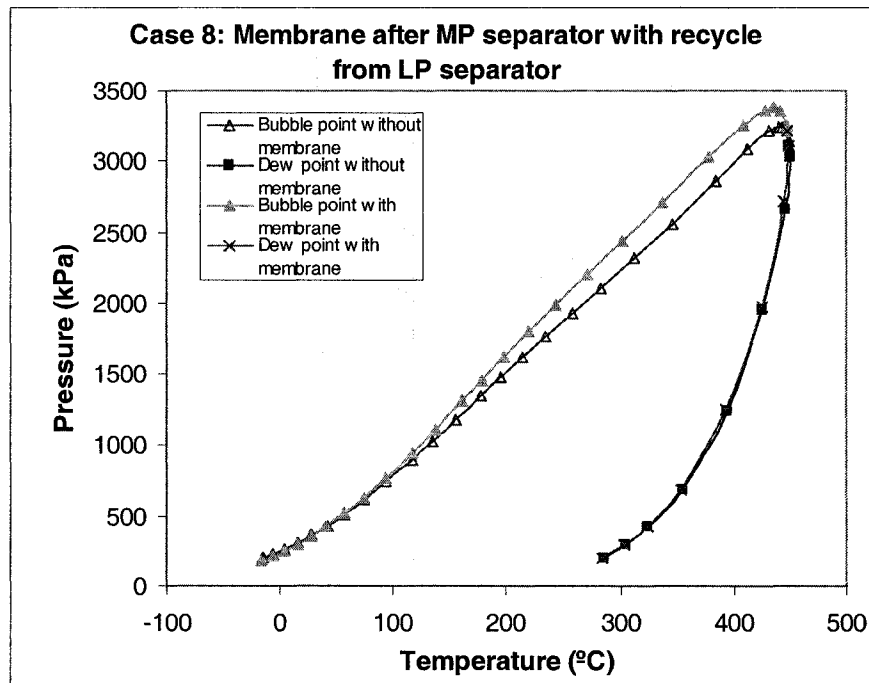


Figure 6.17: Phase envelopes for the stream “Crude Oil Product” for both processes

Table 6.18 outlines the crude oil product composition for Case 8. This process possesses a higher C₂₊, C₃₊ and C₅₊ recovery percentages that the process presented in Case 7. For example, the amount of methane is much lower than the base process, and a

larger proportion of heavy hydrocarbons, is obtained. In addition the RVP value is considerably close to the base RVP value. Therefore, this process can be considered as a promising alternative for offshore NGL production.

Table 6.18: Crude oil production of the process of Case 8

	Mass Flow (kg/h)	Recovery (%)	RVP (psia)	Volume Flow	
				(m ³ /h)	(bbl/day)
Total	1,196,279	82.31	21.908	1,375	207,561
Methane	617	0.34	-	-	-
Ethane Plus	1,195,407	94.68	-	1,373	207,370
Propane Plus	1,191,142	97.29	-	1,366	206,320
C5+	1,153,128	99.90	-	1,307	197,385

6.2.9 Case 9: Membrane after LP separator recycling the permeate to feed the MP separator

In Case 9, a membrane is placed to treat the associated gas from low-pressure separator. Before entering the membrane, the associated gas is compressed to 1,724 kPa and cooled to 35 °C. Then, the permeate stream of the membrane is sent back to feed the medium-pressure separator together with the oil coming from the high-pressure separator at a pressure of 1,724 kPa.

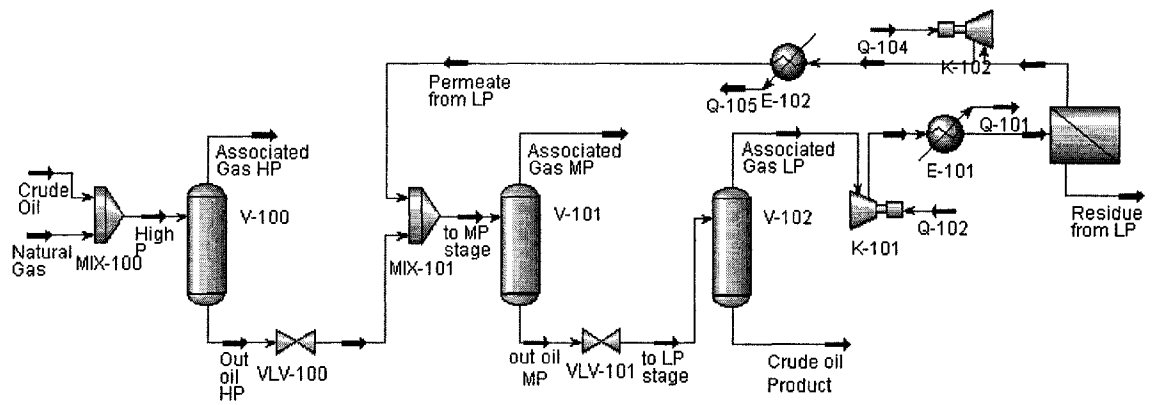


Figure 6.18: Case 9: Membrane after LP separator recycling the permeate to feed the MP separator

In Table 6.19, the mass fractions and mass flow rates of each component are indicated for those streams that differ from the base process.

Table 6.19: Mass fractions and mass flow rates for the streams specified for Case 9

	To MP stage			Associated Gas MP			To LP stage			Associated Gas LP			Crude Oil Product		
	Mass Frac.	Mass Flow (kg/h)	(%)*	Mass Frac.	Mass Flow (kg/h)	(%)*	Mass Frac.	Mass Flow (kg/h)	(%)*	Mass Frac.	Mass Flow (kg/h)	(%)*	Mass Frac.	Mass Flow (kg/h)	(%)*
Total	1.000	1,254,309	1.01	1.000	41,209	1.13	1.000	1,213,100	1.00	1.000	18,974	1.11	1.000	1,194,126	1.00
Methane	0.022	27,010	1.04	0.535	22,059	1.06	0.004	4,950	0.97	0.226	4,295	0.97	0.001	655	0.92
Ethane	0.014	17,188	1.16	0.198	8,171	1.22	0.007	9,017	1.11	0.261	4,961	1.14	0.003	4,057	1.07
Propane	0.026	33,159	1.17	0.178	7,334	1.27	0.021	25,825	1.14	0.359	6,806	1.20	0.016	19,019	1.12
i-Butane	0.005	6,017	1.11	0.016	668	1.22	0.004	5,349	1.10	0.037	694	1.17	0.004	4,655	1.09
n-Butane	0.012	14,968	1.08	0.030	1,226	1.20	0.011	13,742	1.08	0.069	1,305	1.14	0.010	12,437	1.07
i-Pentane	0.003	3,550	1.04	0.003	135	1.15	0.003	3,415	1.03	0.008	144	1.10	0.003	3,271	1.03
n-Pentane	0.003	3,896	1.03	0.003	113	1.15	0.003	3,783	1.03	0.006	121	1.10	0.003	3,662	1.02
Hexane	0.001	1,805	1.01	0.000	19	1.13	0.001	1,787	1.01	0.001	19	1.08	0.001	1,768	1.01
CO2	0.002	2,324	1.04	0.034	1,418	1.08	0.001	906	0.98	0.033	622	1.00	0.000	284	0.94
N2	0.000	67	1.01	0.002	63	1.01	0.000	5	0.93	0.000	5	0.93	0.000	0	0.88
C7+	0.912	1,144,325	1.00	0.000	4	1.16	0.943	1,144,321	1	0.000	3	1.10	0.958	1,144,318	1.00
C3 Plus	0.963	1,207,720	1.01	0.230	9,499	1.25	0.988	1,198,222	1	0.479	9,092	1.18	0.996	1,189,130	1.00
C5 Plus	0.920	1,153,576	1.00	0.007	271	1.15	0.951	1,153,305	1	0.015	287	1.10	0.966	1,153,018	1.00

*With respect to the same stream in the base process

In Figure 6.19, the phase envelopes for the process of Case 9 and for the base process are indicated. The dew point curves of both processes almost exactly overlap, but the bubble point curves differ slightly.

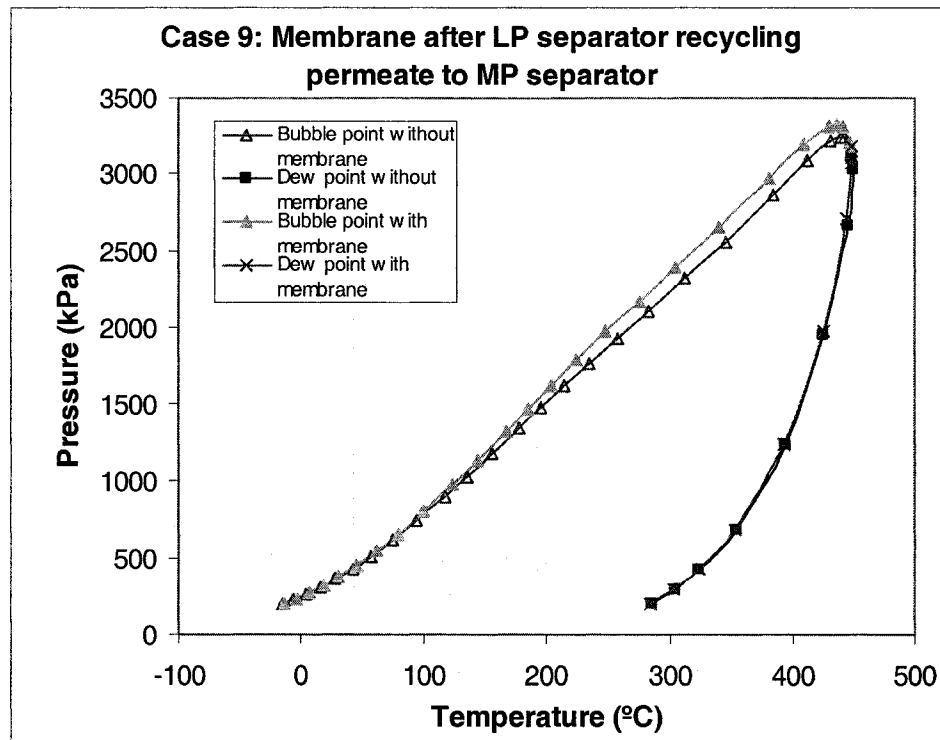


Figure 6.19: Phase envelopes for the stream “Crude Oil Product” for both processes

Table 6.20 outlines the crude oil product for Case 9. As the table illustrates, a better recovery of heavy hydrocarbons with relatively lower amount of methane can be achieved when compared with the base process. However, this process does not approach the large recovery obtained in the process of Case 8. As a result, this configuration of the process is not considered for a further analysis.

Table 6.20: Crude oil production of the process of Case 9

	Mass Flow (kg/h)	Recovery (%)	RVP (psia)	Volume Flow	
				(m ³ /h)	(bbl/day)
Total	1,194,126	82.17	21.162	1,371	207,040
Methane	655	0.36	-	-	-
Ethane Plus	1,193,186	94.50	-	1,370	206,838
Propane Plus	1,189,130	97.12	-	1,363	205,841
C5+	1,153,018	99.89	-	1,307	197,361

6.2.10 Case 10: Membrane after LP separator recycling the permeate to feed the LP separator

In Case 10, a membrane is placed to treat the associated gas from low-pressure separator. Before entering the membrane, the associated gas is compressed to 1,724 kPa and cooled to 35 °C. Then, the permeate stream of the membrane is sent back to feed the low-pressure separator together with the oil coming from the medium pressure separator at a pressure of 413.7 kPa.

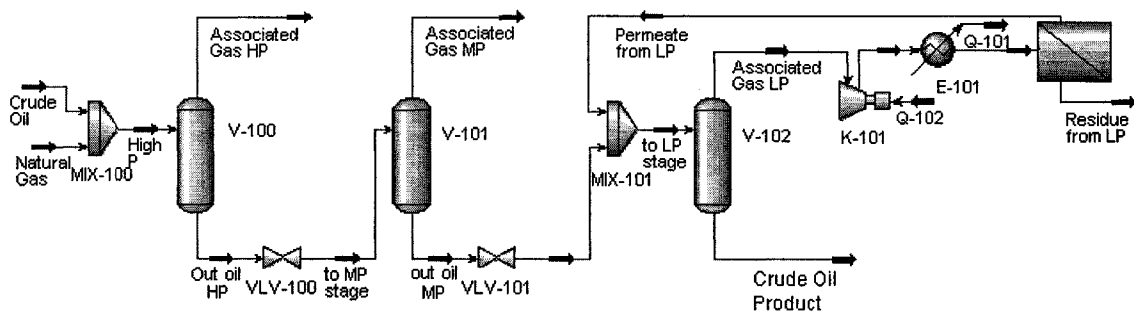


Figure 6.20: Case 10: Membrane after LP separator recycling the permeate to feed the LP separator

In Table 6.21, the mass fractions and mass flow rates of each component are shown for those streams that differ from their values in the base process. These streams are the feed to the low-pressure separator (“to LP stage”), the associate gas LP, and the oil leaving this separator “Crude Oil Product”.

Table 6.21: Mass fractions and mass flow rates for the streams specified for Case 10

	To LP stage			Associated Gas LP			Crude Oil Product		
	Mass Frac.	Mass Flow (kg/h)	(%)*	Mass Frac.	Mass Flow (kg/h)	(%)*	Mass Frac.	Mass Flow (kg/h)	(%)*
Total	1.000	1,218,600	1.01	1.000	24,485	1.44	1.000	1,194,115	1.00
Methane	0.005	6,121	1.19	0.224	5,473	1.24	0.001	648	0.91
Ethane	0.009	10,626	1.31	0.266	6,508	1.50	0.003	4118	1.09
Propane	0.023	27,769	1.23	0.359	8,791	1.55	0.016	18,978	1.12
i-Butane	0.005	5,570	1.15	0.037	902	1.52	0.004	4,668	1.10
n-Butane	0.012	14,124	1.11	0.069	1,692	1.48	0.010	12,432	1.07
i-Pentane	0.003	3,452	1.04	0.008	187	1.43	0.003	3,266	1.03
n-Pentane	0.003	3,814	1.03	0.006	156	1.42	0.003	3,657	1.02
Hexane	0.001	1,791	1.01	0.001	25	1.41	0.001	1,767	1.01
CO2	0.001	1,005	1.09	0.030	742	1.20	0.000	263	0.87
N2	0.000	5	1.07	0.000	5	1.08	0.000	0	0.79
C7+	0.939	1,144,323	1.00	0.000	4	1.44	0.958	1,144,319	1.00
C3 Plus	0.985	1,200,843	1.01	0.480	11,757	1.53	0.996	1,189,086	1.00
C5 Plus	0.946	1,153,380	1.00	0.015	372	1.43	0.966	1,153,009	1.00

* With respect to the same stream in the base process

The introduction of the permeate stream in the feed of the low-pressure separator increases the amount of lighter gases such as CH₄, N₂, and CO₂ as well as the amount of the LPG components. Heavier hydrocarbons do not vary appreciably. In the associated gas all the components are higher in quantity than the base process. In addition, the crude oil leaving the separator is lower in lighter gases (e.g. CH₄, N₂, and CO₂) while the amount of LPG increases compared with the base process.

In Figure 6.21, the two-phase envelopes for the output stream (“Crude Oil Product”) are shown for Case 10 and the base case. The dew point curves are similar, while the bubble point of the process of Case 10 is slightly shifted giving a small increase in the two-phase area.

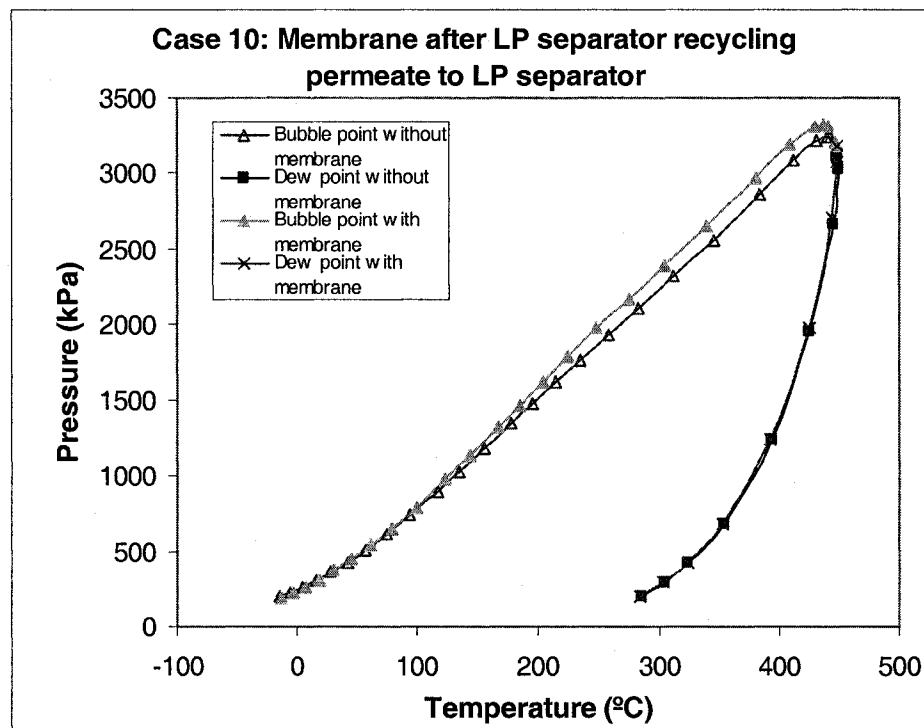


Figure 6.21: Phase envelopes for the stream “Crude Oil Product” for both processes

Table 6.22 outlines the crude oil product for Case 10. In this process, the amount of methane is lower than in the base process. In addition, the recovery of heavier hydrocarbons is also higher than the base process but not as high as Cases 7 and 8. The RVP value is slightly larger than in the base process. Due to the fact other configurations show a better performances, this process is not considered.

Table 6.22: Crude oil production of the process of Case 10

	Mass Flow (kg/h)	Recovery (%)	RVP (psia)	Volume Flow	
				(m ³ /h)	(bbl/day)
Total	1,194,115	82.17	21.176	1,371	207,042
Methane	648	0.36	-	-	-
Ethane Plus	1,193,204	94.50	-	1,370	206,843
Propane Plus	1,189,086	97.12	-	1,363	205,830
C5+	1,153,009	99.89	-	1,307	197,359

6.2.11 Case 11: Membrane after HP separator recycling the permeate to feed process

In Case 11, a membrane is placed after the high-pressure separator (7000 kPa) to treat the associated gas. Then, the permeate stream is sent to feed the high-pressure separator. This stream is mixed with the original feed of the high-pressure separator after compressing and cooling the permeate stream to achieve the condition of the separator (7000 kPa, and 35 °C). In Table 6.23, the mass fractions and mass flows of each component are indicated for all the streams detailed for the base process.

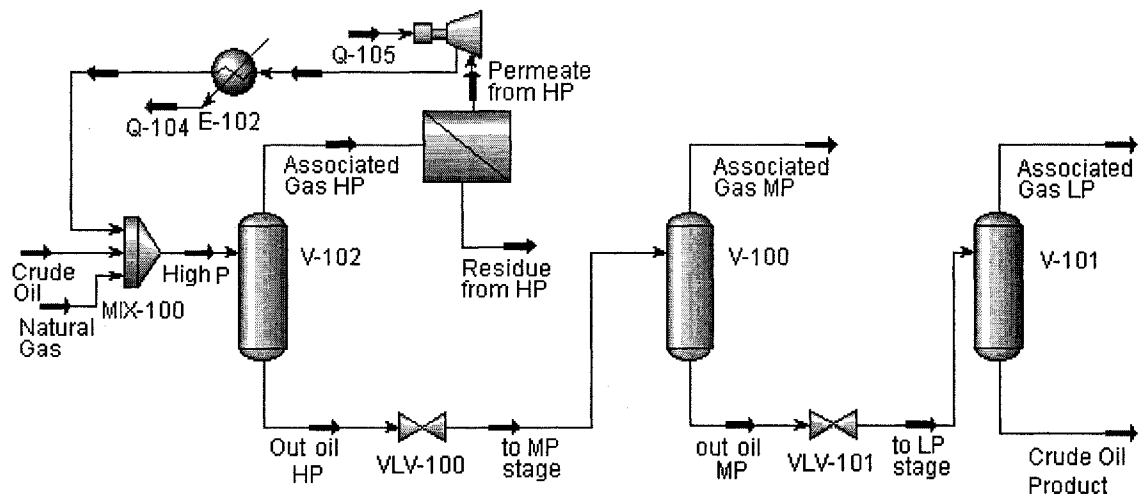


Figure 6.22: Case 11: Membrane after HP separator recycling the permeate to feed process

In Table 6.23, the mass fractions and mass flows of each component are indicated for all the streams indicated for the original process.

Table 6.23: Mass fractions and mass flows for the streams specified for the process of
Case 11

	Associated Gas HP			To MP stage			Associated Gas MP		
	Mass Frac.	Mass Flow (kg/h)	(%)*	Mass Frac.	Mass Flow (kg/h)	(%)*	Mass Frac.	Mass Flow (kg/h)	(%)*
Total	1.000	219,675	1.05	1.000	1,245,897	1.00	1.000	36,892	1.01
Methane	0.741	162,738	1.04	0.021	25,961	1.00	0.565	20,837	1.00
Ethane	0.115	25,198	1.07	0.012	15,203	1.03	0.186	6,860	1.03
Propane	0.086	18,835	1.08	0.024	29,337	1.03	0.162	5,991	1.03
i-Butane	0.008	1,856	1.08	0.004	5,563	1.03	0.015	563	1.03
n-Butane	0.016	3,521	1.07	0.011	14,136	1.02	0.028	1,050	1.02
i-Pentane	0.002	453	1.06	0.003	3468	1.01	0.003	119	1.01
n-Pentane	0.002	394	1.06	0.003	3,830	1.01	0.003	100	1.01
Hexane	0.000	79	1.05	0.001	1,797	1.00	0.000	17	1.01
CO2	0.025	5,488	1.03	0.002	2,203	0.99	0.035	1,292	0.99
N2	0.005	1,041	1.02	0.000	65	0.97	0.002	60	0.97
C7+	0.000	72	1.04	0.918	1,144,333	1.00	0.000	4	1.00
C3 Plus	0.115	25,211	1.08	0.965	1,202,465	1.00	0.213	7,843	1.03
C5 Plus	0.005	999	1.06	0.926	1,153,429	1.00	0.006	239	1.01

	To LP stage			Associated Gas LP			Crude Oil Product		
	Mass Frac.	Mass Flow (kg/h)	(%)*	Mass Frac.	Mass Flow (kg/h)	(%)*	Mass Frac.	Mass Flow (kg/h)	(%)*
Total	1.000	1,209,005	1.00	1.000	17,542	1.03	1	1,191,463	1.00
Methane	0.004	5,124	1.00	0.252	4,421	1	0.001	703	0.99
Ethane	0.007	8,343	1.03	0.256	4,495	1.04	0.003	3,848	1.02
Propane	0.019	23,346	1.03	0.338	5,933	1.05	0.015	17,413	1.03
i-Butane	0.004	5,000	1.03	0.035	620	1.04	0.004	4,380	1.03
n-Butane	0.011	13,086	1.02	0.068	1,185	1.04	0.010	11,901	1.02
i-Pentane	0.003	3,349	1.01	0.008	134	1.03	0.003	3,215	1.01
n-Pentane	0.003	3,730	1.01	0.006	113	1.02	0.003	3,617	1.01
Hexane	0.001	1,781	1.00	0.001	18	1.02	0.001	1,763	1.00
CO2	0.001	911	0.99	0.035	616	0.99	0.000	295	0.98
N2	0.000	5	0.97	0.000	5	0.98	0.000	0	0.96
C7+	0.947	1,144,329	1	0.000	3	1.01	0.960	1,144,327	1.00
C3 Plus	0.988	1,194,622	1	0.456	8,006	1.04	0.996	1,186,616	1.00
C5 Plus	0.954	1,153,190	1	0.015	267	1.03	0.968	1,152,922	1.00

* With respect to the same stream in the base process

The results do not differ largely from the values in the base process. In general, in this process the associated gas streams are richer in heavier hydrocarbons, while the crude oil concentrated streams leaving the separators have similar amounts of heavier hydrocarbons than the base case.

In Figure 6.23, the two phases enveloped of the output stream (“Crude Oil Product”) is shown for both processes. The curves for both processes further demonstrate that this configuration does not obtain a higher recovery of heavier hydrocarbons than the base process.

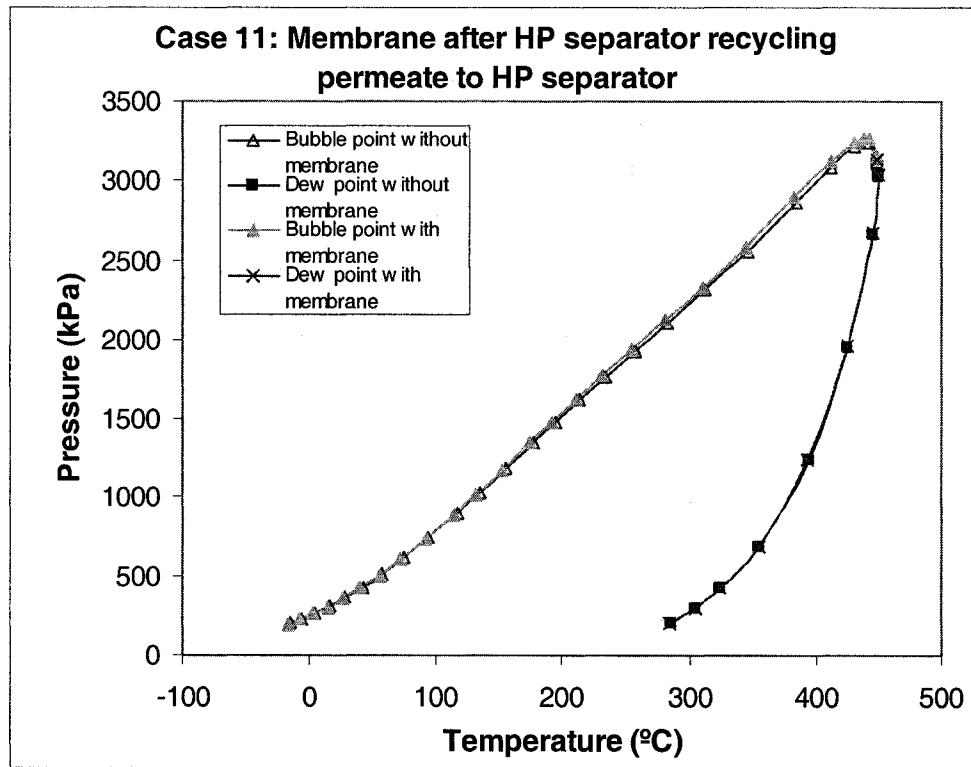


Figure 6.23: Phase envelopes for the stream “Crude Oil Product” for both processes

Table 6.24 outlines the composition and RVP value for the crude oil product for Case 11. The RVP value is also similar than the base values. Since the results achieved by this process do not impact the recoveries from the base process, this process is not considered a possible.

Table 6.24: Crude oil production of the process of Case 11

	Mass Flow (kg/h)	Recovery (%)	RVP (psia)	Volume Flow	
				(m ³ /h)	(bbl/day)
Total	1,191,463	81.98	20.215	1,367	206,400
Methane	703	0.39	-	-	-
Ethane Plus	1,190,465	94.28	-	1,366	206,186
Propane Plus	1,186,616	96.92	-	1,359	205,242
C5+	1,152,922	99.88	-	1,307	197,339

6.2.12 Case 12: Two membranes: one after HP separator recycling the permeate to feed process; and other membrane after MP separator, which receives a recycle from LP separator, and its permeate feeds the MP separator

In Case 12, two membranes are introduced into the original process. A first membrane placed after the high-pressure separator (7000 kPa) to treat the associated gas. Then, its permeate stream is sent to feed the high-pressure separator together with the original feed of this separator (streams “Crude Oil” and “Natural Gas”). The permeate stream is compressed to 7000 kPa and cooled to 35 °C to reach the condition of the separator. The second membrane is placed after the second separator (medium pressure separator, 1724 kPa). The feed of the membrane (“Associated Gas MP mixture”) is constituted by the associated gas of the medium pressure separator and the associated gas

from the low-pressure separator. Before mixing these to streams, the associated gas LP is compressed to 1724 kPa. After mixing the associated gases, the new stream is compressed to 7000 kPa, and then cooled to 35 °C before entering into the membrane. The permeate stream is sent back to feed the medium-pressure separator together with the bottom stream (“to MP stage”) from the high-pressure separator.

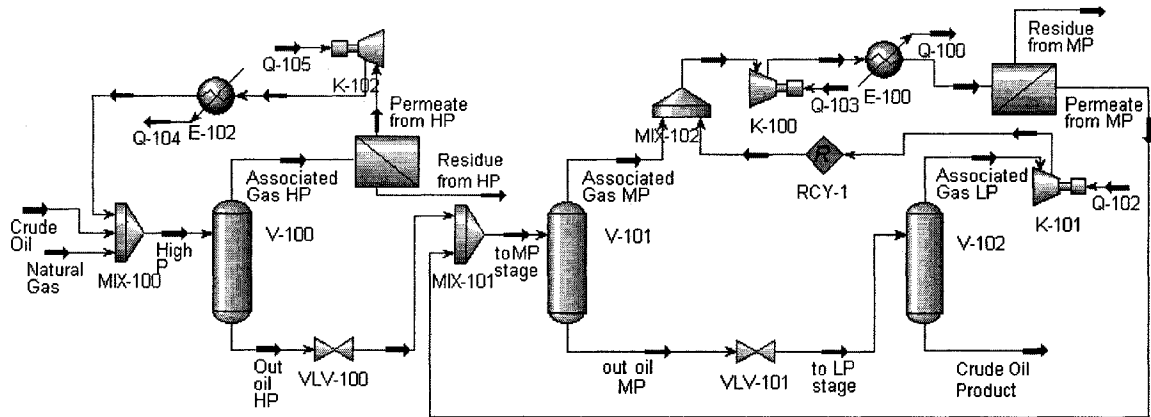


Figure 6.24: Case 12: Two membranes: one after HP separator recycling the permeate to feed process; and other membrane after MP separator, which receives a recycle from LP separator, and its permeate feeds the MP separator

In Table 6.25, the mass fractions and mass flows of each component are indicated for all the streams indicated for the original process.

Table 6.25: Mass fractions and mass flows for the streams specified for the process of
Case 12

	Associated Gas HP			To MP stage			Associated Gas MP		
	Mass Frac.	Mass Flow (kg/h)	(%)*	Mass Frac.	Mass Flow (kg/h)	(%)*		Mass Flow (kg/h)	(%)*
Total	1.000	219,675	1.05	1.000	1,271,239	1.02	1	52,004	1.42
Methane	0.741	162,738	1.04	0.025	31,411	1.21	0.508	26,432	1.27
Ethane	0.115	25,198	1.07	0.017	21,281	1.44	0.213	11,096	1.66
Propane	0.086	18,835	1.08	0.031	38,985	1.37	0.192	9,973	1.72
i-Butane	0.008	1,856	1.08	0.005	6,805	1.26	0.017	897	1.64
n-Butane	0.016	3,521	1.07	0.013	16,342	1.18	0.031	1,602	1.56
i-Pentane	0.002	453	1.06	0.003	3,705	1.08	0.003	171	1.46
n-Pentane	0.002	394	1.06	0.003	4,027	1.06	0.003	143	1.44
Hexane	0.000	79	1.05	0.001	1,829	1.02	0.000	23	1.41
CO2	0.025	5,488	1.03	0.002	2,445	1.10	0.031	1,596	1.22
N2	0.005	1,041	1.02	0.000	70	1.04	0.001	65	1.06
C7+	0.000	72	1.04	0.900	1,144,341	1.00	0.000	6	1.50
C3 Plus	0.115	25,211	1.08	0.957	1,216,033	1.01	0.246	12,815	1.69
C5 Plus	0.005	999	1.06	0.908	1,153,901	1.00	0.007	343	1.45

	To LP stage			Associated Gas LP			Crude Oil Product		
	Mass Frac.	Mass Flow (kg/h)	(%)*	Mass Frac.	Mass Flow (kg/h)	(%)*	Mass Frac.	Mass Flow (kg/h)	(%)*
Total	1.000	1,219,234	1.01	1.000	21,765	1.28	1.000	1,197,469	1.01
Methane	0.004	4,979	0.97	0.201	4,373	0.99	0.001	606	0.85
Ethane	0.008	10,185	1.25	0.269	5,853	1.35	0.004	4,332	1.15
Propane	0.024	29,012	1.28	0.378	8,233	1.45	0.017	20,779	1.23
i-Butane	0.005	5,908	1.22	0.039	838	1.41	0.004	5,069	1.19
n-Butane	0.012	14,739	1.15	0.071	1,537	1.35	0.011	13,202	1.13
i-Pentane	0.003	3,534	1.07	0.008	165	1.26	0.003	3,369	1.06
n-Pentane	0.003	3,884	1.05	0.006	137	1.25	0.003	3,747	1.05
Hexane	0.001	1,805	1.02	0.001	21	1.22	0.001	1,784	1.02
CO2	0.001	849	0.92	0.028	601	0.97	0.000	248	0.82
N2	0.000	4	0.82	0.000	4	0.82	0.000	0	0.71
C7+	0.939	1,144,336	1.00	0.000	3	1.24	0.956	1,144,332	1.00
C3 Plus	0.987	1,203,218	1.01	0.502	10,935	1.43	0.996	1,192,283	1.01
C5 Plus	0.946	1,153,559	1.00	0.015	327	1.25	0.963	1,153,232	1.00

* With respect to the same stream in the base process

Table 6.25 shows concentrations of the components in every stream differ from their values in the base process. In the first separator, the associated gas HP and the bottom stream show increases in all the components. Conversely in the second separator, the associated gas MP has larger amount of all the components, but the bottom stream has

higher amount of heavy hydrocarbons and lower amounts of CH₄, CO₂, and N₂. In the third separator, the associated gas LP and the crude oil product are richer in heavy hydrocarbons with a lower proportion of lighter gases (CH₄, CO₂, and N₂).

In figure 6.25, the two-phase envelopes are shown for both processes. The bubble point curve of the process of case 12 is shifted slightly to the left indicating a larger amount of heavy hydrocarbons.

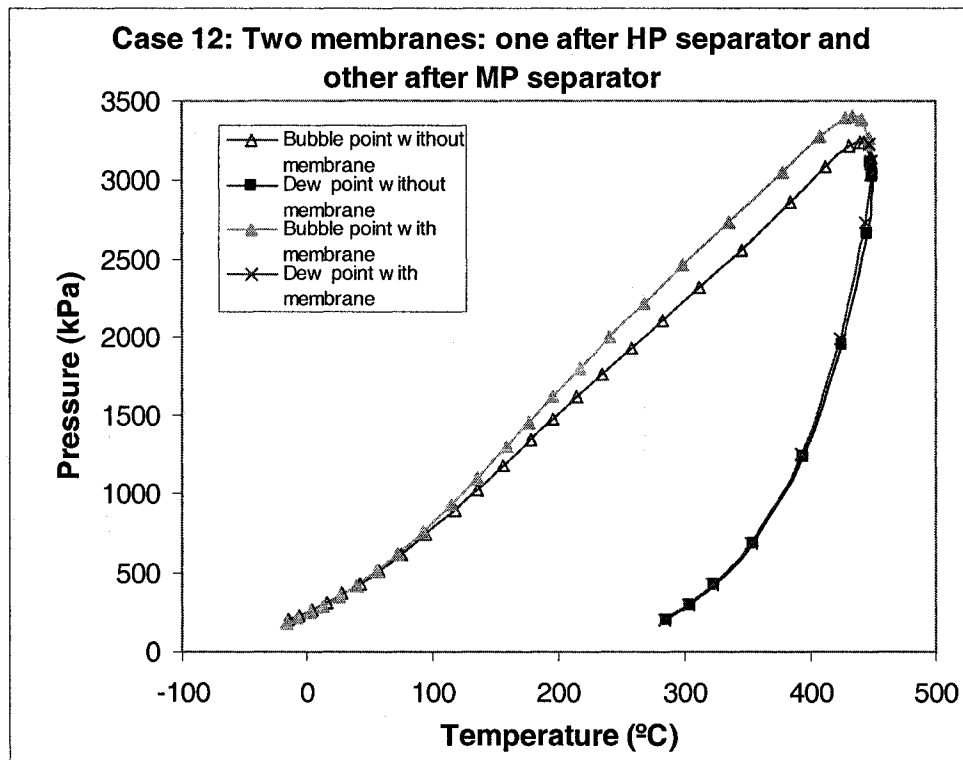


Figure 6.25: Phase envelopes for the stream “Crude Oil Product” for both processes

Table 6.26 outlines the crude oil product composition and RVP value for Case 12. In this process, the heavy hydrocarbons recovery is larger than the base process, while the amount of methane is lower. The RVP value is larger than in the base process. This

process shows favourable recovery; however, it requires many membranes to reach this improved performance.

Table 6.26: Crude oil production of the process of Case 12

	Mass Flow (kg/h)	Recovery (%)	RVP (psia)	Volume Flow	
				(m ³ /h)	(bbl/day)
Total	1,197,469	82.40	22.270	1,377	207,846
Methane	606	0.33	-	-	-
Ethane Plus	1,196,615	94.77	-	1,375	207,659
Propane Plus	1,192,283	97.38	-	1,368	206,590
C5+	1,153,232	99.91	-	1,307	197,408

6.3 Analysis and comparison of the twelve cases presented in the previous section

In Table 6.27, the difference of recovery reached for each alternative process and the base process is indicated. These recoveries are calculated respect to the base values in the input of the process. Positives values indicate that the alternative process has a larger recovery (of methane, C₂⁺, C₃⁺, or C₅⁺) compared to the base process. A negative difference value indicates that the alternative process has a lower recovery than the base process. In terms of methane recovery, a negative value is preferred since the amount of methane present in the crude oil should be minimum to avoid evaporation. On the other hand, in terms of heavy hydrocarbons recovery a positive difference is more preferred since the quality of the crude oil will be increase in this way. In Table 6.27, the preferred values are indicated in bold and the less convenient with a star (*). Also in this table the RVP values of each alternative process are shown. The objective is to reach a higher recovery of the heavy hydrocarbons after the three separation stages by means of the

implementation of membranes with recycling to improve the crude oil quality and production. In order to select a process as a possible alternative to the base process, three specifications are identified; recovery of heavy hydrocarbons should be higher than the base process, the amount of methane in the crude oil should be similar of lower than in the base process, and that the RVP should be similar to the base process. A brief discussion of the results for each alternative processes presented in this chapter is given in the following paragraphs.

Table 6.27: Comparison of the twelve cases

Case	Methane	C ₂ ⁺	C ₃ ⁺	C ₅ ⁺	RVP (psia)	Membranes
1	0.001	0.046	0.048	0.007	19.977	1
2	0.04	-0.177*	-0.15*	-0.007*	18.827	1
3	0.609	0.634	0.477	0.02	29.261	1
4	0.664	0.598	0.481	0.029	28.588	3
5	1.562	0.729	0.564	0.033	36.026	4
6	3.172*	1.197	0.837	0.035	52.182*	1
7	-0.014	0.3	0.301	0.022	20.879	1
8	-0.053	0.475	0.45	0.026	21.908	1
9	-0.032	0.3	0.285	0.017	21.162	1
10	-0.036	0.301	0.282	0.016	21.176	1
11	-0.006	0.084	0.08	0.009	20.215	1
12	-0.059	0.571	0.543	0.035	22.270	2

Case 1 presents slightly higher recoveries of heavier hydrocarbons than the base process but similar recovery of methane than the base process. Therefore, this alternative is not going to produce a larger increment in the crude oil production. Instead Case 2 presents lower recoveries of heavier hydrocarbons, which makes it even less convenient.

Cases 3, 4 and 5 have larger C₂⁺, C₃⁺, and C₅⁺ recoveries than the base process, but the amount of methane is also higher. In addition, these three cases possess larger

RVP values because the large amount of methane and ethane present in the crude oil, which increase the volatility of the crude oil.

Case 6 presents the disadvantage of a large recovery of methane, which diminishes the quality of the crude oil and this is reflected in the RVP value. Nevertheless, this alternative process reaches the largest C_2^+ , C_3^+ , and C_5^+ recoveries among all the alternatives presented.

Cases 7 and 8 are variations of the process of Case 6. Due to the modifications, the methane recovery is reduced considerably such as the recoveries are lower than the base process. In addition, the C_2^+ , C_3^+ , and C_5^+ recoveries are higher than the base process, showing larger recoveries than the process of Case 8.

Cases 9, 10, and 11 show the same trend than Cases 7 and 8 but the heavier hydrocarbon recoveries are lower than these cases. The process of Case 11 presents minimum heavier hydrocarbon recoveries compared to the other two processes.

Case 12 has the lowest recovery of methane among all the alternatives presented. In addition, this process possesses large C_2^+ , C_3^+ , and C_5^+ recoveries values.

After evaluating the results, the processes of Cases 8 and 12 are the most attractive ones because they achieve the specifications mentioned previously in this section. These two processes have larger C_2^+ , C_3^+ , and C_5^+ recoveries than the base process, while the amount of methane is lower. Their RVP values are similar or slightly larger than the value of the base process. As it is explained in section 6.1, these RVP values are not considered high since the oil requires further processing. The oil is treated to break the emulsions at near ambient pressure; therefore, gas is going to be flashed, which is going to reduce the RVP value.

CHAPTER 7

CONCLUSIONS

7.1 Summary

The purpose of this thesis was to evaluate the performance of membranes to recover NGL on Newfoundland and Labrador offshore production platforms. As part of this study the membrane process was compared with traditional processes such as turbo-expander, absorption, adsorption, external refrigeration. After evaluating the main advantages and disadvantages of each process, membranes were reasoned to be a feasible alternative. The model used to simulate the membrane process is based on a set of discrete equations. In order to study the performance of the membrane on a production platform, MATLAB and HYSYS are linked, where MATLAB modelled the membrane and information communicated between the two software packages. The membranes are placed in different locations in a three-stage separation train to evaluate its ability to recover NGL (C_2^+ and for C_3^+) from the associated gas. The effects of pressure, composition, flow pattern, and feed temperature on the NGL recovery are evaluated for each selected position. The results are then applied to determine the enhancement of crude oil production by recycling the permeate and the residue streams of the membranes into the process. Twelve alternative configurations of the original process are proposed and investigated. The objective of this analysis is to evaluate the impact of the membranes on the production of crude oil.

7.2 Conclusion

The produced gas present in Newfoundland is relatively rich in heavier hydrocarbons (C_2^+) with low amounts of inert gases and moderate amounts of CO_2 (between 1 and 2 %), and NGL recovery can be significant. In general the reservoir pressures in Newfoundland are high. Considering these conditions and the composition of the produced gas in this area, absorption and adsorption processes are not suitable. These two processes occupy a large area, consume large amounts of energy, and operations are difficult offshore. The high inlet pressure of the gas favours the use of the turbo expander process; however, turbo expanders are more efficient for lean rather than rich gases, although they could be modified to handle rich gases but this implies higher cost. The application of external refrigeration on platforms is less attractive due to the large area requirement, heavy weight and large energy consumption. Although membranes are new technologies and they have not been proved extensively in the offshore, they present some attractive features. When membranes are compared to other separation technologies advantages such as low energy consumption, mild operating conditions, minimal environmental impacts, process continuity and flexibility, scalability, space saving and modular plant design are apparent. However, the long-term stability of the membranes and material is an issue, as permeabilities will vary in the long-term operation.

To membrane separation model, four models were evaluated: two models (co-current and counter-current) based on differential equations, and two models (co-current and counter-current) based on discrete equations.

The use of the differential equation models results in more complex system of equations. The model requires initial conditions, and for the counter-current model not all

of the initial conditions are known. The “guess” required to run the iteration, which must be close to the actual value or the iteration, could give an initial condition that is not correct. This trial and error iteration could result in long and/or variable simulation times. The co-current differential model has similar simulation times as the discrete model. The use of dimensionless variables presents a problem when a parameter such as area needs to be changed in terms of the simulation code.

The model that uses discrete equations is a relatively less complex. The initial conditions for this model are not as critical as in the previous model, since across the iterations the model converges at the same value. In addition, the solution of the system of equations requires a numerical method such as the Thomas method, but it is simpler in terms of programming than the Runge-Kutta method used to solve the differential equations. The Thomas method uses an iteration procedure, and it stops the calculation when the difference between two consecutive simulation is within the tolerance. Additionally, this model has good flexibility to changes.

The analysis of the recovery of NGL (C_3^+ & C_2^+) was developed with the models based on discrete equations. Membranes were introduced into a three-stage separation train and the effects of different parameters (i.e., pressure, composition, feed process temperature, flow pattern and location into the process) on the recovery of NGL were evaluated. An increase in the pressure of the feed to the membrane produces a higher NGL recovery but also a higher methane loss. An increase in the feed temperature of the process (“Wellhead” stream temperature) results in a higher recovery of NGL while methane is unaffected. A higher concentration of NGL in the feed stream to the membrane resulted in an increase in mass transfer driving force, which translated into

better separation. In addition, the counter-current model showed a better performance since a higher recovery of NGL with less methane could be reached in all cases studied. Both cases (C_2^+ and C_3^+ recovery processes) showed similar behaviour in all simulations. However, C_3^+ recovery had higher separation factors with respect to methane, which indicates lower methane loss in the permeate stream. The membrane treating the associated gas coming from the low-pressure separator obtained the best performance compression since the recovery of NGL was higher than the methane loss in the permeate stream. However, the flow rate of this stream is considerably low compared to the high and medium pressure associated gas flow rates. Therefore, the amount of NGL recovery in this stream is not significantly large. In order to accomplish a complete analysis of the system, it is necessary to include a recycle in the process to return permeate back to feed one of the separators.

Twelve cases were presented, and the performance measure was the highest recovery of heavy hydrocarbons with similar or lower amount of methane in the crude oil than in the base process, and keeping the RVP similar to the base process. Considering all these three factors, Cases 8 and 12 were the most attractive processes.

In Case 8, a membrane is placed after the medium-pressure separator. The associated gas from low-pressure separator is compressed to 1,724 kPa and then mixed with associated gas from the medium-pressure separator. This mixture is then fed to the membrane. Before entering the membrane, the mix is compressed to 7,000 kPa, and then cooled to 35 °C. The permeate stream of the membrane is sent to feed the medium-pressure separator together with the bottom stream coming from the high-pressure separator. The process presented in this case produces a 13.5 % less methane in the crude

product than the base process. In addition, the C_2^+ , C_3^+ and C_5^+ recoveries increased 0.5%, 0.46% and 0.026%, respectively.

In Case 12, two membranes are introduced into the original process. One membrane is placed after the high-pressure separator (7,000 kPa) to treat the associated gas. Then, its permeate stream is sent to feed the high-pressure separator together with the original feed of this separator. The permeate stream is compressed to 7,000 kPa and cooled to 35 °C to reach the condition of the separator. The second membrane is placed after the medium-pressure separator (1,724 kPa). The feed of the membrane is made up of the associated gas from the medium-pressure separator and the associated gas from the low-pressure separator. Before mixing these two streams, the associated gas *LP* is compressed to 1,724 kPa. After mixing the associated gases, the new stream is compressed to 7,000 kPa, and then cooled to 35 °C before entering the membrane. The permeate stream is sent back to feed the medium-pressure separator together with the bottom stream from the high-pressure separator. This process shows a reduction in the amount of methane in the crude product, close to 15 %, from the base process. In addition, the C_2^+ , C_3^+ and C_5^+ recoveries increase in 0.61%, 0.56% and 0.035%, respectively, when this process is compared to the base process.

7.3 Future work

The analysis and conclusions achieved in this thesis with respect to the NGL recovery with membranes were based on computational simulations. Therefore, several assumptions had to be considered to perform this study. In order to accomplish a more complete analysis, it is necessary to develop an experimental study. First, it is

recommended to develop a set of experiments with different membrane materials under diverse operational conditions. Once an optimal material was selected for the recovery of NGL, a pilot plant needs to be design and constructed to confirm that the observations achieved in the computational simulations were correct. In addition, this experimental stage could allow the mathematical model of the membrane to improve since correction factors can be incorporated in the model. Such factors could be the variation of the permeability of the components with pressure, and the variation of the permeability due to the interaction among the components. This incorporation could permit to develop a more realistic model; therefore, a more complex simulation analysis could be achieved.

On the simulation side, the combination of membranes with other conventional or more modern techniques of NGL recovery in hybrid processes can be evaluated. For instance turbo expanders are very attractive processes for NGL recovery where footprint area is a factor. The NGL recovery efficiency when membranes are combined with turbo expanders deserves a closer study. The current research proved that membranes are more efficient when the richer gas from low-pressure separator is treated. Turbo expanders are efficient for leaner gases at higher pressures. It would be interesting to see how a hybrid process where a turbo expander treats the gas from the high- and medium-pressure separators and a membrane that processes the gas from the low-pressure separator enhance crude production.

REFERENCES

- [1] Chang S., “Comparing Exploitation and Transportation Technologies for Monetisation of Offshore Stranded gas”, the SPE Asia Pacific Oil & Gas Conference and Exhibition, Jakarta, Indonesia, SPE Paper 68680, 17-19, 2001.
- [2] Anon, “Estimates of Recoverable Reserves/Resources – Resource Information”, The Canada-Newfoundland and Labrador Offshore Petroleum Board (CNLOPB), <http://www.cnlopb.nl.ca/>
- [3] Meisen A. and Beronich E., “Monetizing Stranded Gas Off Newfoundland and Labrador”, The 2005 College Chemistry Canada (C3) National Conference, St. John’s NL, Canada, June 17-18, 2005.
- [4] Strosher M., “Characterization of Emissions from Diffusion Flare Systems”, Air & Waste Management Association, 50, 1723-1733, 2000.
- [5] Neff J.M., “Polycyclic aromatic hydrocarbons in the aquatic environment: sources, fates, and biological effects”, London: Applied Science Publi. Ltd, 262, 1979.
- [6] Rovinski F., Teplitskaya T., Alekseeva T., “Background monitoring of the polycyclic aromatic hydrocarbons”, Leningrad: Gidrometeoizdat, 224, 1988.
- [7] International Association of Oil and Gas Producers (2002), Aromatics in produced water: occurrence, fate and effect, and treatment, Report No 1.20/324, January 2002.
- [8] Lokhandwala K. and Jacobs M., “New Membrane Applications in Gas Processing”, Gas Processor Association Annual Convention, Atlanta, GA, March 2000.
- [9] Anon., Advanced Membrane Technology for Processes and Environment – NGL Recovery, Borsig Membrane Technology, <http://www.borsig-mgp.com/>

- [10] Russell, T. H., "Truck-Mounted Plant Speeds Gas Processing Flexibility", Oil & Gas Journal, (), 129-133, 1982.
- [11] Section 16, "Hydrocarbon Recovery", GPSA Engineering Data Book, 11th edition, Gas Processors Suppliers Association, Tulsa, Oklahoma, USA, 1998.
- [12] Barnwell J., Wong W., "Expanders Do Payout Offshore North Sea", Society of Petroleum Engineers, SPE Paper 12381, May 1985.
- [13] Moins, G., "Associated Gas Treatment On Site" International Petroleum Exhibition and Technical Symposium of the Society of Petroleum Engineers, Houston, TX, SPE Paper 9998, March 18-26, 1982.
- [14] Markiewicz G., Losin M., and Campbell K., "The Membrane Alternative for Natural Gas Treating: Two Case Studies", the 63rd Annual Technical Conference and Exhibition of the Society of Petroleum Engineers, SPE 18230, October 1986.
- [15] The Canada-Newfoundland and Labrador Offshore Petroleum Board (CNLOPB), Hibernia Field Production History 2004.
- [16] Aggarwal, V. and Singh, S., "Improve NGL recovery – Processing conditions and product specifications determine the best method to recover NGLs", Hydrocarbon Processing, 80 (5), 41-45, May 2001.
- [17] Economou I., Raptis V., Melissas V., Theodorou D., Petrou J., and Petropoulos J.; "Molecular simulation of structure, thermodynamic and transport properties of polymeric membrane materials for hydrocarbon separation", Fluid Phase Equilibria, 228-229, 15-16, 2005.

- [18] Basu, A.; Akhtar, J.; Rahman, M.; and Islam, M. "A Review of separation of Gases using Membrane Systems" *Petroleum Science and Technology*, 22 (9-10), 1343-1368, 2004.
- [19] Geankoplis C. J., "Transport Processes and Separation Process Principles", Fourth edition editorial: Prentice Hall PTR, 2003
- [20] Kalyuzhnyi, N.; Sidorenko, V.; Shishatskii S.; Yampol'skii, Y.; "Membrane separation of oil gas hydrocarbons", *Petroleum Chemistry*, 31 (3), 260-270, 1991.
- [21] Schultz, J. and Peinemann K.; "Membranes for separation of higher hydrocarbons from methane", *Journal of Membrane science*, 110 (1), 37, 1996.
- [22] Ilinitich O., Semin G., Chertova M., and Zamaraev K.; "Novel polymeric membranes for separation of hydrocarbons", *Journal of Membrane Science*, 66 (1), 1-8, 1992.
- [23] Pinnau I., Casillas C., Morisato A., and Freeman B.; " Hydrocarbon/Hydrogen Mixed Gas Permeation in Poly(1-trimethylsilyl-1-propyne) (PTMSP), Poly(1-phenyl-1-propyne) (PPP), and PTMSP/PPP Blends", *Journal of Polymer Science: Part B: Polymer Physics*, 34, 2613-2621, 1996.
- [24] Alentiev A., Shantarovich V., Merkel T., Bondar V., Freeman B., and Yampolskii Y., "Gas and Vapor Sorption, Permeation and Diffusion in Glassy Amorphous Teflon AF1600", *Macromolecules*, 35, 9513-9522, 2002.
- [25] Pinnau I., and He Z.; "Pure- and mixed-gas permeation properties of polydimethylsiloxane for hydrocarbon/methane and hydrocarbon/hydrogen separation", *Journal of Membrane Science*, 244 (1-2), 227-233, 2004.

- [26] Finkelshtein E., Ushakov N., Krasheninnikov E., and Yampolskii Y.; "New polysilalkylenes: synthesis and gas-separation properties", Russian Chemical Bulletin, International Edition, 53 (11), 2604-2610, 2004.
- [27] Shindo, Y., Hakuta T., Yoshitome H., and Inoue H., "Calculation Methods for Multi-component Gas Separation by Permeation", Sep. Sci. and Tech., 20, 445, 1985.
- [28] Coker D., and Freeman B., "Modelin Multi-component Gas Separation Using Hollow-Fiber Membrane Contactors", AIChE Journal, 44 (6), 1998.
- [29] Barrer R., Barrie A., and Raman N., "Solution and Diffusion in Silicone Rubber: I. A Comparison with Natural Rubber", Polymer, 3, 595, 1962.
- [30] Ghosal K., Freeman B., "Gas Separation Using Polymer Membranes: An Overview", Poly. For Adv. Technol., 5, 673, 1994.
- [31] Graham T., "On the Absorption and Dialytic Separation of Gases by Colloid Septa: I. Action of a Septum of Caoutchouc" Phil. Mag., 32, 401, 1866.
- [32] King, C. J., Separation Processes, 2nd ed., McGraw Hill, New York, p. 466, 1980.
- [33] Geankoplis C., Transport Processes and Unit Operations, 3rd ed., Prentice Hall, Englewood Cliffs, NJ, 921, 1993.
- [34] Manning F. S. and Thompson R. E., "Oilfield Processing of Petroleum", vol 1, Natural Gas, Pennwell Publishing Company, 1995.
- [35] Odello R., "Systematic Method Aids Choice of Field Gas Treatment", Oil Gas Journal, 79 (6), 103-110, 1981.
- [36] Beronich E., Hawboldt K., and Abdi M., "Linking a Process Simulator (HYSYS) with MATLAB, a Powerful Modeling Tool for Continuous Process Industry: a Tutorial",

Newfoundland Electrical and Computer Engineering Conference 2005, NECEC 2005, St
John's, NL, Canada, November 8, 2005.

APPENDIX A

A.1 Co-current Model

A.1.1 C-ocurrent model with differential equation

CUCURRENT FLOW (Calculated by hand the Runge Kutta Method)

```
global Pa Pb Pc lambda Qa Qb Qc Ph Pl xa xb xc ya Ff ya yb yc qa qb qc gamma D
nstage
```

```
xa(1)=0.3333;
xb(1)=0.3333;
xc(1)=0.3334;
cte = 7.501e-12;
Pa = 500*cte; % GPU -> m^3[STP]/(m^2*s*Pa)
Pb = 100*cte;
Pc = 10*cte;
xaf=0.3333;
xbf=0.3333;
xcf=0.3334;
gamma = 0.1; % gamma = Pl/Ph
qa = Pa/Pa; %Pa/Pa
qb = Pb/Pa; %Pb/Pa
qc = Pc/Pa; %Pc/Pa
Lf = 0.0786; %m^3/s %Lf = 283.2; %m^3[STP]/h -> m^3/s
nstage = 1000;
Am = 377/nstage*0.1; %m^2 el area seria 37.7
Ph=1000000; %Ph = 10; %Bar -> Pa (pascal)
Pl = 100000; %Pl = 42.4; %Bar -> Pa
f(1) = 1; % f = F/Ff ; f =1 -> initial value of f at A=0 or S=0
```

```
%CALCULATION OF PERMEATE FRACTIONS YA, YB, YC AT G=0 (A=0)
```

```
%Call to the function to calculate the ya at G=0
```

```
x0 = [0.001]; % Make a starting guess at the solution
```

```
options=optimset('Display','iter'); % Option to display output
```

```
[x,fval] = fsolve(@initialPermFract,x0,options); % Call optimizer
```

```
ya(1)=x(1)
```

```
%Call to the function to calculate the yb and yc at G=0
```

```
x0 = [0.001 0.0001];
```

```
options=optimset('Display','iter');
```

```
[y,fval] = fsolve(@initialPermComp,x0,options);
```

```

yb(1)=y(1)
yc(1)=y(2)
ya(1)+yb(1)+yc(1);

*****
INITIAL CALCULATION
*****
D = 0.001; % delta of area (value fixed)
fin = 1799;
Area(1)=1;
Delta=0.001;
for m=1:1:fin %0.001*1000 = 1 = Area %|Delta|*fin = 0.01*100 = 1 = Area
Area(m+1)=Area(m)-Delta;

%CALCULATION OF RUNGE KUTTA DELTA COEFFICIENTS AT A=0
%Calculation of D1f, D2f, D3f, D4f AT G=0 (A=0)
f(m+1) = RK41(xa(m),xb(m),xc(m),ya(m),yb(m),yc(m),f(m)); %eq1

%Calculation of D1a, D2a, D3a, D4a AT G=0 (A=0)
xa(m+1) = RK42(xa(m),xb(m),xc(m),ya(m),yb(m),yc(m),f(m)); %eq2

%Calculation of D1b, D2b, D3b, D4b AT G=0 (A=0)
xb(m+1) = RK43(xa(m),xb(m),xc(m),ya(m),yb(m),yc(m),f(m)); %eq3

%CALCULATION OF THE OTHER MOLAR FRACTIONS: xc, ya, yb, yc
xc(m+1) = 1-xa(m+1)-xb(m+1); %f

%Calculation of permeate side molar fractions
if(f(m)==1)
ya(m+1) = ya(1);
yb(m+1) = yb(1);
yc(m+1) = yc(1);
else
ya(m+1) = (xa(1)-f(m)*xa(m))/(1-f(m)); %f != 1 -> m!=1
yb(m+1) = (xb(1)-f(m)*xb(m))/(1-f(m)); %f != 1 -> m!=1
yc(m+1) = 1-ya(m+1)-yb(m+1); %f != 1 -> m!=1
end

end
theta=1-f(fin);
matrix = [f' xa' xb' xc' ya' yb' yc' Area'];
st=-Area(fin)+Area(1);
At = st*Lf/(Ph*Pa);

```

```

% EQUATION TO CALCULATE YA AT G=0 (A=0)

function y= initialPermFract(x)

global Pa Pb Pc lambda xa xb xc gamma

% equation number 4.13 of the paper, the component i selected is A
%y(1)= xaf/(xaf/x(1))+ (xbf*Pb/Pa)/((Pl/Ph)*((Pb/Pa)-
1)+xaf/x(1))+ (xcf*Pc/Pa)/((Pl/Ph)*((Pc/Pa)-1)+xaf/x(1))-1;

y(1)= xa/(xa/x(1))+ (xb*Pb/Pa)/(gamma*((Pb/Pa)-
1)+xa/x(1))+ (xc*Pc/Pa)/(gamma*((Pc/Pa)-1)+xa/x(1))-1;

%EQUATIONS TO CALCULATE YB AND YC AT G=0 (A=0)

function y = initialPermComp(x)

global Pa Pb Pc gamma xa xb xc ya

%equation number 4.12 of the paper to calculate yb at G=0, the component i selected is A
y(1)= (xb*(Pb/Pa))/(gamma*((Pb/Pa)-1)+xa/ya) - x(1);

%equation number 4.12 of the paper to calculate yc at G=0, the component i selected is A
y(2)= (xc*(Pc/Pa))/(gamma*((Pc/Pa)-1)+xa/ya) - x(2);

%RUNGE KUTTA 4 order for "f"

function f = RK41(xA,xB,xC,yA,yB,yC,fo)

global qa qb qc gamma D

% y(1)= delta1f
% y(2)= delta2f
% y(3)= delta3f
% y(4)= delta4f

%Runge Kutta for the equation df/ds expressed as:
%df/ds = - ( qa*(xa-gamma*ya) + qb*(xb-gamma*yb) + qa*(xc-gamma*yc));

%form of the equation in the initial step
%y(2) = D*(-1)*( qa*(xaf-gamma*yao) + qb*(xbf-gamma*ybo) + qa*(xcf-
gamma*yco));

```

```

y(1) = D*(-1)*( qa*(xA-gamma*yA) + qb*(xB-gamma*yB) + qc*(xC-gamma*yC));
y(2) = D*(-1)*( qa*(xA-gamma*yA) + qb*(xB-gamma*yB) + qc*(xC-gamma*yC));
y(3) = D*(-1)*( qa*(xA-gamma*yA) + qb*(xB-gamma*yB) + qc*(xC-gamma*yC));
y(4) = D*(-1)*( qa*(xA-gamma*yA) + qb*(xB-gamma*yB) + qc*(xC-gamma*yC));

```

```
f = fo + (1/6)*y(1) + (1/3)*y(2) + (1/3)*y(3) + (1/6)*y(4);
```

```
%RUNGE KUTTA 4 order for "xa"
```

```
function xa = RK42(xA,xB,xC,yA,yB,yC,F)
```

```
global qa qb qc gamma D
```

```
%Definition of Delta Coefficients
```

```
%f = dy/dt = xxxxxx
```

```
%D = delta of area (value fixed)
```

```
%delta1 = D* f(t,y)
```

```
%delta2 = D* f(t + 1/2*D , y + 1/2*delta1)
```

```
%delta3 = D* f(t + 1/2*D , y + 1/2*delta2)
```

```
%delta4 = D* f(t + D , y + delta3)
```

```
%Runge Kutta for the equation dxa/ds expressed as:
```

```
% y = xa
```

```
% t = S
```

```
%dxa/ds = - qa/f*(xA-gamma*yA) + xA/f*( qa*(xA-gamma*yA) + qb*(xB-gamma*yB)+
qa*(xC-gamma*yC));
```

```
y(1) = D*(- qa/F*(xA-gamma*yA) + xA/F*( qa*(xA-gamma*yA) + qb*(xB-
gamma*yB)+ qc*(xC-gamma*yC)));
```

```
y(2) = D*(- qa/F*((xA+1/2*y(1))-gamma*yA) + (xA+1/2*y(1))/F*( qa*((xA+1/2*y(1))-
gamma*yA) + qb*(xB-gamma*yB)+ qc*(xC-gamma*yC)));
```

```
y(3) = D*(- qa/F*((xA+1/2*y(2))-gamma*yA) + (xA+1/2*y(2))/F*( qa*((xA+1/2*y(2))-
gamma*yA) + qb*(xB-gamma*yB)+ qc*(xC-gamma*yC)));
```

```
y(4) = D*(- qa/F*((xA+y(3))-gamma*yA) + (xA+y(3))/F*( qa*((xA+y(3))-gamma*yA) +
qb*(xB-gamma*yB)+ qc*(xC-gamma*yC)));
```

```
xa = xA + (1/6)*y(1) + (1/3)*y(2) + (1/3)*y(3) + (1/6)*y(4);
```

%RUNGE KUTTA 4 order for "xb"

function xb = RK43(xA,xB,xC,yA,yB,yC,F)

global qa qb qc gamma D

%Definition of delta coefficients

%f = dy/dt

%D = delta of area (value fixed)

%delta1 = D* f(t,y)

%delta2 = D* f(t + 1/2*D , y + 1/2*delta1)

%delta3 = D* f(t + 1/2*D , y + 1/2*delta2)

%delta4 = D* f(t + D , y + delta3)

%Runge Kutta for the equation dx_a/ds expressed as:

% y = xb

% t = S

% $dx_b/ds = - qb/f*(x_b-gamma*y_b) + x_b/f*(qa*(x_a-gamma*y_a) + qb*(x_b-gamma*y_b)+ qa*(x_c-gamma*y_c))$;

$y(1) = D*(- qb/F*(x_B-gamma*y_B) + x_B/F*(qa*(x_A-gamma*y_A) + qb*(x_B-gamma*y_B)+ qc*(x_C-gamma*y_C))$);

$y(2) = D*(- qb/F*((x_B+1/2*y(1))-gamma*y_B) + (x_B+1/2*y(1))/F*(qa*(x_A-gamma*y_A) + qb*((x_B+1/2*y(1))-gamma*y_B)+ qc*(x_C-gamma*y_C))$);

$y(3) = D*(- qb/F*((x_B+1/2*y(2))-gamma*y_B) + (x_B+1/2*y(2))/F*(qa*(x_A-gamma*y_A) + qb*((x_B+1/2*y(2))-gamma*y_B)+ qc*(x_C-gamma*y_C))$);

$y(4) = D*(- qb/F*((x_B+y(3))-gamma*y_B) + (x_B+y(3))/F*(qa*(x_A-gamma*y_A) + qb*((x_B+y(3))-gamma*y_B)+ qc*(x_C-gamma*y_C))$);

$xb = x_B + (1/6)*y(1) + (1/3)*y(2) + (1/3)*y(3) + (1/6)*y(4)$;

A.1.2 Cocurrent model with discrete equations

```
clc
clear all

nstage = 25;
Am = 37.7/nstage; %m^2
Ph=1000000;
Pl = 100000; Pa
cte = 7.501e-12;
QA = 500*cte; % GPU -> m^3[STP]/(m^2*s*Pa)
QB = 100*cte;
QC = 10*cte;
xAf = 0.3333;
xBf = 0.3333;
xCf = 0.3334;
Lf = 0.0786; %m^3/s %Lf = 283.2; m^3[STP]/h -> m^3/s
Lfa = Lf*xAf;
Lfb = Lf*xBf;
Lfc = Lf*xCf;

%Initial values:
V = [Lf-Lf/(nstage+1):-Lf/(nstage+1):0];
L = [Lf/(nstage+1):Lf/(nstage+1):Lf];

la(nstage+1) = Lfa;
lb(nstage+1) = Lfb;
lc(nstage+1) = Lfc;
va(nstage+1) = 0;
vb(nstage+1) = 0;
vc(nstage+1) = 0;
ya(nstage+1) = 0;
yb(nstage+1) = 0;
yc(nstage+1) = 0;
xa(nstage+1) = xAf;
xb(nstage+1) = xBf;
xc(nstage+1) = xCf;

Vcomp=1;
Lcomp=1;
count=0;

while((abs(Vcomp)>1e-8)|(abs(Lcomp)>1e-8))
    for k=nstage:-1:1
```

%CALCULATION OF MOLAR FEED FLOW

%Component A

$la(k) = (va(k+1) + la(k+1) * (1 + V(k)/(QA * Am * PI))) / (1 + V(k)/(QA * Am * PI) + (Ph * V(k))/(PI * L(k)))$;

%Component B

$lb(k) = (vb(k+1) + lb(k+1) * (1 + V(k)/(QB * Am * PI))) / (1 + V(k)/(QB * Am * PI) + (Ph * V(k))/(PI * L(k)))$;

%Component C

$lc(k) = (vc(k+1) + lc(k+1) * (1 + V(k)/(QC * Am * PI))) / (1 + V(k)/(QC * Am * PI) + (Ph * V(k))/(PI * L(k)))$;

% Save previous V and L

Voutant = V(1);

Loutant = L(1);

% RECALCULATE TOTAL FEED FLOW RATES

$L(k) = la(k) + lb(k) + lc(k)$;

% RECALCULATE TOTAL PERMEATE FLOW RATES

$V(k) = L(k+1) + V(k+1) - L(k)$;

% Save actual V and L

Voutact = V(1);

Loutact = L(1);

% CRITERIA VERIFICATION

$Vcomp = (Voutact - Voutant) / Voutact$;

$Lcomp = (Loutact - Loutant) / Loutact$;

% PERMEATE FLOW RATES OF EACH COMPONENT ON EACH STAGE ON THE LOW-PRESSURE SIDE

%Component A

$va(k) = la(k+1) - la(k) + va(k+1)$;

%Component B

$vb(k) = lb(k+1) - lb(k) + vb(k+1)$;

%Component C

$vc(k) = lc(k+1) - lc(k) + vc(k+1)$;

```
% CALCULATION OF THE MOLE FRACTION OF EACH COMPONENT ON FEED  
SIDE
```

```
  % Component A  
  xa(k)=la(k)/L(k);  
  % Component B  
  xb(k)=lb(k)/L(k);  
  % Component C  
  xc(k)=lc(k)/L(k);
```

```
% CALCULATION OF THE MOLE FRACTION OF EACH COMPONENT ON  
PERMEATE SIDE
```

```
  % Component A  
  ya(k)=va(k)/V(k);  
  % Component B  
  yb(k)=vb(k)/V(k);  
  % Component C  
  yc(k)=vc(k)/V(k);
```

```
end
```

```
count=count+1; % This indicated how many iterations were required to converge the  
system  
end
```

```
xaout = xa(1)  
xbout = xb(1)  
xcout = xc(1)  
yaout = ya(1)  
ybout = yb(1)  
ycout = yc(1)
```

```
[xa(1) xb(1) xc(1) ya(1) yb(1) yc(1)]
```

```
% METHOD THOMAS TO ESTIMATE THE COEFFICIENTS OF THE MATRICES  
THAT CALCULATE THE FEED AND PERMEATE MOLAR FLOWS ON EACH  
STAGE
```

```
function [l] = Tmethod(Qx,xXf,lX1)
```

```
global Ph Pl nstage Am Lf V L
```

```
E = 1:1:nstage;  
E(:)=0;
```

```

for k=2:nstage+1
B(k-1) = -V(k-1)/(Pl*Am*Qx)*(1+Qx*Am*Ph/L(k-1));
C(k-1) = 1+V(k-1)/(Pl*Am*Qx)+V(k)/(Pl*Am*Qx)*(1+Qx*Am*Ph/L(k));
D(k-1) = -V(k)/(Pl*Am*Qx)-1;
end
E(1) = -B(1)*lX1;
E(nstage) = -D(nstage)*Lf*xXf;

W(1) = C(1);
u(1) = D(1)/W(1);
g(1) = E(1)/W(1);

```

A.2 Countercurrent Model

A.2.1 Countercurrent model with differential equation

```

clear all
clc

```

% COUNTERCURRENT FLOW (Calculated by hand the Runge Kutta Method)

```

global Pa Pb Pc lambda Qa Qb Qc Ph Pl xa xb xc xao xbo xco ya yb yc qa qb qc
gamma nstage

```

```

%Constants values
cte = 7.501e-12;
QA = 500*cte; % GPU -> m^3[STP]/(m^2*s*Pa)
QB = 100*cte;
QC = 10*cte;
Pa = QA; % (mol/s.m.Pa)
Pb = QB ; % (mol/s.m.Pa)
Pc = QC;% (mol/s.m.Pa)
Lf = 0.0786; %m^3/s
Ph=1000000; Pa (pascal)
Pl = 100000; Pa
gamma = 0.1; % gamma = Pl/Ph
qa =QA/QA ; %Pa/Pa
qb = QB/QA; %Pb/Pa
qc = QC/QA; %Pc/Pa
D = -0.01; % delta of area (value fixed)

```

```

%*****
% CALCULATION
%*****
xao = 0.1076;
xbo = 0.3629;
xco = 0.5295;
theta = 0.3933;

%CALCULATION OF PERMEATE FRACTIONS YA, YB, YC AT G=0
%Call to the function to calculate the ya at G=0
x0 = [0.001]; % Make a starting guess at the solution
options=optimset('Display','iter'); % Option to display output
[x,fval] = fsolve(@finalPermFract,x0,options); % Call optimizer
ya(1)=x(1)

%Call to the function to calculate the yb and yc at G=0
x0 = [0.001 0.0001];
options=optimset('Display','iter');
[y,fval] = fsolve(@finalPermComp,x0,options);
yb(1)=y(1)
yc(1)=y(2)
ya(1)+yb(1)+yc(1)

xa(1) = 0.1076;
xb(1) = 0.3629;
xc(1) = 0.5295;

f(1)=1-theta;
%f(fin+1)=1-theta;
fin = 1770;
Area(1)=1;
Delta=-0.001;
for m=1:1:fin %|Delta|*fin = 0.01*100 = 1 = Area
Area(m+1)=Area(m)+Delta;

%CALCULATION OF RUNGE KUTTA DELTA COEFFICIENTS AT A=0
%Calculation of D1f, D2f, D3f, D4f AT G=0 (A=0)
f(m+1) = RK41(xa(m),xb(m),xc(m),ya(m),yb(m),yc(m),f(m),Delta); %eq1

%Calculation of D1a, D2a, D3a, D4a AT G=0 (A=0)
xa(m+1) = RK42(xa(m),xb(m),xc(m),ya(m),yb(m),yc(m),f(m),Delta); %eq2

```

```

%Calculation of D1b, D2b, D3b, D4b AT G=0 (A=0)
xb(m+1) = RK43(xa(m),xb(m),xc(m),ya(m),yb(m),yc(m),f(m),Delta); %eq3

%CALCULATION OF THE OTHER MOLAR FRACTIONS: xc, ya, yb, yc
xc(m+1) = 1-xa(m+1)-xb(m+1); %f

%Calculation of permeate side molar fractions
ya(m+1) = ( xa(m+1)*f(m+1)-xao*(1-theta) )/( f(m+1)-(1-theta) ); %f != 1 -> m!=1
yb(m+1) = ( xb(m+1)*f(m+1)-xbo*(1-theta) )/( f(m+1)-(1-theta) ); %f != 1 -> m!=1
yc(m+1) = 1-ya(m+1)-yb(m+1);

%ya(m+1) = ( xa(m+1)*f(m+1)-xao*(1-theta) )/((xa(m+1)*f(m+1)-xao*(1-theta))
+(xb(m+1)*f(m+1)-xbo*(1-theta))+xc(m+1)*f(m+1)-xco*(1-theta)); %f != 1 -> m!=1

%yb(m+1) = ( xb(m+1)*f(m+1)-xbo*(1-theta) )/((xa(m+1)*f(m+1)-xao*(1-theta))
+(xb(m+1)*f(m+1)-xbo*(1-theta))+xc(m+1)*f(m+1)-xco*(1-theta)); %f != 1 -> m!=1

%yc(m+1) = ( xc(m+1)*f(m+1)-xco*(1-theta) )/((xa(m+1)*f(m+1)-xao*(1-theta))
+(xb(m+1)*f(m+1)-xbo*(1-theta))+xc(m+1)*f(m+1)-xco*(1-theta)); %f != 1 -> m!=1
%yc(m+1) = 1-ya(m+1)-yb(m+1);
end

matrix = [f' xa' xb' xc' ya' yb' yc' Area'];
st = 1-Area(fin);
At = st*Lf/(Ph*QA);

% EQUATION TO CALCULATE YA AT G=0 (A=0)

function y= initialPermFract(x)

global Pa Pb Pc lambda xa xb xc gamma

% equation number 4.13 of the paper, the component i selected is A
%y(1)= xaf/(xaf/x(1))+ (xbf*Pb/Pa)/((Pl/Ph)*((Pb/Pa)-1)+xaf/x(1))
+(xcf*Pc/Pa)/((Pl/Ph)*((Pc/Pa)-1)+xaf/x(1))-1;

y(1)= xa/(xa/x(1))+ (xb*Pb/Pa)/(gamma*((Pb/Pa)-
1)+xa/x(1))+xc*Pc/Pa)/(gamma*((Pc/Pa)-1)+xa/x(1))-1;

```

```

%EQUATIONS TO CALCULATE YB AND YC AT G=0 (A=0)

function y = initialPermComp(x)

global Pa Pb Pc gamma xa xb xc ya

%equation number 4.12 of the paper to calculate yb at G=0, the component i selected is A
y(1)= (xb*(Pb/Pa))/(gamma*((Pb/Pa)-1)+xa/ya) - x(1);

%equation number 4.12 of the paper to calculate yc at G=0, the component i selected is A
y(2)= (xc*(Pc/Pa))/(gamma*((Pc/Pa)-1)+xa/ya) - x(2);

%RUNGE KUTTA 4 order for "f"
function f = RK41(xA,xB,xC,yA,yB,yC,fo,D)

global qa qb qc gamma
% y(1)= delta1f
% y(2)= delta2f
% y(3)= delta3f
% y(4)= delta4f

%Runge Kutta for the equation df/ds expressed as:
%df/ds = - ( qa*(xa-gamma*ya) + qb*(xb-gamma*yb) + qa*(xc-gamma*yc));

%form of the equation in the initial step
%y(2) = D*(-1)*( qa*(xaf-gamma*yao) + qb*(xbf-gamma*ybo) + qa*(xcf-
gamma*yco));

y(1) = D*(-1)*( qa*(xA-gamma*yA) + qb*(xB-gamma*yB) + qc*(xC-gamma*yC));
y(2) = D*(-1)*( qa*(xA-gamma*yA) + qb*(xB-gamma*yB) + qc*(xC-gamma*yC));
y(3) = D*(-1)*( qa*(xA-gamma*yA) + qb*(xB-gamma*yB) + qc*(xC-gamma*yC));
y(4) = D*(-1)*( qa*(xA-gamma*yA) + qb*(xB-gamma*yB) + qc*(xC-gamma*yC));

f = fo + (1/6)*y(1) + (1/3)*y(2) + (1/3)*y(3) + (1/6)*y(4);

%RUNGE KUTTA 4 order for "xa"
function xa = RK42(xA,xB,xC,yA,yB,yC,F,D)

global qa qb qc gamma

```

```

%Definition of delta coefficients
%f = dy/dt
%D = delta of area (value fixed)
%delta1 = D* f(t,y)
%delta2 = D* f(t + 1/2*D , y + 1/2*delta1)
%delta3 = D* f(t + 1/2*D , y + 1/2*delta2)
%delta4 = D* f(t + D , y + delta3)

%Runge Kutta for the equation dxa/ds expressed as:
% y = xa
% t = S
%dxa/ds = - qa/f*(xa-gamma*ya) + xa/f* (qa*(xa-gamma*ya) + qb*(xb-gamma*yb)+
qa*(xc-gamma*yc));

%forma de la ecuacion en el paso inicial
y(1) = D*(- qa/F*(xA-gamma*yA) + xA/F* (qa*(xA-gamma*yA) + qb*(xB-gamma*yB)
+ qc*(xC-gamma*yC)));

y(2) = D*(- qa/F*((xA+1/2*y(1))-gamma*yA) + (xA+1/2*y(1))/F* (qa*((xA+1/2*y(1))-
gamma*yA) + qb*(xB-gamma*yB)+ qc*(xC-gamma*yC)));

y(3) = D*(- qa/F*((xA+1/2*y(2))-gamma*yA) + (xA+1/2*y(2))/F* (qa*((xA+1/2*y(2))-
gamma*yA) + qb*(xB-gamma*yB)+ qc*(xC-gamma*yC)));

y(4) = D*(- qa/F*((xA+y(3))-gamma*yA) + (xA+y(3))/F* (qa*((xA+y(3))-gamma*yA) +
qb*(xB-gamma*yB)+ qc*(xC-gamma*yC)));

xa = xA + (1/6)*y(1) + (1/3)*y(2) + (1/3)*y(3) + (1/6)*y(4);

%RUNGE KUTTA 4 order for "xb"
function xb = RK43(xA,xB,xC,yA,yB,yC,F,D)

global qa qb qc gamma

%Definition of delta coefficients
%f = dy/dt
%D = delta of area (value fixed)
%delta1 = D* f(t,y)
%delta2 = D* f(t + 1/2*D , y + 1/2*delta1)
%delta3 = D* f(t + 1/2*D , y + 1/2*delta2)
%delta4 = D* f(t + D , y + delta3)

```

```

%Runge Kutta for the equation dxa/ds expressed as:
% y = xb
% t = S
%dxb/ds = - qb/f*(xb-gamma*yb) + xb/f* (qa*(xa-gamma*ya) + qb*(xb-gamma*yb)+
qa*(xc-gamma*yc));

y(1) = D*(- qb/F*(xB-gamma*yB) + xB/F* (qa*(xA-gamma*yA) + qb*(xB-gamma*yB)
+ qc*(xC-gamma*yC)));

y(2) = D*(- qb/F*((xB+1/2*y(1))-gamma*yB) + (xB+1/2*y(1))/F* (qa*(xA-gamma*yA)
+ qb*((xB+1/2*y(1))-gamma*yB)+ qc*(xC-gamma*yC)));

y(3) = D*(- qb/F*((xB+1/2*y(2))-gamma*yB) + (xB+1/2*y(2))/F* (qa*(xA-gamma*yA)
+ qb*((xB+1/2*y(2))-gamma*yB)+ qc*(xC-gamma*yC)));

y(4) = D*(- qb/F*((xB+y(3))-gamma*yB) + (xB+y(3))/F* (qa*(xA-gamma*yA) +
qb*((xB+y(3))-gamma*yB)+ qc*(xC-gamma*yC)));

xb = xB + (1/6)*y(1) + (1/3)*y(2) + (1/3)*y(3) + (1/6)*y(4);

```

A.2.1 Countercurrent model with differential equation

```

global Ph Pl nstage Am Lf V L laOut lbOut lcOut Vf Lo

```

```

nstage = 25;
Am = 37.7/nstage; %m^2
Ph=1000000;
Pl = 100000;
cte = 7.501e-12;
QA = 500*cte; % GPU -> m^3[STP]/(m^2*s*Pa)
QB = 100*cte;
QC = 10*cte;
xAf = 0.3333;
xBf = 0.3333;
xCf = 0.3334;
Lf = 0.0786; %m^3/s
Lfa=Lf*xAf;
Lfb=Lf*xBf;
Lfc=Lf*xCf;

```

```

%Initial values for the feed and permeate flows in each stage

```

```

V = [0:Lf/(nstage+1):Lf-Lf/(nstage+1)];

```

```

L = [Lf/(nstage+1):Lf/(nstage+1):Lf];

```

```

% initial condition to calculate coefficient Ea
IA1= Lf/(5*(nstage+1));
% initial condition to calculate coefficient Eb
IB1 = Lf/(5*(nstage+1));
% initial condition to calculate coefficient Ea
IC1= Lf/(5*(nstage+1));

Vcomp=1;
Lcomp=1;

while(abs(Vcomp)>1e-8&abs(Lcomp)>1e-8)
la = Tmethod(QA,xAf,IA1); %Thomas Method for A
lb = Tmethod(QB,xBf,IB1); %Thomas Method for B
lc = Tmethod(QC,xCf,IC1); %Thomas Method for C

% Save previous V and L
Voutant = V(nstage+1);
Loutant = L(1);

% RECALCULATE TOTAL FEED FLOW RATES
L=la+lb+lc;
L(nstage+1)=Lf;

% RECALCULATE TOTAL PERMEATE FLOW RATES
% Independent from number of components
V(1)=0;
for k=1:nstage
V(k+1)=L(k+1)+V(k)-L(k);
end

% Values needed to use in the Thomas Method suce.aprox.
IA1 = la(1);
IB1 = lb(1);
IC1 = lc(1);

Voutact = V(nstage+1);
Loutact = L(1);

% CRITERIA VERIFICATION
Vcomp=(Voutact-Voutant)/Voutact;
Lcomp=(Loutact-Loutant)/Loutact;
end
%*****END WHILE*****

```

```
% PERMEATE FLOW RATES OF EACH COMPONENT ON EACH STAGE ON THE  
LOW-PRESSURE SIDE
```

```
  %Component A  
la(nstage+1)=Lfa;  
va(1)=0;  
  for k=1:nstage  
    va(k+1)=la(k+1)+va(k)-la(k);  
  end  
  %Component B  
lb(nstage+1)=Lfb;  
vb(1)=0;  
  for k=1:nstage  
    vb(k+1)=lb(k+1)+vb(k)-lb(k);  
  end
```

```
  %Component C  
lc(nstage+1)=Lfc;  
vc(1)=0;  
  for k=1:nstage  
    vc(k+1)=lc(k+1)+vc(k)-lc(k);  
  end
```

```
%CALCULATION OF mj  
% mj: the mass flow rate of each component that leaves stage k due to permeation  
through the membrane
```

```
  %Component A  
  for k=1:nstage  
    ma(k)=la(k+1)-la(k);  
  end  
  %Component B  
  for k=1:nstage  
    mb(k)=lb(k+1)-lb(k);  
  end  
  %Component C  
  for k=1:nstage  
    mc(k)=lc(k+1)-lc(k);  
  end
```

```
%Total Mass Flow Rate that leaves stage k due to permeation through the membrane  
M=ma+mb+mc;
```

```
% CALCULATION OF THE MOLE FRACTION OF EACH COMPONENT ON FEED  
SIDE
```

```
    % Component A  
xa(nstage+1)=xAf;  
    for k=1:nstage  
    xa(k)=la(k)/L(k);  
    end  
    % Component B  
xb(nstage+1)=xBf;  
    for k=1:nstage  
    xb(k)=lb(k)/L(k);  
    end  
    % Component C  
xc(nstage+1)=xCf;  
    for k=1:nstage  
    xc(k)=lc(k)/L(k);  
    end
```

```
% CALCULATION OF THE MOLE FRACTION OF EACH COMPONENT ON  
PERMEATE SIDE
```

```
    % Component A  
%ya(1)=0;  
    for k=2:nstage+1  
    ya(k)=va(k)/V(k);  
    ya(1)=0;  
    end  
    % Component B  
%yb(1)=0;  
    for k=2:nstage+1  
    yb(k)=vb(k)/V(k);  
    yb(1)=0;  
    end  
    % Component C  
%yc(1)=0;  
    for k=2:nstage+1  
    yc(k)=vc(k)/V(k);  
    yb(1)=0;  
    end
```

```
[xa(1) xb(1) xc(1) ya(nstage+1) yb(nstage+1) yc(nstage+1)]
```

```
% METHOD THOMAS TO ESTIMATE THE COEFFICIENTS OF THE MATRICES
THAT CALCULATE THE FEED AND PERMEATE MOLAR FLOWS ON EACH
STAGE
```

```
function [l] = Tmethod(Qx,xXf,lX1)
```

```
global Ph Pl nstage Am Lf V L
```

```
E = 1:1:nstage;
```

```
E(:)=0;
```

```
for k=2:nstage+1
```

```
    B(k-1) = -V(k-1)/(Pl*Am*Qx)*(1+Qx*Am*Ph/L(k-1));
```

```
    C(k-1) = 1+V(k-1)/(Pl*Am*Qx)+V(k)/(Pl*Am*Qx)*(1+Qx*Am*Ph/L(k));
```

```
    D(k-1) = -V(k)/(Pl*Am*Qx)-1;
```

```
end
```

```
E(1) = -B(1)*lX1;
```

```
E(nstage) = -D(nstage)*Lf*xXf;
```

```
W(1) = C(1);
```

```
u(1) = D(1)/W(1);
```

```
g(1) = E(1)/W(1);
```

```
for k=2:nstage
```

```
    W(k) = C(k)-B(k)*u(k-1);
```

```
    u(k) = D(k)/W(k);
```

```
    g(k) = (E(k)-B(k)*g(k-1))/W(k);
```

```
end
```

```
l(nstage) = g(nstage);
```

```
for k=nstage-1:-1:1
```

```
    l(k) = g(k)-u(k)*l(k+1);
```

```
end
```

APPENDIX B

Linking a Process Simulator (HYSYS) with MATLAB, a Powerful Modeling Tool for Continuous Process Industry: a Tutorial

Erika L. Beronich
email: beronich@enr.mun.ca

Kelly Hawboldt
email:
hawboldt@enr.mun.ca

Majid A. Abdi
email: abdi@enr.mun.ca

Faculty of Engineering and Applied Science, Memorial University of Newfoundland
St. John's, NL, Canada A1B 3X5

Abstract— Process simulators are critical in achieving cost and timesaving during design stages. Simulators such as HYSYS can be used to design and optimize processes systems using well-established routines available within the software package. Computing tools such as MATLAB can be used to model new technologies or modify existing ones. However, MATLAB lacks the extensive thermophysical property and equipment database. The connection between these two software packages leads to an integral powerful simulation tool for the study of new processes. This paper presents a procedure to link HYSYS and MATLAB with a simple tutorial. From the educational point of view, this work is also a very useful guide for engineers and students in training.

Introduction

Process simulators are currently used to study the performance of well-established technologies or to develop new technologies for the process industry. These simulators present important advantages with respect to experimental work, pilot scale systems, and process design. HYSYS - a typical and very widely used process simulator - presents special features for oil and gas processes and allows for steady state and dynamic simulation. Most unit operations and an extensive thermodynamic database and solving routines are contained in HYSYS. Nevertheless, new unit operations are constantly being developed and may not be contained in HYSYS. Computing tools such as MATLAB can be used to model these new unit operations or modify existing ones. However, MATLAB lacks the extensive thermophysical property and equipment database. Thus, the connection between these two software packages leads to an integral powerful simulation tool for the study of new processes.

This paper presents a procedure to link HYSYS and MATLAB with a simple tutorial. In the first part of the paper, a brief description of HYSYS and MATLAB is presented with the purpose of providing background information of both software packages. Readers who are familiar with them can skip this section. Then, important concepts and terminology used in the connection are explained followed by a step-by-step connection procedure. Finally, a working example is presented.

The objective of this paper is to provide a simple method to perform a connection of these two powerful programs. This work is intended for engineers in the Process or Engineering fields who wish to rapidly combine MATLAB and HYSYS.

DESCRIPTION OF HYSYS AND MATLAB

HYSYS

HYSYS models processes for steady state and dynamic simulations. HYSYS Using process modelling software to simulate the process improves designs, optimizes production and enhances decision-making.

HYSYS offers the following [1]:

- Physical properties, transport properties, and phase behaviour can be predicted. The components database is extensive including most organic components and inorganic components.
- Most traditional unit operations (reactors, distillation columns etc...) are included in HYSYS.
- New unit operations, proprietary reaction kinetic expressions, and specialized property packages are included into HYSYS by means of a link with programs such as Microsoft Excel, MATLAB and Visual Basic.
- An extensive understanding of unit operations.
- HYSYS. Both steady state and dynamic simulations are possible. In addition, adding control systems to the process is possible.
- Evaluation of the equipment performance is also possible.
- HYSYS produces a reduction in engineering cost. For example, the analysis of the process and data can be achieved quickly and effectively, which without this program can take an uncounted time.
- An easy graphic representation in Portable Document Format (PDF) of the process flowsheet and its correspondent sub-flowsheets.
- An economic evaluation of the process design can be estimated. HYSYS simulation models are exported to special program such as Aspen Icarus Process Evaluator or Aspen Icarus Project Manager to effectuate the economic evaluation.

MATLAB

MATLAB is an interactive, numeric computation and visualization environment that combines hundreds of pre-packaged advanced math and graphic functions with the flexibility of a high level language to customize and add new functions as needed. As a result, MATLAB performs computationally intensive tasks faster than traditional programming languages such as C, C++, and Fortran. Numerous applications can be accomplished with this software such as signal and image processing, communications, control design, test and measurement, financial modeling and analysis, and computational biology [2]. The algorithms created with this software can be integrated with external application and languages, such as HYSYS.

CONNECTION

A. Fundamental Definitions

In this section, important terminologies and concepts to establish the communication between HYSYS and MATLAB will be expanded [3].

1) Automation

Automation is the action of operating one application from another. HYSYS presents its objects (i.e. distillation column, material stream, etc...) as exposed, which permits access through automation. Programs with ability to connect to applications that have exposed objects can programmatically interact with HYSYS. Such programs could be any language programs since the automation is language independent. In this case, MATLAB (version 7.0.1) is selected due to its extensive use in the Engineering field and its ease when compared with other languages.

2) Objects

An object involves a set of related function and variables, which describe the object's general attributes. In the terminology used in automation, the functions of an object are referred to as methods and the variables as properties. Each property possesses a value associated with it, while methods are functions and subroutines related with the object. The properties and methods are used to describe, manage and control objects.

An object can include other objects that are subgroup of the main object. An example of an object that contains other objects is a "Flowsheet". The object Flowsheet contains other objects such as material streams or energy streams. At the same time, the object material stream also contains other properties such as temperature, pressure, molar flow, composition, and other properties that described this stream.

3) Hierarchy

The route to access a specific property may contain various objects. Therefore, a hierarchy must be followed. The route starts from the main object followed by the next objects ordered in importance of appearance to the specific property or method of interest. The initial object in a hierarchy route might be an object from which all other objects can be accessed. In MATLAB, this route is built up through the dot operator (.) function, where each dot operator in the route is a function call.

When a property is required to access several times in the code, it is useful to declare a new variable that represents the route to reach this property frequent used.

4) Spreadsheet

The spreadsheet allows complete access to all process variables, and it is extremely powerful with many applications in HYSYS. In general, the spreadsheet is used to perform calculations that are not provided by HYSYS the unit operation such as calculation of pressure drop during dynamic operation of a Heat Exchanger.

The spreadsheet has access to any variable by importing them. Any variable in the simulation may be imported virtually into the Spreadsheet. In the same way, a cell's

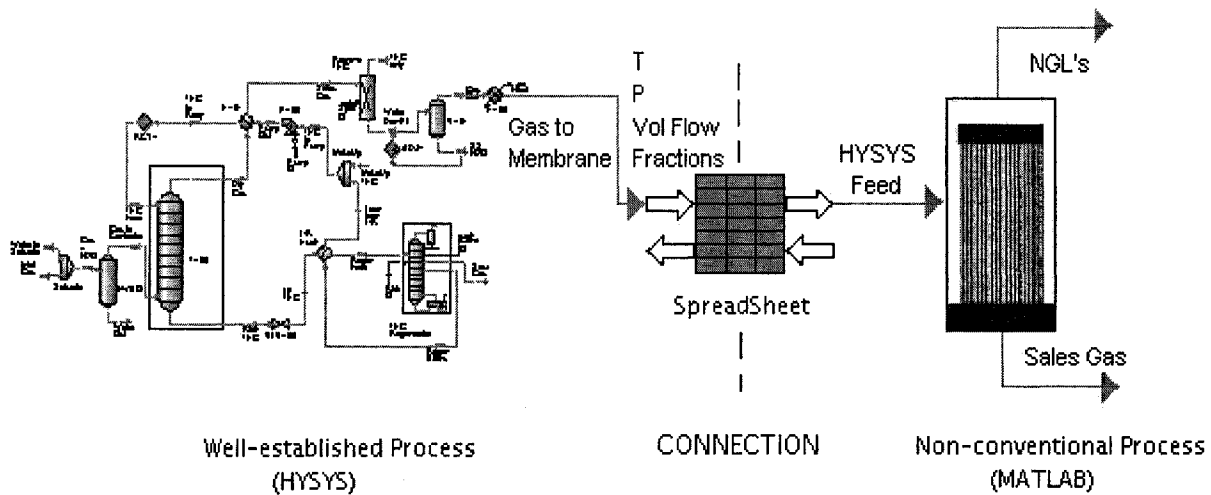


Fig. 1 Conceptual schematic of a connection between MATLAB and HYSYS using a spreadsheet

value, such as a calculation result, can be exported to any specifiable input field in the simulation.

In this paper, all the variables needed for the MATLAB program code are imported to the spreadsheet. This simplifies the task of reading the variables from MATLAB since the routes toward the variables are not always clear (i.e., number of plates in a distillation column). In Figure 1, a conceptual schematic of a connection between MATLAB and HYSYS using a spreadsheet is presented. This figure represents the application example explained in section IV, where the communication of both programs is through the spreadsheet.

B. Steps for connections

1) Communication

First, the HYSYS file or HYSYS application of interest should be opened. The line of the code that connects MATLAB to the current HYSYS file is:

```
hsys=feval('actxserver','Hysys.Application');
```

2) Solver

Once the connection is established, HYSYS method "solver" can be accessed from MATLAB using:

```
hysolver=hsys.ActiveDocument.Solver;
```

Here “hysolver” summarizes the method “Solver” for the HYSYS simulation from MATLAB. The route to access to the method “Solver” is formed by “hysys”, which represents the connection between both programs, followed by “ActiveDocument”, which refers to the active document of HYSYS; and “Solver” is the property solve of the simulation. The dots in this route determined the order of hierarchy followed.

Now, from MATLAB an order to stop solving the simulation is sent. The instruction to stop the simulation from MATLAB is:

```
hysolver.CanSolve = 0;
```

Here “Cansolve” is a method that stops the simulation when it is zero, and it enables the simulation (or solve) when it is one using the following code:

```
hysolver.CanSolve = 1;
```

3) Read a value

In order to read a value of a specific property, the route to achieve this property needs first to be declared. For example, if the temperature value of a material stream requires to be read, the route is declared as follow.

```
StreamRoute=hysys.ActiveDocument.Flowsheet.MaterialStreams.  
Item('nameofthematerialStream')
```

In this example the variable that determines the route is called “StreamRoute”. The name of the stream, which the temperature is read from, is placed between the brackets.

After that, the temperature value can be read. The instruction to access temperature property of the material stream selected is defined as a new variable; in this case it is temp1:

```
temp1 = StreamRoute.TemperatureValue
```

Here “TemperatureValue” is the method that executes the reading of the temperature property of the object specified (material stream).

4) Set a Value

A value of an input material stream can be changed from MATLAB. For example, if the value of the temperature of the previous case wishes to be changed at 310 K, the instructions are as follow:

```
StreamRoute.Temperature.SetValue(310, 'K')
```

Here “StreamRoute” establishes the route to achieve the object (material stream) that is going to be modified. “Temperature” describes the specific property of the object materialstream that is going to be changed. “SetValue” is the method to change a property, where the new value with its respective unit is described between brackets (new temperature value, unit). In this example, the temperature value is set to 310 K.

After that, the simulation with the new set value is solved from MATLAB.

```
hysolver.CanSolve = 1;
```

Then, the simulation is stopped from MATLAB in order to read the updated temperature value.

```
hysolver.CanSolve = 0;
```

The new temperature value can be read to verify the change. This new reading is again defined as a variable as:

```
Temp2 = StreamRoute.TemperatureValue
```

5) Read a value from Spreadsheet

From the spreadsheet, any value imported or exported can be read from MATLAB. For that, the route to arrive at the spreadsheet need to be specified, and it is defined as a variable as follows:

```
hySS=hysys.ActiveDocument.Flowsheet.Operations.Item('SPRDSHT-1');
```

In this example the variable that determines the route is called “hySS”. The name of the spreadsheet, which called in this case “SPRDSHT-1”, is placed between the brackets.

Once the spreadsheet access route is determined, the desired cell to be read is determined. The cell is described as column/row; the columns are defined with capital letters and the rows with numbers. The specification of the cell is declared as a variable such as “hyCell”.

```
hyCell=hySS.Cell('A1');
```

Once the cell is declared, the cell value can be read from MATLAB using the method “CellValue”, and this value is assigned to the variable named Value:

```
Value = hyCell.CellValue
```

In the same manner, the text of the cell is read using the method “CellText”, and it is also defined as a variable:

```
Text = hyCell.CellText
```

Also, the name and unit of the cell can be read from MATLAB using the methods “VariableName” and “Units”, respectively.

```
Name = hyCell.VariableName  
Units = hyCell.Units
```

6) Change a value of the spreadsheet from MATLAB

Any value imported to the spreadsheet, which is an input data, can be modified from MATLAB. For that, the route to the spreadsheet needs to be specified. Then, the desired cell to be modified needs also to be specified in the same manner as before:

```
hySS=hsys.ActiveDocument.Flowsheet.Operations.Item('SPRDSHT-1');  
  
hyCell=hySS.Cell('C1');
```

The instruction to modify an import value from MATLAB is shown as follow:

```
hyCell.CellValue = 25;
```

Here “hyCell” describes the route to achieve the cell of the object spreadsheet that is going to be changed, and “CellValue” is the method to read a property value. In order to change this value, these two methods are called and made equal to the new value without specifying the units. The new value has to possess the same units as in the cell being modified. In this example, the temperature of the material stream “Inlet Gas” is going to be modified. The actual value of the cell is 29.44 °C. The new value to be set is 25 °C. After that, the simulation with the new set value is solved from MATLAB.

```
hysolver.CanSolve = 1;
```

Then, the simulation is stopped from MATLAB in order to read the updated temperature value.

```
hysolver.CanSolve = 0;
```

The new temperature value can be read to verify the change. This new reading is again defined as a variable as:

```
Temp3 = hyCell.CellValue
```

As the changed value is an imported value, it will change the value in the flowsheet automatically.

2) Brief description of the Separation Process

The purpose of the membrane is to remove heavier hydrocarbons or natural gas liquids (NGLs) from the natural gas. NGLs consist of ethane, propane, and butanes. This separation process consists of a non-porous membrane, which separates the components according to their affinity with the membrane material.

This process is not available in HYSYS case as it is a relatively new application. For this reason, this process is executed in a MATLAB code using the data obtained from the HYSYS simulation. The membrane model used is a counter current flow model for a hollow-fiber membrane system [5].

B. Connection

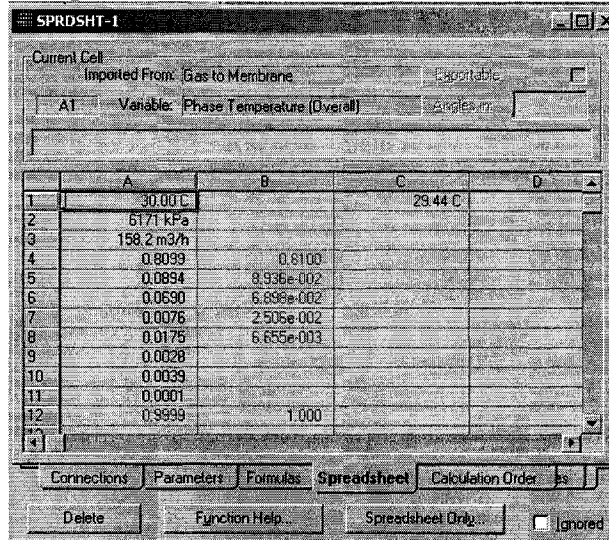
1) Spreadsheet

The data necessary for the MATLAB simulation are composition of the natural gas, pressure, and molar flow exiting the dehydrator. These data are imported from the flowsheet to the spreadsheet.

Figure 3 shows the spreadsheet. The first two cells in column A are input data (A1 and A2), which are indicated by HYSYS in blue). Cells A3-A11 in column A are results of the HYSYS simulation, which are indicated by HYSYS in black. The cells of column B are calculated values, which are indicated by HYSYS in red. The calculated values can be exported to the flowsheet. The four first values in column A of the spreadsheet are temperature, pressure, molar flow and volumetric flow of the material stream specified, which in this case is named "Gas to Membrane". The next values in column A are the mole fraction of the components. The mole fractions of similar components (i.e. n-butane and i-butane) are added, and this calculation is represented in column B.

2) MATLAB reading

The data specified in the spreadsheet are read from MATLAB, as is show below:



	A	B	C	D
1	30.00 C		29.44 C	
2	6171 kPa			
3	158.2 m3/h			
4	0.8099	0.8100		
5	0.0894	8.936e-002		
6	0.0690	6.896e-002		
7	0.0076	2.505e-002		
8	0.0175	6.655e-003		
9	0.0028			
10	0.0039			
11	0.0001			
12	0.9999	1.000		

Fig. 3: Spreadsheet

```

% Connect MATLAB to the current HYSYS application

hysys=feval('actxserver','Hysys.Application');

% Stop the solver
hysolver = hysys.ActiveDocument.Solver;
hysolver.CanSolve = 0;

% READ FROM THE SPREADSHEET
    %Connecting to SPRDSHT-1
hySS=hysys.ActiveDocument.Flowsheet.Operations.Item('SPRD
SHT-1');

    %Temperature
    hyCell = hySS.Cell('A1');
    TemHYSYS = hyCell.CellValue;
    Units = hyCell.Units;

    %Pressure
    hyCell = hySS.Cell('A2');
    PhHYSYS = hyCell.CellValue ;
    Units = hyCell.Units;

    %Act Volume Flow
    hyCell = hySS.Cell('A3');
    LfHYSYS = hyCell.CellValue;
    Units = hyCell.Units;

    %Molar Fraction Methano
    hyCell = hySS.Cell('B4');
    fc1 = hyCell.CellValue;

    %Molar Fraction Ethano
    hyCell = hySS.Cell('B5');
    fc2 = hyCell.CellValue;

    %Molar Fraction Propane
    hyCell = hySS.Cell('B6');
    fc3 = hyCell.CellValue ;

    %Molar Fraction Butanes
    hyCell = hySS.Cell('B7');
    fc4 = hyCell.CellValue;

```

```

%Molar Fraction Pentanes
hyCell = hySS.Cell('B8');
fC5 = hyCell.CellValue;

```

3) MATLAB Code

Once the data from HYSYS are collected in MATLAB, the correspondent code to model the membrane can be performed and the results returned to HYSYS for further processing. The results obtained from the model are shown in Figure 4. This figure represents the change of volumetric flow rate of the C_2^+ components (ethane, propane, butanes and pentanes) in the material streams “NGL” (permeate) and “Sales Gas” (residue), which flow in opposite directions (counter flow).

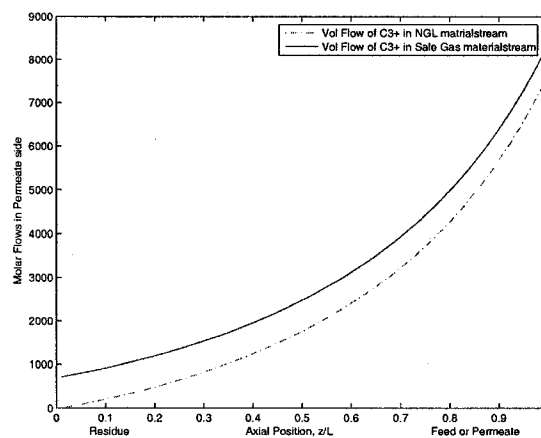


Figure 4: Volumetric Flow rates of the C_2^+ components along the membrane in the permeate side (material stream “NGL”) and in the residue side (material stream “Sales Gas”).

Conclusion

In this paper, a procedure to connect HYSYS and MATLAB, two powerful software packages, was presented. The connection of these two programs allows the modelling of a new technology by exploiting the wealth of information contained in HYSYS.

The application example shows a case that combines a well-established technology (simulated with HYSYS) with new technology (MATLAB model). From this example case, it can be seen that the connection is simple and straight forward, and the results obtained can represent great advantages for the continuous process industry.

ACKNOWLEDGMENT

The authors wish to thanks Natural Science and Engineering Research Council of Canada (NSERC) for the support.

REFERENCES

- [1] HYSYS.Process 2.2 Documentation. Customization Guide – Chapter 1: Welcome to HYSYS.
- [2] Anonymous MATLAB student version “Learning MATLAB 6.5”, The Math Works, Inc. (2002).
- [3] HYSYS.Process 2.2 Documentation. Customization Guide – Chapter 2: Automation.
- [4] Manning F. and Thompson R., “Oil Field Processing of Petroleum, Volume 1: Natural Gas”, Pennwell Publishing, 1991, ISBN: 0-87814-343-2
- [5] D. Coker, B. Freeman, and G. Fleming, “Modeling Multicomponent Gas Separation Using Hollow-Fiber Membrane Contactors”, AIChE Journal, v44, n6, 1289 (1998).

APPENDIX C

C.1 Typical gas composition in the Newfoundland Offshore Area

Components	Composition (%)
Methane	78
Ethane	8.82
Propane	7.15
ii-Butane	0.84
n-Butane	2.02
i-Pentane	0.37
n-Pentane	0.4
Hexane	0.15
Nitrogen	0.27
Dioxide carbon	1.18